Mucoadhesive Nanocarriers for Nasal Delivery of Vaccines

Inaugural-Dissertation
to obtain the academic degree
Doctor rerum naturalium (Dr. rer. nat.)
submitted to the Department of Biology, Chemistry and Pharmacy
of Freie Universität Berlin

by

RAHUL ASHOK SONAWANE

from Nasik, India

Berlin, 2016

Die vorliegende Arbeit wurde von October 2012 bis Juni 2016 unter der Leitung von Prof. Dr. Roland Bodmeier im Institut für Pharmazie angefertigt.

1. Gutachter:	Prof. Dr. Roland Bodmeier
2. Gutachter:	Prof. Dr. Philippe Maincent

Tag der mündlichen Prüfung: 12.07.2016

To my Family

Acknowledgements

I would like to thank Prof. Dr. Roland Bodmeier who accepted me as his Ph.D. student. I am very thankful for his support and supervision during my academic tenure as a doctoral student at Institute of Pharmaceutical Technology, Freie Universität Berlin. Without his supervision, professional guidance, and encouragement, this thesis would not have materialized.

I would like to thank Prof. Dr. Philippe Maincent for co-evaluating my Ph.D. dissertation.

I am very thankful to German Academic Exchange Service (DAAD) for providing financial support for my Ph.D. study.

I would also like to show my gratitude to Dr. Onkar Kulkarni, Dr. Vamsi Krishna Venuganti, Dr. Shrikant Charde and Mr. Suman Labala for their help, support and scientific input for the collaboration work at BITS Pilani Hyderabad campus, India. I would also like to thank Prof. Dr. Karl Lang and Mr. Vishal Khairnar for the interesting collaborative work at Institut für Immunologie, Universitätsklinikum Essen, Germany. I am also thankful to Dr. Vikash Singh and Dr. Karsten Tedin from Institut für Mikrobiologie und Tierseuchen, Berlin for performing cytotoxicity assay.

I would like to extend the deepest gratitude to Dr. Shrikant Mulay and Dr. Ujjwal Mahajan for sharing crucial scientific expertise and help and support extended during my Ph.D. tenure. I am also thankful to Dr. Harshad Harde and Dr. Sachin Surwase for the scientific inputs in my Ph.D. work. I am thankful to Dr. Vikram Paradkar from Biological E Ltd. Hyderabad, India for providing Tetanus toxoid as a gift sample. I am also thankful to Prof. Dr. Gerald Brezesinski and Mr. Janos Keller for their help in Circular Dichroism analysis at Max Planck Institute of Colloids and Interfaces, Potsdam, Germany.

I am thankful to Kathrin, Luisa, Marius, Benjamin, Dr. Fitsum, Marina and Prutha for proofreading parts of my thesis. I would also like to thank my colleagues Dr. Anis, Dr. Rebaz, Dr. Gaith, Dr. May, Jelena, Rick, Zoha, Reza, Fenny and Jia for their help and encouragement. I am very thankful to Nadeem Ishaque Khan for being a very nice lab colleague and creating

an enjoyable environment in the lab. I am grateful to all lab colleagues for their help and support during my stay in the group.

I am very thankful to Mr. Stefan Walter, Ms. Eva Ewest and Mr. Andreas Krause for their generous help and technical support; to Mrs. Gabriela Karsubke for her assistance with administrative issues.

Lastly and most importantly, my deepest gratitude to my Family and my friends in India for their love, support and persistent encouragement which provided me great strength to counter all odds and successfully finishing my Ph.D. study.

Table of contents

List of Figures

List of Tables

List of Abbreviations

ALG	Sodium alginate
APC	Antigen presenting cell
BCA	Bicinchoninic acid
BSA	Bovine serum albumin
CD	Cluster of differentiation
CD	Circular dichroism
CMC	Sodium carboxymethylcellulose
ConA	Concanavalin A
CPCSEA	Committee for the Purpose of Control And Supervision of Experiments on Animals
CTL	Cytotoxic T-lymphocytes
DAPI	4’,6-diamidino-2-phenylindole
DC	Dendritic cell
DEAE	Diethylaminoethyldextran
DMEM	Dulbecco’s modified Eagle’s medium
DMSO	Dimethyl sulfoxide
DPT	Diphtheria, Pertussis, and Tetanus combination vaccine
EDTA	Ethylenediaminetetraacetic acid
EE	Encapsulation efficiency
ELISA	Enzyme-linked immunosorbent assay
FACS	Fluorescence activated cell sorting
FBS	Fetal bovine serum
FCS	Fetal calf serum
FDA	Food and Drug Administration
FITC	Fluorescein isothiocyanate
FTIR	Fourier transformer infrared
GIT	Gastrointestinal tract
HA	Sodium hyaluronate
HIV	Human Immunodeficiency Virus
HRP	Horseradish peroxidase
i.m.	Intramuscular

i.n.	Intranasal
ICH	International Conference on Harmonization
IFN	Interferon
IgG	Immunoglobulin G
IL	Interleukin
LDH	Lactose dehydrogenase
Lf	Limits of flocculation
LPS	Lipopolysaccharides
MCC	Mucociliary clearance
M cell	Microfold cell
MHC	Major histocompatibility complex
MTT	3-(4,5-dimethylthiazol-2-yl)-2,5-diphenyltetrazolium bromide
MW	Molecular weight
MWCO	Molecular weight cut-off
NALT	Nasal-associated lymphoid tissues
NP	Nanoparticles
OD	Optical density
OVA	Ovalbumin
PAGE	Polyacrylamide gel electrophoresis
PBS	Phosphate buffered saline
PCT	Sodium pectinate
PDI	Polydispersity index
PEG	Polyethylene glycol
pI	Isoelectric point
RH	Relative humidity
Ri	Redispersibility index
RPMI	Roswell Park Memorial Institute
SD	Standard deviation
SDS	Sodium dodecyl sulfate
SEM	Standard error of mean
sIgA	Secretory immunoglobulin A
SNES	Simulated nasal electrolyte solution
Th	T-helper

TMB	3,3′,5,5′-Tetramethylbenzidine
TPP	Sodium tripolyphosphate
TT	Tetanus toxoid
UV	Ultraviolet
WHO	World Health Organization

List of Symbols

kDa	Kilo Dalton = 1000 Dalton
%	Percentage
λ	Lambda
®	Registered
°C	Degree Celsius
µg	Microgram= 10^{-6} Gram
µl	Microliter= 10^{-6} Liter
g	Gram(s)
g	Gravitation force (9.897 m/s^2)
h	Hour(s)
L	Liter(s)
M	Molar
mg	Milligram= 10^{-3} Gram
min	Minute(s)
ml	Milliliter= 10^{-3} Liter
mV	Millivolts= 10^{-3} Volts
N	Newton
N	Normal
nm	Nanometer= 10^{-9} meter
pH	Negative log of H^+ ion concentration
RSD	Relative standard deviation
SD	Standard deviation
™	Trademark
v/v	Volume by volume basis
w/v	Weight by volume basis
w/w	Weight by weight basis

1. Introduction

1.1 Vaccines

Over the last two decades, medical science has advanced at a phenomenal pace. Medical researchers have successfully traversed one after another milestone towards the development of "effective therapies" for most of the life-threatening diseases and disorders. Yet, the infectious diseases are one of the major leading causes of deaths amongst infants, grown-up children and adults, as well. As prevention is always a better option than cure, immunization against these diseases is crucial. Needless to mention, vaccines are deployed to realize this purpose. By definition, vaccines are the immune system stimulators which stimulate the production of antibodies against specific antigens. The conventional vaccines whether live attenuated or heat-killed pathogens have been proved effective for the prevention and treatment of several life-threatening infectious diseases such as smallpox, polio, and diphtheria. Still, there are major diseases where no effectual vaccine is available or the vaccine, even on hand, affords partial protection. Such diseases lead to millions of deaths every year and is considered as a primary challenge to be tackled by medical practitioners. The World Health Organization (WHO) and the health ministry of every nation have primarily focused on the vaccination program with an aim to completely eradicate a number of dreadful diseases like polio, cholera, malaria, Human Immunodeficiency Virus (HIV) and hepatitis (Gamvrellis et al., 2004; Plotkin, 2005).

The infectious diseases like smallpox, hepatitis, dengue, malaria, viral fever, bird flu and many more are the primary cause behind the millions of deaths worldwide. Vaccines were developed to prevent such life-threatening diseases in the human being as well as animals. Simply speaking, vaccines are nothing but immunity boosters or in other words, immune stimulants which contribute to active immunity. By origin, vaccines are antigens derived from viruses or bacteria which are either inactivated or killed and thus produces immunity against particular bacteria or viruses. Thus to prevent infections in the newborns vaccination program is being carried out which includes vaccines like hepatitis B, polio, measles, rubella, diphtheria, pertussis, tetanus (DPT) and Haemophilus influenza type B. Along with children, the adults are also vaccinated against influenza, pneumococcal and DPT infections.

Vaccines available for the prevention of infectious diseases, including type, route of administration and efficacy, are summarized in Table 1.

Table 1 Vaccines available on the market for the prevention of infectious diseases worldwide. Table adapted and modified from (Chadwick et al., 2010) with permission.

Vaccine	Type Of Vaccine	Route Of Administration	Resulting Efficacy
Adenovirus Type 4 and 7	Live	Oral	M
Anthrax[a]	Inactivated	SC	S
BCG	Live attenuated	IM	S
Cholera	Toxin B subunit + inactivated	Oral	M
Cholera	Live attenuated	Oral	M
Diphtheria	Toxoid	IM	S
Hepatitis A	Inactivated/recombinant	IM	S
Hepatitis B	Inactivated/recombinant	IM	S
Haemophilus influenza type b	Conjugate	SC	S
Human Papillomavirus	Subunit	IM	S
Influenza A (H1N1)	Inactivated	SC or IM	S
Influenza	Live attenuated	Nasal	M/S
Japanese encephalitis	Inactivated	SC	S
Lyme disease[b]	Protein subunit	IM	S
Measles	Live virus	SC	S
Meningococcal	Purified bacterial capsular polysaccharide	IM (MCV)/ SC (MPSV)	S
Mumps	Live attenuated virus	SC	S
Plague	Inactivated	IM	S
Pertussis	Whole-cell or acellular	IM	S
Pneumococcal	Polysaccharide	IM or SC	S
Poliomyelitis (IPV)	Inactivated organism	IM or SC	S
Poliomyelitis (OPV)	Live attenuated organism	Oral	M
Rabies	Cell-cultured inactivated	IM	S
Rotavirus	Live attenuated	Oral	M
Rubella	Live attenuated	SC	S
Smallpox	Live virus	PC	S
Tetanus	Toxoid	IM	S
Typhoid	Live attenuated mutant	Oral	M
Typhoid	Vi polysaccharide	IM/ deep SC	S
Tuberculosis	Live organism	ID	S
Varicella (chickenpox)	Live attenuated	SC	S
Yellow Fever	Live viral	SC	S
Zoster	Live attenuated	SC	S

Abbreviations: SC= subcutaneous, IM= intramuscular, ID= intradermal, S= systemic, M= mucosal, BCG= Bacillus of Calmette and Guerin, MCV= meningococcal conjugate vaccine, MPSV= meningococcal polysaccharide vaccine, IPV= inactivated polio vaccine, OPV= live attenuated oral polio vaccine. [a] Not routinely available, [b] No longer available in the US.

1.1.1 Principle of vaccination

As mentioned above, vaccines are the specific components derived from pathogenic organisms (e.g. viruses, bacteria) which are either inactivated or killed to generate immune response specific to organisms. In principle, the vaccine should provide long-term protection by eliciting innate and adaptive immune response.

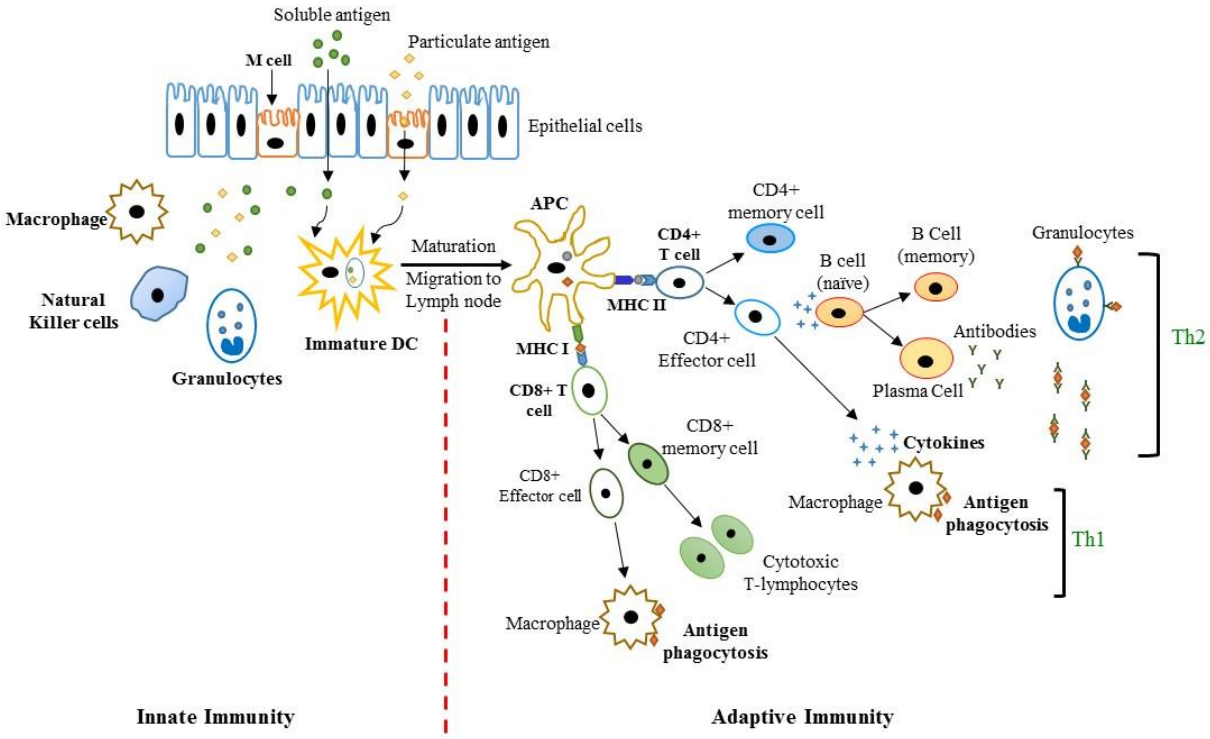

Figure 1 Schematic presentation of immune response generated in response to invading pathogens/vaccine antigens.

The principle of vaccination is similar to the interactions between invading pathogens and human body's defense system. The cascade of the immune response following entry of pathogens/administration of vaccines is presented in Figure 1. The antigen crosses the epithelial membrane through intracellular route (soluble antigens) or actively taken up by specialized microfold cells (M cells) (particulate antigens). These antigens are then captured by the immature dendritic cells (DC) which are patrolling throughout the body. The surface proteins of antigen act as pathogen-associated molecular patterns (PAMP) and attracts the macrophages, natural killer cells, and granulocytes, which either engulf them or release cytokines to destroy these antigens. This is a part of innate immunity which is brisk and short-lasting.

After sampling the antigens, the immature DCs undergo brisk maturation, activates specific surface receptors and migrate towards secondary lymph nodes. The matured DCs are called as antigen presenting cells (APC) which process the antigens and present them to T-lymphocytes

through major histocompatibility complex (MHC) molecules. The activation of T-lymphocytes and the further immune response is a part of adaptive immune response which is antigen-specific and last for a longer period (in some cases lifetime). Depending on the nature of vaccine antigens, the APC either present them to $CD4^+$ T cells via class II MHC (MHC II) or to the $CD8^+$ T cells via MHC I molecules. The antigenic parts from intracellular pathogens and viruses are presented to $CD8^+$ T cells also called as cytotoxic T lymphocytes (CTL) via MHC I molecules which then kills the infected cells and/or release virus-specific cytokines to destroy them. The memory $CD8^+$ T cells keep the memory of the virus recognition pattern and release CTLs and specific cytokines upon re-exposure in future. While the antigenic parts of extracellular pathogens and bacteria, after processing by APC, are presented to the $CD4^+$ T cells via MHC II molecules which further matures and differentiate into $CD4^+$ effector cells and $CD4^+$ memory cells. The $CD4^+$ effector cells also celled as T helper cells (Th) are commonly subdivided into T helper 1 (Th1) and T helper 2 (Th2) subtypes/lineage based on their secretion of different cytokines. Th1 cells secrete interleukin-2 (IL-2) and interferon-γ (IFN-γ) as main cytokines which in turn activates CTLs and recruit macrophages to perform phagocytosis. Th2 cells secrete IL-4, IL-5, IL-6, IL-10 and IL-13 cytokines which activate naïve B cells to mature and differentiate into plasma B cells and memory B cells. The plasma B cells then produce antigen-specific antibodies (IgG and IgA) which are circulate throughout the body to clear pathogens from other parts of the body. The memory B cells store the memory of specific antigen patterns and produce the antigen-specific antibodies upon re-exposure. This is also called as humoral immunity which is long lasting and ensures better protection for a longer period (Nordly et al., 2009; Siegrist, 2008).

Most of the vaccines stimulate both T- and B-cells response and thus activates cellular and humoral immune response to ensure better protection against the invading pathogens.

1.1.2 Types of vaccines

Depending upon the immunogenic components of pathogens used for the vaccine preparation, they can be divided into following types:

1. Live, attenuated vaccines: These are the weakened versions (attenuated) of the disease causing organisms which cannot cause disease but are potent enough to trigger an immune response. As they are very close to the living organisms, elicit stronger cellular as well as a humoral immune response which is long lasting (lifetime). In general, it is easier to create live, attenuated vaccines with viruses than with bacteria, since former contains less

number of genes which need to be controlled to avoid infection. The major disadvantage of this type is the reversion of the avirulent organisms to an original virulent organism which can cause disease. Another limitation is the storage and transport are difficult and costly as these vaccines need to be refrigerated to retain potency. Vaccines against measles, mumps, and chickenpox are some of the examples of live, attenuated vaccines.

2. Inactivated vaccines: They are produced by killing the targeted pathogens with heat, chemicals or radiation treatment. They are more safe and stable than the live, attenuated vaccines as dead microbes cannot revert back to virulent form. Moreover, they don't need refrigeration if stored and transported in freeze-dried form. The major limitation with inactivated vaccines is the weaker immune stimulation (mostly humoral immunity) and thus, there is a need to take booster doses frequently to maintain immunity. Examples of this type include Hepatitis A vaccine and Japanese Encephalitis virus vaccine.
3. Subunit vaccines: These are consisting of antigenic components of microbes which can elicit a stronger immune response. The selecting and isolating antigenic components is a tricky and time-consuming work at it needs a thorough understanding of immune response generated by each antigenic part of micro-organism. The subunit vaccines produce a weak immune response when administered alone. The adjuvants are used to potentiate their actions. Hepatitis B recombinant vaccine is an example of a subunit vaccine.
4. Toxoids vaccines: These vaccines were developed to prevent the infections from toxin secreting bacteria. The toxins secreted by these microbes are the primary cause of infection. The toxoid vaccines are prepared by inactivating bacterial toxins with formalin (formaldehyde treated). The immune system produces toxin-specific antibodies and thus confers the protection. Tetanus and Diphtheria toxoid vaccines are the examples of this type.
5. Conjugate vaccines: This is the modified/advanced type of subunit vaccine, which is developed to boost immature immune system of infants and young children. The immature immune system of infants failed to recognize polysaccharide coatings of some bacteria as a foreign antigen and thus failed to generate an immune response. These polysaccharides are thus separated and conjugated with toxoids to elicit a strong immune response against toxoid and thus polysaccharide containing bacteria. Haemophilus b conjugate, meningococcal conjugate, and Pneumococcal conjugate vaccines are the examples of this type.

6. Naked DNA vaccines: These vaccines are still in the developmental stage and will take some more time to be materialized. The basic principle behind developing these vaccines is genes which encode (DNA) for the antigen can be injected into the body and the cells will uptake the DNA and produce antigen and present it on the surface. The immune cells will generate strong immune response against these antigens and thus will ensure better protection.
7. Recombinant vector vaccines: These are also in the developmental stage and uses the attenuated viruses or bacteria to carry DNA encoding antigens from other microbes in the human body. The virus loaded with these DNA will inject it into the body cells and produce the immune response similar to naked DNA vaccines. (NIAID, 2012)

1.1.3 Adjuvants

In recent years, vaccine technology has experienced a tremendous leap. Yet vaccines for many life-threatening infections like HIV and some recent viral originated infections are not available, till date. The other vaccines which are available in the market are also ineffective in severely immune-compromised individuals due to poor or lack of immune components in the body. For such individuals, the vaccines are administered along with some vaccine adjuvant which not only boost up the immune response but also helps to reach the antigen to their site of action i.e. receptors on class I/II Major histocompatibility complex (MHC) molecules or dendritic cells (Gamvrellis et al., 2004; Nordly et al., 2009; Sproul et al., 2000).

Moreover, the non-live vaccines (attenuated/subunit) produces a poor immune response which lasts for shorter duration as compared to live vaccines. These vaccines need an additional component to provide an initial boost. These components were termed as “adjuvants” by Roman *et al.* and described them as compounds that enhance the antibody response against antigens (Kwak and Longo, 1996; Marciani, 2003). From the early 1920s, adjuvants were employed to improve vaccine efficacy (Cox and Coulter, 1997; Lewis and Loomis, 1924). Although it is well established that adjuvants improve the efficacy of vaccine antigens significantly, the exact mechanism of immune stimulation for most of the adjuvants is not clear. Most of the vaccine adjuvants play an important role in guiding CD4 T cells induction and further differentiation, thereby stimulating components of innate and adaptive immune system. This influence the quality and quantity of immune response.

Table 2 Current status of commonly used and newly developed vaccine adjuvants. Table adapted from (O'Hagan and Fox, 2015) with permissions.

Adjuvant (Examples)	Description	Development Status
Aluminium salts	Insoluble particles of hydroxide, phosphate or hydroxy phosphate sulfate salts	Included in licensed products for routine childhood vaccines and many others
Oil-in-water emulsions (MF59, AS03, etc.)	Oil dispersed nanoemulsions stabilized with non-ionic surfactants	Included in licensed products for seasonal influenza (MF59) or pandemic influenza (MF59, AS03)
Liposomes (AS01)	Dispersed lipid vesicles containing TLR4 ligand and saponin	Phase III, submitted for licensure for malaria
Virosomes	Dispersed lipid vesicles including viral membrane (influenza) proteins	Licensed products for influenza and hepatitis A
Topical cream w/TLR7 ligand	Topical ointment of TLR7 ligand (Aldara) applied in conjunction with intradermal vaccination	Phase III for influenza
Polymeric microparticles (PLG)	Biodegradable polymeric microparticles	Phase I
Saponin complexes (ISCOM, Matrix-M)	Lipid, purified saponins and cholesterol cage-like nano-complexes	Phase II for influenza
AS04	Natural product TLR4 ligand (MPL) adsorbed to aluminum hydroxide	Licensed products for HBV and HPV
RC-529	Synthetic TLR4 ligand adsorbed to aluminum hydroxide	Was licensed product in Argentina for HBV
CpG ODN (1018 ISS)	Soluble TLR9 ligand (oligonucleotide)	Phase III, submitted for licensure for HBV
AS02	Oil-in-water nanoemulsion with TLR4 ligand (MPL) and saponin	Phase III
GLA-SE	Oil-in-water nanoemulsion with synthetic TLR4 ligand (GLA)	Phase II
IC31	Cationic peptide complexed with TLR9 ligand (oligonucleotide)	Phase II
Flagellin	TLR5 ligand protein linked to antigen	Phase II
Poly(I:C) (Ampligen)	Double-stranded RNA polymer analog (PolyI:C12U) TLR3 ligand	Phase II
Delta inulin (Advax)	Plant-derived crystallized microparticulate polysaccharide	Phase II
CAF01	Cationic liposome including a synthetic CLR ligand	Phase I
Alum/TLR7	Small molecule synthetic TLR7 ligand adsorbed to aluminum hydroxide	Phase I

The most commonly used adjuvants includes mineral compounds (Alum/aluminium salts), water-in-oil (incomplete Freund's adjuvant [IFA]) or oil-in-water emulsions (MF59), chemically or genetically detoxified bacterial toxins (cholera toxin (CT) or lymphotoxin (LT) from Escherichia coli), saponins (QuilA, QS21), muramyl di- or tripeptides and derivatives (MTP-PE), copolymers, ISCOMS, cytokines (IL-2, IL-12) , CpG oligonucleotides (CpG ODN), and combinations thereof (Aguado et al., 1999; Moingeon et al., 2002; Moingeon et al.,

2001; Schijns, 2000). Moreover, there are many new adjuvants developed and are currently under clinical investigations (Table 2). These adjuvants can be classified based on their chemical nature, origin or physical properties (Cox and Coulter, 1997; Kwak and Longo, 1996). However, it has been observed that some compounds belonging to same class show divergent immunomodulating properties, for example, different saponins stimulate Th1 or/and Th2 pathways of immunity (Press et al., 2000). Thus, it is logical to classify adjuvants based on type (Th1/Th2) immune response modulated and then sub-classify based on their chemical structure and other properties (Marciani, 2003).

Adjuvants stimulate the immune response by different mechanisms depending upon their chemical nature and physical properties. Most common mechanisms of immune stimulation by adjuvants are as follows (Cox and Coulter, 1997; Marciani, 2003):

i. Depot generation: This is observed in the case of alum, emulsion based and particulate antigens. The antigens are released slowly over a longer period of time from the depot formed at the site of action and are presented to APCs (macrophages, DCs). Polymeric microparticles of size >10 μm forms depot at the site of injection and releases antigen for a longer duration (Eldridge et al., 1990).

ii. Immunomodulation: Adjuvants, depending upon their nature can upregulate the secretion of specific cytokines thereby activating specific components of adaptive innate and immune systems. These adjuvants direct either Th1 or Th2 pathways of $CD4^+$ T cells to provide cellular or humoral immune response, respectively. Aluminum salts predominantly produce Th2 type immune response while bacterial endotoxin or lipid adjuvants predominantly induce a Th1 type immune response.

iii. Antigen presentation: The adjuvants which preserve the conformational integrity of antigen until they are presented to immune effector cells improves the antibody response and increase the shelf life of antigens. Generally complex forming and amphipathic molecules fall under this class.

iv. Induction of cytotoxic T-lymphocyte (CTL) responses: The CTL responses are triggered only when antigens are processed inside cell cytosol. The viruses/live attenuated vaccines activate CTL responses while subunit vaccine antigens are processed outside cytosol and thus failed to generate CTL responses. When subunit/killed vaccine antigens are incorporated in o/w emulsions, they attract more DCs to uptake antigens and at the same time protect the antigen from proteolysis before reaching to lymphoid tissues. In lymphoid tissues, the antigens are presented to the T cells (including $CD8^+$ T cells) to stimulate CTL responses.

v. Targeting: The particulate adjuvants delivers antigens to immune effector cells via APCs mainly by protecting antigens from enzymatic degradation. A higher number of antigens presented to immune effector cells ensures the better efficacy of the vaccine antigens. Nano-/microparticles increase uptake of vaccine antigens by macrophages and DCs thereby generating stronger immune responses.

Thus, careful selection of the vaccine adjuvants should be made based on the type of vaccine antigens and desired the type of immune response to achieve maximum efficacy. Moreover, these adjuvants sometimes cause severe immune responses and, therefore, should be initially tested for their safety in human beings.

1.2 Nasal anatomy and physiology

1.2.1 Anatomy of nose

Exteriorly, the nose is an irregular pyramidal shaped part of the human face which plays a vital role in the process of inhalation. The external nose surrounds a pair of the nostril and one-third of the total nasal cavity. The entire nasal cavity is about 12-14 cm in length, around 5 cm in height with a total surface area of about 150-160 cm^2 and total volume is about 15-20 ml. The nasal cavity is divided vertically by the nasal septum into two approximately equal sized halves. The nasal septum begins anteriorly at the nares and extended posteriorly to the nasopharynx where the two halves join together. The septum is much thinner in the middle than at the perimeter and is generally bent towards one of the side (Gizurarson, 2012). The internal ostium (or nasal valve) is located approximately 1.5 cm from the nares and have a cross-sectional area of about 30 mm^2 on each side It is the narrowest portion of the entire airway (Figure 2). The nasal valve accounts for approximately 50% of the total resistance to respiratory airflow from the nostrils to the alveoli (Merkus and Verhoef, 1994; Mygind and Dahl, 1998). This high resistance to airflow, the relatively high linear velocity of the air stream, combined with an almost 90° angle of the flow passage at the ostium, and turbulences facilitate the impaction of the majority of particles carried in the inspired air stream in the anterior of the nasal cavity from where they are mainly removed by mucociliary clearance (Hinchcliffe and Illum, 1999).

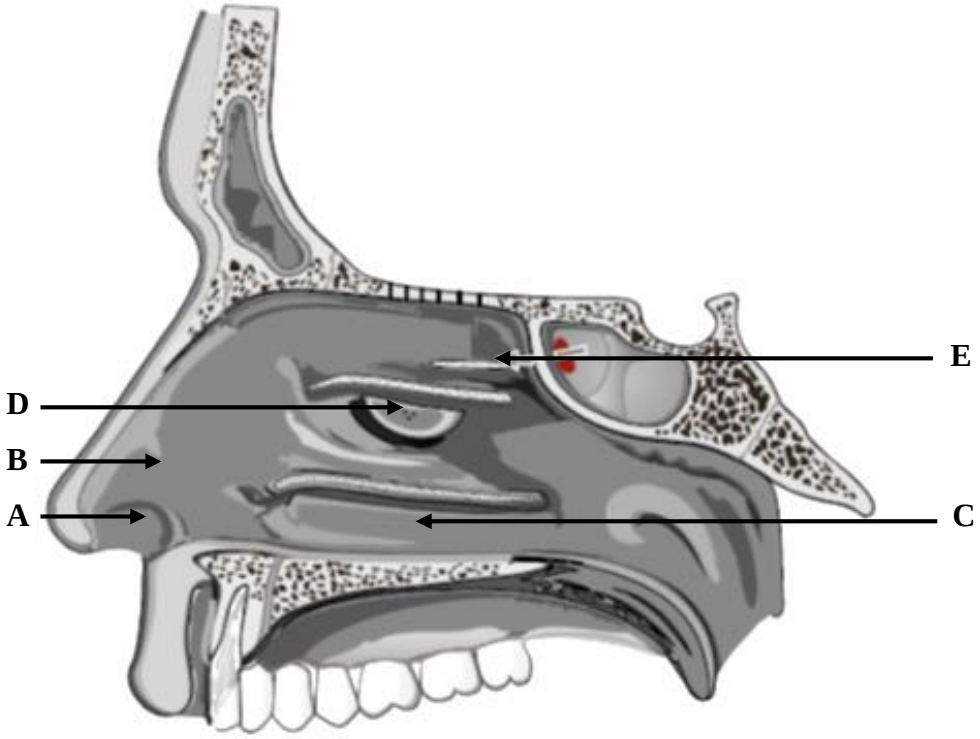

Figure 2 Schematic presentation of the sagittal section of the lateral wall of the nasal cavity. A: nasal vestibule, B: internal ostium, C: inferior concha, D: median concha, E: superior concha. (Image downloaded from http://www.slideshare.net/ on 11/05/2016)

The septal wall and the lateral wall further divides each half of the nasal cavity into inferior, middle and superior concha (turbinates). Bony scroll-like conchae (or turbinates) are attached to the lateral wall and project into the main part of the cavities (Figure 2). The presence of these conchae generates a turbulent air flow through the nasal passages which ensures a better contact between the mucosal surface and the inhaled air, additionally facilitating its humidification and temperature regulation (Gizurarson, 1990; Illum, 1996; Mygind and Dahl, 1998).

The passages present beneath and lateral to each of the concha are called the inferior, middle, and superior meatus. The inferior and middle meatus receive the openings of the nasolacrimal duct and the paranasal sinuses. The mucous membrane in a meatus will not be hit by an ordinary nasal spray (Mygind and Dahl, 1998).

1.2.2 Physiology of nose

The nasal cavity is divided into three regions based on the functions as:

i. The vestibular region, which occupies the anterior 10-20 cm^2 part and is posteriorly limited by the internal ostium. It is covered with a stratified squamous epithelium, which

is continuous with the facial skin. Short rigid hairs filter the larger particles from the incoming air stream.

ii. The respiratory region occupies the majority (about 130 cm^2) of the posterior nasal cavity and is important for the absorption of drugs into the systemic circulation. The epithelium consists of pseudostratified columnar epithelial cells.

iii. The olfactory region (10-20 cm^2) at the roof of the nasal cavities comprises of the small patch of columnar cells containing the smell receptors (Merkus and Verhoef, 1994).

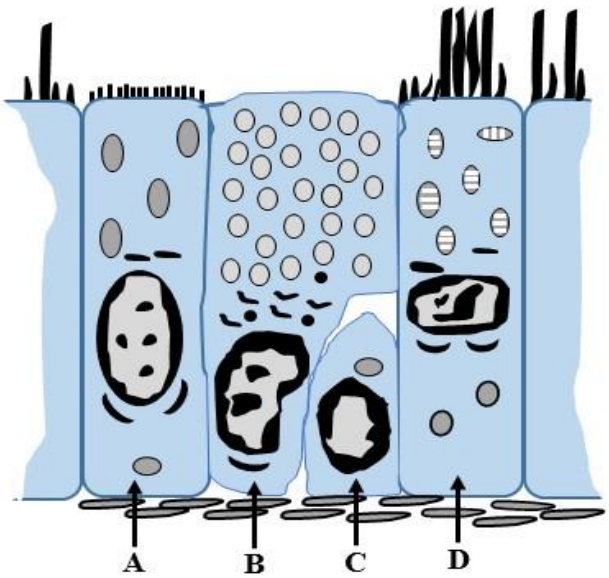

Figure 3 Epithelial cell types present in the nasal cavity. A) Non-ciliated columnar epithelial cells with numerous microvilli, B) Goblet cells with mucus granules, C) Basal cells, D) Ciliated columnar cells with mitochondria in the apical region.

The nasal/respiratory epithelium is approximately 100 μm in thickness and consists of four major types of cell as mentioned below: (Figure 3) (Merkus and Verhoef, 1994; Mygind and Dahl, 1998)

A. Non-ciliated columnar epithelial cells are connected to neighboring cells by tight junctions. The entire apical surface of these columnar cells is covered uniformly by about 300 microvilli (Ugwoke et al., 2005b). Microvilli are short, slender fingerlike cytoplasmic expansions which increase the surface area of the epithelial cells. The microvilli also prevent drying of the surface by retaining moisture essential for ciliary function.

B. Goblet cells are mucous secreting cells lining the respiratory epithelium. Their number is slightly larger in the posterior part than in the anterior part of the nasal cavity. The average number of goblet cells (4,000-7,000 cells/mm^2) are similar to the trachea and the bronchi (Tos, 1983; Ugwoke et al., 2005a). The goblet cells probably contribute less to the nasal

secretions as compared to the submucosal glands. The secretions from submucosal glands are under the control of parasympathetic system while mechanism behind secretions from the goblet cells is little known. The physical and chemical irritants present in the nasal microenvironment might be triggering secretions from the goblet cells (Mygind and Dahl, 1998).

C. Basal cells, which are ancestors of the other cell types are located on the basement membrane and are not connected to the airway lumen.

D. The ciliated columnar epithelial cells are covered with fingerlike protrusions (0.2-0.3 μm wide and 5 μm in length) called cilia and microvilli on the apical surface. Each ciliated cell is covered with about 100-300 cilia (Batchelor, 2014; Petruson et al., 1984). The cytoplasm of ciliated columnar cells contains numerous mitochondria in the apical part, which in an indication of active metabolism.

The anterior 1/3rd of the nasal cavity is covered with non-ciliated epithelial cells while ciliated cell layer starts just afterward the front edge of the inferior turbinate. The posterior part of the nasal cavity, as well as the paranasal sinuses, are densely covered with cilia. The baseline pH in the human nasal cavity is in the range of 5-6.5.

Submucosal glands, mucus, and mucociliary clearance

Lamina propria or submucosa is present below the respiratory epithelium and composed of a loose mesh of fibro-elastic tissue which is rich in blood vessels, nerves, and glands. These submucosal glands possess both serous and mucous secretory cells. The sections, also called as nasal secretions from these cells are directly released on the apical surface of the epithelium. Other minor contributors are goblet cells and plasma exudation, especially during inflammatory processes.

Mucus is a thin, clear, viscoelastic watery fluid which covers the entire nasal epithelial surface. A normal resting nose produces approximately 0.5 to 1 ml of mucus/cm^2 mucosa per day (Quraishi et al., 1998). The mucus is a complex mixture of many substances and composed of almost 95% of water, 2.5-3% mucus glycoproteins (mucin), 1% electrolytes, and 1% of other proteins such as albumin, immunoglobulins, lysozyme and lactoferrin, and <1% lipids (Ugwoke et al., 2005b). The mucus glycoproteins (mucin) consist of a protein core (20%) with oligosaccharide side chains (80%), cross-linked by disulfide and hydrogen bonds (Kaliner et al., 1986). These glycoproteins impart characteristic viscoelastic property to the mucus, which

essentially provide a protective coating to the nasal epithelium and helps in mucociliary clearance.

The mucus layer, approximately 5 μm in thickness, consists of two fluid layers: a viscous gel layer which floats on a less viscous sol layer. The cilia of the columnar cells move with regular, symmetric beats at a frequency of about 10 Hz in the lower sol phase (Duchateau et al., 1985). This beat frequency propels the gel layer backward with no effect on the relatively stationary sol layer (Sleigh et al., 1988). During the recovery stroke, the cilia move backward exclusively through the sol layer. Thus by this action, the particles entrapped in upper mucus layer are transported towards the nasopharynx from where the mucus is swallowed (Hua et al., 2010). This synchronized action of mucus layer and cilia is called mucociliary clearance. It is a vital nonspecific physiological first-line defense mechanism to protect the body against harmful inhaled materials. The velocity of mucus transport is approximately 5-8 mm/min (Smith et al., 2011) which results in the renewing of the nasal mucous layer every 10-20 min. The mucociliary clearance is responsible for the rapid clearance of nasally administered drugs from the nasal cavity to the nasopharynx and thus poor absorption of the drugs. Conversely, inhibition of the mucociliary clearance by drugs and drug delivery systems results in longer contact times of the nasal mucosa with inhaled bacteria, viruses, carcinogens etc.

Formulation of mucoadhesive drug delivery system can improve the absorption of the nasally administered drugs.

Vasculature and innervation

The lamina propria or submucosa is rich in blood vessels and has an extensive blood supply (about 40 ml/min/100 g) along with large, well-developed lymph drainage system, especially in the respiratory region of the nasal cavity (Bende et al., 1983; Hinchcliffe and Illum, 1999). The vasculature of nasal cavity differs in three ways from the vasculature of the tracheobronchial tree:

i. The nose contains venous sinusoids, which are localized in the inferior turbinates. The cavernous sinusoids are specialized vessels, actively involved in the heating and humidification of inhaled air (Mygind and Dahl, 1998).
ii. Arteriovenous anastomoses help the blood to bypass capillary bed in the nasal cavity. Their role is most probably associated with the temperature and water control. The arterio-venous anastomoses shunt at least 50% of the blood flow in the nose (Anggard, 1974).

iii. Nasal vasculature shows cyclic changes of congestion, giving rise to nasal cycle (Widdicombe, 1997). Enlargement of venous plexuses with blood leads to a swelling of the mucosa which can temporarily occlude the airway and make the tissue appear engorged. This occlusion of the airway occurs alternately between the two sides of the nasal cavity and thus, preventing the drying out of the mucous membrane (Hinchcliffe and Illum, 1999). The effect of the nasal cycle on the absorption drugs is still unclear. The total clearance of radiolabelled saline was not affected by the nasal patency, even though the initial clearance was higher in the more patent half of the nasal cavity (Washington et al., 2000).

The venous blood draining from the nose passes directly into the systemic circulation, thereby circumventing hepatic first pass elimination which is predominant in the gastrointestinal tract.

The lamina propria of the nasal mucosa also surrounds the nerves. Afferent nerve fibers run in the trigeminal nerve. Stimulation of the trigeminus in the nasal mucosa results in the sneezing reflex. There is a rich parasympathetic innervation of the glands. Nervous stimulation of the glandular choline receptors causes marked hypersecretion and is often part of the reflex arc. Nasal blood vessels are both sympathetically and parasympathetically innervated but are mainly controlled by sympathetic fibers (Mygind and Dahl, 1998).

1.2.3 Function of the nose

The average human breathing rate is about 12-24 times/min. Thus, a human being inhales approximately 10,000 liters of air of differing temperature and humidity every day. As the main entrance for inspired air, the nose has to perform the following functions (Jones, 2001):

i. **Olfaction:** Human nose can detect more than 10,000 different odors and discriminate between about 5,000 of them, thanks to the rich innervation. The olfactory epithelium at the roof of the nasal cavity has several million olfactory sensory neurons (Jones and Rog, 1998). The precise mechanism by which different smells are recognized and discriminated still remains unclear. Specific odorant-receptor interactions might be playing a crucial role in this function.
ii. **Sensation:** Free nerve endings in the nasal mucosa senses the signals of irritation or burning via the trigeminal nerve when stimulated by substances like chili, peppers or ammonia. These sensations can initiate the sneezing reflex, tears or nasal secretions thereby playing a protective role.

iii. **Immunology:** The nasal passage is associated with the immunologically active lymphatic tissue. Nasal secretions contain immunoglobulins and enzymes. Neutrophils and lymphocytes are also found in the nasal mucosa. Fokkens et al. (Fokkens et al., 1989) have identified antigen-presenting Langerhans cells in the epithelial surface as well as in lamina propria.

iv. **Clearing of inspired air:** Larger particles in the air are filtered out by the stiff hairs in the nasal vestibular region. Approximately 90° angles in the nasal air passage at the internal ostium and posteriorly prior to the nasopharynx lead to impaction of the majority of airborne particles. 80% of the particles larger than 12.5 μm are filtered from the air before it reaches the nasopharynx (Jones, 2001).

v. **Heating and humidification of inspired air:** The highly vascularized mucosa of nasal concha/turbinates warm the inhaled air to approximately 34-36°C. Secretions of the goblet cells and submucosal glands as well as tear fluid reaching the nose via the nasolacrimal duct lead to a saturation of inhaled air with water vapor, reaching a relative humidity of 80-90%.

vi. **Resonance organ and isolation:** The air-filled nasal cavity and the sinuses (sinus maxillaries, sinus frontalis, sinus sphenoidales, sinus ethmoidales) influence the tone of the voice and act as thermal isolators (Jones, 2001).

Thorough understanding of nasal anatomy and physiology helps in the development of successful nasal formulations. It is very important that nasally administered drugs and drug delivery systems/their components should not interfere with any of these physiological functions of the nose.

1.3 Mucoadhesion

In 1986, Longer and Robinson coined the term “bioadhesion” for the “attachment of a synthetic or natural macromolecule to mucus and/or an epithelial surface/membrane” (Longer and Robinson, 1986). In general, the adherence of a polymeric material to biological surfaces is termed as “bioadhesion” while their adherence to mucosal surfaces is termed as “mucoadhesion”.

The exact mechanisms of polymer adhesion to mucosal/biological surfaces are not yet completely understood. However, several theories have been put forward to explain the mechanism behind mucoadhesion of polymers/macromolecules. At the beginning, the wetting

of the mucoadhesive polymer leads to proper swelling which provides a larger surface area to strongly interact with the mucosal surface. Later on, the mucoadhesive polymers penetrate into the mucosal tissue crevices due to interactions between the mucoadhesive polymer chains and components of the mucus. Consequently, low chemical bonds become operational to further strengthen the interaction (Jimenez-Castellanos et al., 1993; Ugwoke et al., 2005b).

Based on the above-mentioned mechanisms, six theories have been suggested to play a major role in bioadhesion, thoroughly explained below (Khutoryanskiy, 2011; Ponchel et al., 1987; Salamat-Miller et al., 2005; Sosnik et al., 2014):

i. Adsorption theory: States that upon initial contact between the mucus and mucoadhesive polymers, chemical bonds of the covalent and non-covalent (electrostatic and van der Waals forces, hydrogen and hydrophobic bonds) types are formed. Although the individual forces are weak, the high number of interaction sites can produce intense adhesive strength. This is the most widely accepted theory of mucoadhesion/bioadhesion.

ii. Diffusion theory: It proposes that interpenetration and entanglement between mucoadhesive polymer chains and mucus glycoproteins produce semi-permanent adhesive bonds. The bond strength increases with the degree of the polymer chain penetration into the mucus layer. Penetration and entanglement of mucoadhesive polymers into the mucus network dependents on the polymer chain flexibility, adequate contact time, chemical structure, concentration gradients and the diffusion coefficients. Cross-linking of either component deters the interpenetration but small chains and chain ends can still entangle.

iii. Electronic theory: It is based on the assumption that the electrostatic attraction between negatively charged mucin and positively charged materials is responsible for the adhesion. When these two surfaces come in contact, the electron transfer leads to the formation of the electric double layer at the interface.

iv. Fracture theory: It relates adhesion to the forces required for interfacial detachment of two previously joint surfaces. When determining fracture properties of an adhesive union from separation experiments, failure of the adhesive bond must be assumed to occur at the bioadhesive interface.

v. Mechanical theory: According to this theory, adhesion depends on the roughness of two different interacting surfaces as well as the area available for interaction.

vi. Wetting theory: It assumes that the adhesion of a mucoadhesive polymer, when present in liquid form, depends on its ability to spread over the mucus layer. It uses interfacial tension to predict spreading and in turn adhesion.

Based on this concept, bioadhesive/mucoadhesive drug delivery systems have been extensively investigated for various mucosal routes of administration including the nasal cavity. The drug absorption and thus bioavailability of the drugs/proteins can be improved by extending the residence time of the delivery system on the mucosa (Illum and Fisher, 1997). In this context, the detailed study of mucoadhesive polymers is of prime importance.

Different techniques/methods used for the measurement of mucoadhesive potentials of polymers or drug carriers prepared from mucoadhesive polymers are presented in Table 3.

Table 3 Summary of different methods used to evaluate mucoadhesive potential. Table adapted and modified from (das Neves et al., 2011; Sosnik et al., 2014) with permissions.

Methods	**Mechanism**	**Real-time Measurement**	***In vivo* relevance**	**Feasibility**	**Cost**
Indirect methods					
Mucin particle method	Low	No	Low	High	Low
Micro-gravimetric methods	Medium	Yes	Low	Medium	Medium
Atomic force microscopy	High	Yes	Low	Low	High
Optical techniques	Medium	Yes	Low/medium	Medium	High
Diffusion/particle tracking methods	High	Yes	Medium	High	Medium
Direct methods					
Cytoadhesion methods	Medium	Optional	Medium	Medium	Medium
Ex vivo methods	Low	Optional	Medium	Medium	Medium
In vivo administration/*ex vivo* analysis	Low	No	High	Medium	Medium
In vivo imaging	Low	Yes	High	Low	High

1.3.1 Mucoadhesive polymers

The mucoadhesive polymers used in mucosal delivery can be broadly classified into natural polymers, synthetic polymers, and semi-synthetic polymers.

1. Natural polymers

Natural polymers are widely used in the development of drug delivery system due to their superior biocompatibility, ease of availability, and low cost among other benefits. Commonly used natural mucoadhesive polymers include alginate, chitosan and its derivatives, guar gum, pectin, hyaluronic acid, xanthan gum, gluco- and galactomannan, carrageenan and gelatin (Sosnik et al., 2014). Among these natural polymers, alginates and chitosan and its derivatives are of prime importance for nasal delivery of vaccines and are discussed in detail below:

Alginates:

Alginates (ALG) are a group of natural polymers mainly extracted from brown algae such as *Laminaria hyperborea*, *Ascophyllum nodosum* and *Macrocystis pyrifera* for commercial use (Draget et al., 2005; Sosnik et al., 2014). These are unbranched polyanionic polysaccharide consisting of β-d-mannuronic acid (M) and α-l-guluronic acid (G) linked by1→4 linkages and arranged in MMMMM and GGGGG homo-sequences inter-dispersed with MGMGMG hetero-sequences (Goh et al., 2012; Haug et al., 1974; Penman and Sanderson, 1972). There are more than 200 types of ALG currently available in the market which differ in molecular weight (32-400 kg/mol), molecular arrangements and different G/M composition (Tønnesen and Karlsen, 2002). Moreover, in regulatory point of view, the US FDA has enlisted ALG under "Generally Recognized as Safe" (GRAS) category that applies to substances that are accepted as safe for alimentary use by qualified experts (Chang and Chang, 2007). ALG is widely used in the production of wound dressings due to its mucoadhesive, non-irritant properties as well as excellent biocompatibility (Boateng et al., 2008). Moreover, ALG has been used in cell encapsulation and immunoisolation due to its gelation capacity (de Vos et al., 2006; Rowley et al., 1999), as well as for the encapsulation and sustained release of a broad spectrum of drugs (Goh et al., 2012; Penman and Sanderson, 1972). ALG is also commonly used in different pharmaceutical formulations as thickening, stabilizing and gel forming agent, especially for oral administration. Concurrently, the use of ALG in depot forming drug delivery systems is also growing (Butoescu et al., 2009).

Chitosan and its derivatives

Chitosan is a natural cationic polymer, derived from chitin. It is the second most abundant polymer in the world, consisting of repeating units of N-acetylglucosamine and D-glucosamine, with pKa of 6.5. Chitin, a water insoluble precursor of chitosan is extracted from shrimps and other crustacean shells and converted to chitosan by deacetylation with sodium hydroxide (Muzzarelli and Muzzarelli, 2005). The degree of deacetylation varies depending on reaction conditions, giving rise to different grades of chitosan with differences in properties. Its biopharmaceutically relevant characteristics include good blood, cell biocompatibility and biodegradability (Kean and Thanou, 2010; Richardson et al., 1999). In general, commercial grade chitosan is composed of 80% β-D-glucosamine and 20% N-acetyl-β-D-glucosamine units (Sandford and Steinnes, 1991). Chitosan has been widely used in the areas of food, cosmetics, biomedical and pharmaceutical applications, (Rinaudo, 2006), due to its excellent biocompatibility and other advantageous properties.

Chitosan is considered as fundamental mucoadhesive polymer due to its ability to establish ionic, hydrogen and hydrophobic bonds with the negatively charged mucin (Sogias et al., 2008). The mucoadhesive potential of chitosan has already been studied for a broad variety of administration routes such as oral (Chen et al., 2013; Thanou et al., 2001b), ocular (de la Fuente et al., 2010), nasal (Illum et al., 2001), inhalation (Andrade et al., 2011) and topical (Ueno et al., 2001) with different categories of therapeutics. In addition, chitosan has been chemically modified to fine tune its properties toward the encapsulation and delivery of different drugs, genes, and proteins (Andrade et al., 2011). Furthermore, modifications in the chemical structure of chitosan can improve the mucoadhesive potential thereby increasing the interactions with components of the mucus. Incorporation of thiol (-SH) group in the backbone of chitosan is one of the commonly used strategies (Leitner et al., 2003); the process is known as thiolation. In an attempt, the mucoadhesive potential of thioglycolic acid/glycol chitosan NPs was compared to that of non-thiolated counterparts when administered intratracheally in rats (Makhlof et al., 2010). Chitosan also enhances the transport of drugs across the epithelial membrane by transiently disrupting tight junctions between cells (Thanou et al., 2001a). The chitosan also showed immune modulation potential when antigens were encapsulated or adsorbed on chitosan nano/micro-particles and tested on different laboratory animals (Bacon et al., 2000; Boonyo et al., 2007; Gogev et al., 2004; Jabbal-Gill et al., 1998; Westerink et al., 2001).

However, the thiolated derivatives of chitosan also found to be associated with toxicity, limiting their use (Guggi et al., 2004). Moreover, the stronger mucoadhesive potential of chitosan and its derivatives could also limit the penetration of chitosan nanocarriers due to stronger interactions with mucin components.

2. Semi-synthetic polymers

Semi-synthetic polymers were introduced by fine tuning desired properties of natural polymers. Natural polymers are subjected to chemical modifications to obtain semi-synthetic derivatives. In the context of pharmaceutical products, cellulose derivatives are most commonly used semi-synthetic polymers. Cellulose is the most abundantly available polysaccharide biopolymer in nature, composed of a linear chain of β (1→4) linked D-glucose units. In addition to its insolubility in water and most of the organic solvents, various other functional and technological limitations necessitated the development of different semi-synthetic cellulose derivatives (ether and ester) (Kamel et al., 2008). Most commonly used cellulose ethers include

methylcellulose (MC), ethylcellulose (EC), hydroxyethyl cellulose (HEC), hydroxypropyl cellulose (HPC), hydroxypropylmethylcellulose (HPMC), and carboxymethylcellulose (CMC) salts- calcium (CaCMC) or sodium (NaCMC); while for esters, cellulose acetate and cellulose acetate phthalate are the most commonly used pharmaceutical excipients (Dahl et al., 2009; Sosnik et al., 2014). Most of these cellulose derivatives are considered as biocompatible and non-irritating and thus included in GRAS list.

Among cellulose derivatives, HEC presents considerable mucoadhesive potential at intestinal pH 6.8 but usually lower than that of HPC and NaCMC (Grabovac et al., 2005). Thiolation of HEC with thiourea and HEC-cysteamine conjugation further improved its mucoadhesive potential (Rahmat et al., 2011; Sarti et al., 2010). HPC and HPMC possess high mucoadhesive potential in the solid state but it significantly reduced when used in a liquid state when measured by rheological methods (Madsen et al., 1998). Another polymer, NaCMC has been reported to present only mild mucoadhesive properties when compared to other polymers such as HPMC, polycarbophil, Carbopol® 934, and NaCMC in the solid state (Sosnik et al., 2014). However, thiolation of NaCMC (NaCMC-cysteine) was shown improvement in mucoadhesive potential. Methylcellulose (MC) and ethylcellulose (EC) shows mild to poor mucoadhesive potential (Tachaprutinun et al., 2013).

3. Synthetic polymers

Synthetic polymers used in mucosal delivery includes poly(ethylene glycol) (PEG) and poly (ethylene oxide) (PEO) and their derivatives, poly(acrylic acid) (PAA) and poly(methacrylic acid) (PMA) derivatives, poly(vinyl pyrrolidone) (PVP), poly(vinyl amine) (PVA) and boronate containing polymers (BCC) (Sosnik et al., 2014). Lack of amine and/or carboxylic functional side groups makes the mucoadhesive potential of PEG/PEO polymers debatable. However, the faster interpenetration of PEG polymers through mucus layer might play a role in the improved mucosal delivery of drugs. Several attempts were made to improve the mucoadhesive potential of PEG by its surface modification with PAA polymers (Bromberg et al., 2004; Cleary et al., 2004). The block copolymers of PEO-like poly(ethylene oxide)-co-poly(propylene oxide) (PEO–PPO) were also explored extensively with some modifications, due to their environment responsive properties (Chiappetta and Sosnik, 2007). Research groups of Cohn *et al.* and Bromberg *et al.* have performed several chemical modifications of PEO-PPO block polymers and PAA polymers to improve their mucoadhesiveness (Bromberg, 1998; Bromberg et al., 2007; Bromberg et al., 2004; Cohn et al., 2006; Cohn and Sosnik, 2003; Cohn

et al., 2003; Cohn et al., 2007; Sosnik and Cohn, 2005). In addition to chemical modifications in structure, polymer blends are a relatively simple strategy to achieve mucoadhesion as well as desired release of drug/antigen. In such an attempt, Bilensoy *et al.* formulated Pluronic® F127 (20%) vaginal gel with low concentrations of mucoadhesive polymers (e.g., poly(acrylate)s and HPMC) for the localized release of clotrimazole (Bilensoy et al., 2006). Moreover, Majithiya *et al.* used a similar composition for the nasal delivery of sumatriptan (Majithiya et al., 2006). In another study, tetanus toxoid encapsulated poly(lactic acid) (PLA) NPs were coated with PEG to improve their penetration through the nasal mucosa (Vila et al., 2002).

Another class of synthetic mucoadhesive polymers, PAA, also called as carbomer is a high molecular weight polymer of acrylic acid used as a viscosity modifier in semi-solids. PAA exhibits very high adhesive bond strength, owing to the presence of numerous side carboxylic acid groups. To improve other properties of PAA, copolymers with PEG has been developed and studied by some research groups (Serra et al., 2006). Following this rationale, PAA–PEG NPs have been developed and reported to improve the trans-corneal diffusion of pilocarpine (Vasi et al., 2014). In a similar approach, cysteine/PAA microparticles increased the permeation of vitamin B12 across the intestinal mucosa (Sarti et al., 2012).

Poly(methacrylates) (PMA) are hydrophobic synthetic polymers composed of primeval and modified methacrylic acid monomers (PMMA). They show a good degree of biocompatibility with very limited biodegradability. Eudragit® is one of the most widely used copolymers derived from PMA polymers and have been approved by regulatory agencies for use in medical devices and non-parenteral pharmaceutical products (Eidi et al., 2010). In context to vaccine delivery, PMMA NPs for the nasal delivery of bovine para-influenza type 3 virus (BPI-3) proteins have been reported (Shephard et al., 2003). Moreover, amphiphilic PMAA-grafted-PEG NPs were prepared by dispersion polymerization and assessed for the oral administration of calcitonin (Torres-Lugo and Peppas, 2002). Similar NPs were prepared by emulsion polymerization for DNA vaccine applications, which induced significant antigen-specific humoral and cellular responses and greatly increased Th1-type T cell responses, and cytotoxic T cells against HIV-1 (Castaldello et al., 2006).

Poly(vinyl pyrrolidone) (PVP), also commonly called as povidone, is a non-ionic synthetic linear polymer comprising of 1-vinyl-2-pyrrolidone groups. It is soluble in various aqueous and organic solvents, chemically inert and principally non-toxic for non-parenteral administration (Folttmann and Quadir, 2008). It is widely used in pharmaceutical industry as an excipient for solid and liquid dosage forms. Although it is considered as mucoadhesive

polymer and being explored for mucosal applications, it possesses mild mucoadhesive potential. The chemical characteristics and molecular weight of PVP may have an impact on its mucoadhesive property (Sosnik et al., 2014).

Another group of the synthetic polymer, poly(vinyl amine) or poly(amino ethylene) is a hydrophilic linear cationic polymer, commonly used to coat nanoparticles (Sakuma et al., 1999) or drug-polymer complex (Sakuma et al., 2007) to improve mucoadhesion. Boronate-containing copolymers (BCCs) displayed lectin-like receptor (LLR) binding capacity and thus gathered attention as a potential synthetic mucoadhesive polymer. Due to their specific polysaccharide binding capacity, soluble BCCs are employed in cell separation techniques (Ivanov et al., 2009; Ivanov et al., 2006) and for targeted delivery of drugs to specific tumor cells (Chen et al., 2012; Ellis et al., 2012; Li et al., 2012).

1.4 Nasal route for vaccine delivery

Most of the vaccines are administered via a parenteral route which causes pain, local irritation reactions in many individuals and thus making it patient incompliant. The parenteral route administration requires the sterile formulation and also an expert person for its administration, which, in turn, increases the cost.

From the past few years, the emphasis is being given on formulating the vaccines for the oral or nasal route by the scientific community. This strategy not only improves the patient compliance but also reduces local side effects. The oral polio vaccine (OPV), nasal Flu Mist® and Nasovac-S™ are only vaccines available in the market for the prevention of polio, influenza virus, and swine-flu respectively. Apart from these marketed vaccines, many vaccines were tested for human efficacy by the intranasal route (Table 4). These includes the vaccines targeted against adenovirus-vectored influenza (Van Kampen et al., 2005), proteosome-influenza (Treanor et al., 2006), influenza A (Treanor et al., 1992), influenza B (Obrosovaserova et al., 1990), meningococcal outer membrane vesicle (Oftung et al., 1999), and a combination respiratory syncytial virus (RSV) and parainfluenza 3 virus (PIV3) live, attenuated intranasal vaccine (Belshe et al., 2004).

Table 4 Development in nasal vaccine products and their current status. Table adapted and modified from (Jabbal-Gill, 2010) with permissions. (Updated from https://clinicaltrials.gov/ct2/home)

Product	Indication	Development status	Company
DeltaFLU	Pandemic influenza	Phase II	Green Hills Biotechnology AG
FluGEM, Mimopath®-based influenza vaccine	Influenza	Phase I	Mucosis
FluINsure™	Influenza	Phase II (discontinued)	ID Biomedical Corporation
FluMist®	Seasonal influenza	Marketed, approved in June 2003	MedImmune (now Astra-Zeneca)
FluVac	Seasonal influenza	Phase II	Green Hills Biotechnology AG
HIV and tuberculosis vaccines	HIV, tuberculosis prophylaxis	Preclinical	Polymun Scientific Immunobiologische Forschung GmbH
Invaplex 50	Against Shigella flexneri 2a 2457T strain	Phase II	The United States Department of Defense
Liposomal influenza vaccine	Influenza	Phase I completed	Hadassah Medical Organization
MEDI 534	Parainfluenza virus type 3/respiratory syncytial virus	Phase II (discontinued)	MedImmune (now Astra-Zeneca)
MEDI 559	Respiratory Syncytial Virus	Phase I/IIa	MedImmune (now Astra-Zeneca)
MEDI 560	Parainfluenza virus type 3	Phase I/IIa	MedImmune (now Astra-Zeneca)
NB-1008 (Fluzone®)	Influenza	Phase I	NanoBio Corp.
NanoVax®-Panflu	Influenza	Preclinical	NanoBio Corp.
Nasalflu®	Influenza virus infections	Withdrawn	Berna Biotech
NASOVAC-S™	H1N1 swine flu	Marketed, approved in July 2010	Serum Institute of India, Licensed from BioDiem Ltd.
NasoVAX based on RespirVec™ platform	Influenza	Phase I completed	Vaxin Inc. (name changed to Altimmune Inc.)
Norwalk VLP	Norovirus	Phase I-II completed	LigoCyte (now Takeda Pharmaceuticals Ltd.)
Protesomal Vaccine	Influenza	Phase II completed	hVIVO
QLAIV	HIV infection	Phase II	University of Colorado, Denver
rFla-MBP	Diarrhea	Phase I completed	U.S. Army Medical Research and Materiel Command
SeV2 0401 and others	Various including HIV, tuberculosis, influenza, malaria, Alzheimer's, Parkinson's, cancers	Preclinical/No development reported	DNAVEC Corporation (now ID Pharma Co., Ltd.)
Vacc-4x	HIV infection	Phase I/II	Oslo University Hospital

To formulate effective vaccine formulation for nasal delivery, it is important to first understand the nasal immunology thoroughly. The nasal immunology is explained comprehensively in the following section.

1.4.1 Nasal immunology

Since most of the pathogens get entry into the human body through tissues lined by a mucosal membrane, it is important to generate a 'first line of defense' by establishing pathogen-specific immunity at the site of entry (Partidos, 2000).

The epithelial layer of mucosal surfaces acts as a barrier and separates it from the external environment. It provides protection to mucosal layer by non-specific defense mechanisms like mucus secretion, mucociliary clearance, and enzymatic degradation. While mucosa-associated lymphoid tissue (MALT) which are scattered along mucosal linings, provides specific protection against invading micro-organisms. Depending upon their location at different anatomical sites in the body, MALT differs slightly in structural and functional characteristics. Thus, depending on the site they are termed as nasal-associated lymphoid tissue (NALT), bronchus-associated lymphoid tissue (BALT), gut-associated lymphoid tissue (GALT), lacrimal duct-associated (LDALT), larynx-associated lymphoid tissue (LALT) and salivary duct-associated lymphoid tissue (DALT) (Cesta, 2006).

As described above, NALT is an organized lymphoid tissue located at the base of the nasal mucosal surface (Kuper et al., 1992). During evolution, the NALT has adapted itself to perform several functions like protection of nasal epithelium from invading pathogens, acts as barrier for absorption of macromolecules, antigen sampling, production of secretory IgA (sIgA) antibodies, distribution of effector T- and B-cells to local and distant mucosal sites for further protection (Partidos, 2000). To perform the defense mechanism effectively, the NALT contains a variety of immunocompetent cells, including B-lymphocytes, T-lymphocytes ($CD4^+$ and $CD8^+$), phagocytic antigen presenting cells (APC) such as macrophages and various subsets of dendritic cells (DCs) (Bienenstock and McDermott, 2005).

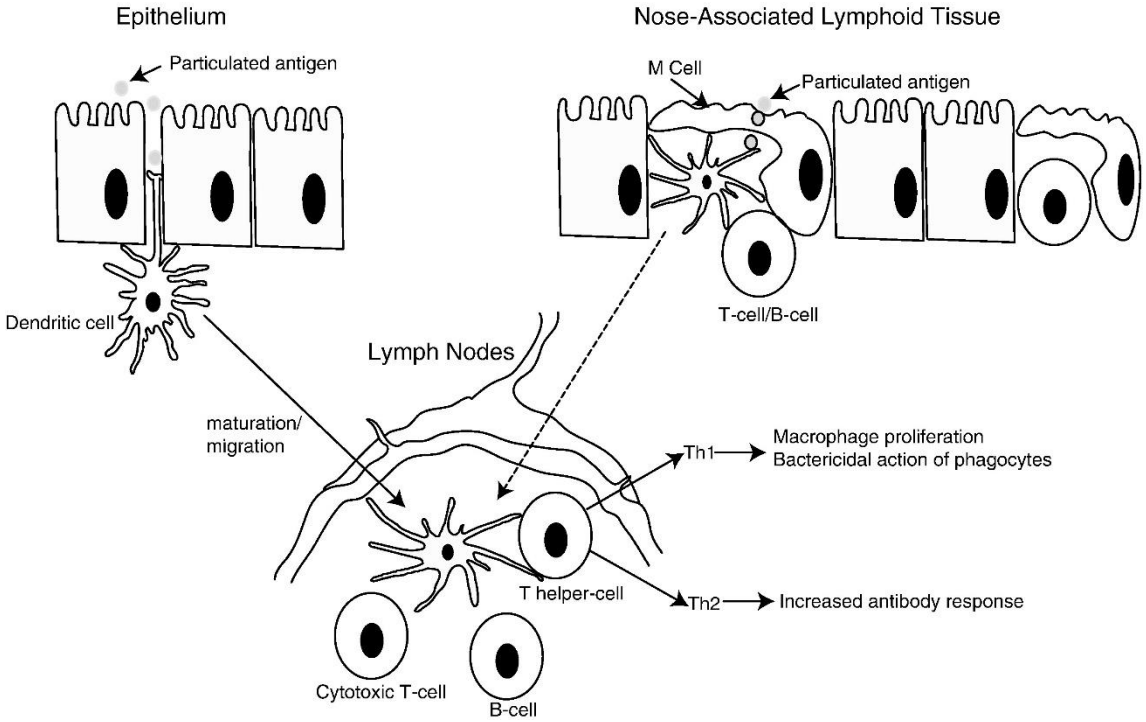

Figure 4 Schematic presentation of pathways involved in local and systemic mucosal immune response triggered by vaccine antigens. (Csaba et al., 2009) (Reproduced with permission from Elsevier Limited)

A schematic presentation of the mechanism involved behind immune response generated by nasal mucosa and NALT is presented in Figure 4. The small soluble antigens and particulate antigens can cross the nasal epithelium through loosely arranged follicle associated epithelium or taken up by microfold cells (M cells) present in NALT. The soluble antigens generally enter through follicular associated epithelium while particulate antigens (also nanoparticles) are taken up by M cells. After the entry of antigens, they are captured by the patrolling dendritic cells which then migrates to the draining lymph nodes. During migration, the dendritic cells matures and becomes antigen presenting cells (APCs) which process the antigens and present them to $CD4^+$ T cells via class II major histocompatibility complex (MHC II) or to the $CD8^+$ T cells via MHC I depending upon the nature of antigens (viruses, intracellular pathogens, extracellular pathogens). The $CD4^+$ T cells are also called T helper cells while $CD8^+$ T cells are called cytotoxic T lymphocytes (CTL).

The $CD4^+$ T helper cells upon activation either produce Th1 or Th2 or mixed Th1-Th2 type of immune response depending upon nature of the antigen, tissue microenvironment and cytokine milieu (Partidos, 2000). The Th1 phenotype of effector $CD4^+$ T cell activates after infection with viruses or intracellular bacteria and produces specific cytokines (IL-2, IFN-γ) while Th2 phenotype is activated by exogenous antigens (e.g. parasites) and produces IL-4, IL-5, IL-6 and IL-10 cytokines (Mosmann and Coffman, 1989). The Th1 phenotype promotes the

developments of cellular immunity (proliferation of macrophages, microbicidal activity) while Th2 phenotype promotes the activation of humoral immune response by activating B cells to secrete antigen specific antibodies (IgG, sIgA). The $CD8^+$ T cells or CTLs limit the spread of infection by recognizing and killing infected cells through natural killer cells as well as secreting specific antiviral cytokines (Siegrist, 2008).

Following activation of B cells by Th2 phenotype of effector $CD4^+$ T cells, immunoglobulin A (IgA) are secreted at the mucosal surface. The synthesis and secretion of IgA by mucosal plasma cells is mediated by precursors originated from organized lymphoepithelial structures. These precursors mature in the regional lymph nodes and later enter the systemic circulation via the thoracic duct. The precursors then enter and stay in the lamina propria of distant mucosal sites (e.g. intestines, respiratory tract, genital tract, etc.) where they can further differentiate to produce region-specific IgA. As a result, secretory IgA (sIgA) antibodies can appear in parallel at different mucosal sites followed by pathogen invasion as a part of a common mucosal immune system (Mestecky et al., 1997).

In conclusion, cells of the NALT can regulate both cellular and humoral immune responses locally and also at distant sites, providing extra protection against invading pathogens. This characteristic feature of NALT makes the nasal route particularly attractive for the administration of vaccines (Csaba et al., 2009).

1.4.2 Advantages and disadvantages of nasal route

The nasal route is recently explored as potential route for delivery of vaccine since it has advantages like (Charalambos D, 2000; Csaba et al., 2009):

i. Better patient compliance due to the ease of administration and needle-free drug application when compared to parenteral administration (Pontiroli et al., 1989).
ii. Moderately permeable epithelium ensures better penetration of lipophilic and low molecular weight drugs through the nasal mucosa. For example, the absolute nasal bioavailability of fentanyl is about 80% (Striebel et al., 1993).
iii. Less enzymatic activity in nasal cavity as compared to the gastrointestinal tract (GIT) protects the drugs from degradation.
iv. The lower dose required as compared to oral route due to circumvention of hepatic first pass metabolism.
v. Especially for vaccination, high availability of immune-reactive sites ensures generation of a better immune response.

vi. Nasal epithelium is thin, porous and highly vascularized which helps in rapid onset of action of drugs administered through this route.

vii. Large absorption area available due to the presence of numerous microvilli governs the rapid absorption of drugs. For example, the t_{max} of fentanyl after nasal administration was $\leq$ 7 min comparable which was comparable to intravenous administration (Striebel et al., 1993).

viii. It is a promising route for direct delivery of drugs to the central nervous system via the olfactory region and bypassing the blood-brain-barrier (Dahlin et al., 2001; Dufes et al., 2003; Illum, 2000, 2015)

Despite these advantages, the nasal route of administration suffers from a few disadvantages like (Csaba et al., 2009; Pires et al., 2009; Ugwoke et al., 2005b):

i. Degradation of proteins remaining for longer duration in nasal cavity by mucosal enzymes is a less considered but contributing factor for low nasal bioavailability of therapeutic proteins.

ii. The limited volume of the nasal cavity restricts the total amount of the formulation to be administered. Administration of large volume results in a disturbance in the normal functioning of the nose.

iii. Nasal mucociliary clearance (MCC) limits the absorption of therapeutic proteins. The proteins which are not absorbed within first 15-20 min. are cleared from nasal cavity by MCC.

iv. The high sensitivity of nasal mucosa towards irritation reactions limits the use of a variety of formulation excipients.

It is, therefore, necessary to come up with some novel delivery systems that effectively surpass the disadvantages of the nasal route while providing an easy way for vaccination.

1.5 Nanoparticles for vaccine delivery

Nanoparticles for the pharmaceutical purposes are defined as solid, colloidal, submicron-sized drug carriers (ranging in size from 1 to 1000 nm) that may or may not be biodegradable (Couvreur et al., 1995; Pinto Reis et al., 2006). The nanoparticles can be broadly divided into two categories: nanospheres and nanocapsules. Nanospheres are matrix type system in which drug molecules are either encapsulated within the matrix or may be adsorbed on the particle surface. Nanocapsules are vesicular structures in which the drug is either confined to a cavity

consisting of an inner liquid core or dispersed in the surrounded polymeric membrane, depending on the nature of drug (Pinto Reis et al., 2006).

The nanocarriers approach is currently focused on the delivery of drugs or active agents to the site of action in an appropriate concentration. Entrapment of drug within nanocarriers may radically transform their bioavailability and tissue distribution profiles. These changes can augment the site-specific delivery with reduced side effects. Therefore, nanoparticles can improve the therapeutic efficiency and are excellent carriers for biological molecules, including enzymes, recombinant proteins, and nucleic acid. The nanocarriers also protect the drug molecules from the enzymatic or chemical degradation. The controlled release of drug from the formulation is one of the most important advantages of the nanocarrier system.

In the context of the nasal route the nanocarriers delivers the antigen to the immune system and also provide control release of antigens over a prolonged duration of time. These nanocarriers can also modulate the immune response and thus enhances the potency of vaccines. The different nanopharmaceuticals which are currently in the development phase for clinical uses (Table 5) includes micelle, liposomes, solid lipid nanoparticles, polymeric nanoparticles, PEGylated nanostructures, cyclodextrin, dendrimers, carbon nanotubes, metallic nanoparticles etc. (Jain et al., 2011a; Jain et al., 2011b; Marcato and Duran, 2008).

Table 5 Current status of the nanoparticulate system developed for delivery of vaccine antigens. Table adapted and modified from (Cordeiro et al., 2015) with permissions and updated information from https://clinicaltrials.gov/ct2/home.

Name/Type of delivery system	Antigen	Development status	Route of administration
MF59™ (squalene oil-in-water nanoemulsion stabilized with Tween® 80 and Span® 85)	Influenza (H5N1 inactivated virus)	Not disclosed	IM
	Influenza (H7N9 inactivated virus)	Phase I (ongoing)	IM/IN
		Phase II (completed)	IM
		Phase II (ongoing)	IM
	Influenza (killed virus, trivalent subunit vaccine)	Phase I (completed)	IM
		Phase II (completed)	IM
	RSV (RSV F protein)	Phase I (ongoing)	IM
	Cytomegalovirus (CMV) (group B)	Phase II (completed)	IM
AS03™ (oil-in-water nanoemulsion containing squalene, DL-α-tocopherol, and Tween® 80)	Influenza (H5N1 inactivated virus)	Phase I/II (completed)	IM
		Phase I (completed)	IM
		Phase II (completed)	IM
MF59™ and AS03™	Influenza (H7N9 inactivated virus)	Phase II (completed)	IM

AS01B (Liposomes containing 3-O-desacyl-4′-monophosphoryl lipid A (MPL), and QS-21 saponin	Malaria (FMP012; FMP2.1; RTS, S proteins)	Phase I (ongoing)	IM
		Phase I/II (completed)	IM
		Phase I/II (completed)	IM
		Phase II/III (ongoing)	IM
AS01E and AS03B	Dengue (inactivated virus)	Phase I (ongoing)	IM
		Phase I (ongoing)	IM
AS02 (An o/w emulsion containing QS21 and 3 De-O-acylated monophosphoryl lipid A (3D-MPL))	Malaria (FMP1; RTS,S proteins)	Phase I/IIa (completed)	IM
ISCOM (Immune stimulating complex, composed of cholesterol, lipid, immunogen, and saponins)	HSV (GEN-003 protein)	Phase II (completed)	IM
		Phase II (ongoing)	IM
	Malaria (viral vector with ME-TRAP protein)	Phase I (completed)	IM
	Influenza (H7N9 VLP)	Phase I/II (completed)	IM
ISCOMATRIX™ (Contains immunostimulatory component, cholesterol, and phospholipids)	Cancer (tumor cell lysates)	Phase I/II (ongoing)	IM
ViscoGel® (Chitosan based hydrogel)	Influenza (Act-HIB® vaccine)	Phase I/II (completed)	IM
Virosomes (unilamellar phospholipid membrane vesicles containing virus components)	Hepatitis A (inactivated virus)	Phase II (completed)	IM
	Vulvovaginal candidiasis (RVVC)	Phase I (completed)	IM/intravaginal
PLGA microspheres	Cancer (HER-2/Neu peptide)	Phase I (completed)	ID/SC
Liposomes	Influenza	Phase I/II (completed)	IN
	Ovarian/Breast/Prostatic neoplasms	Phase I (completed)	SC
	Tuberculosis	Phase I (completed)	IM
	Non-Small Cell Lung Cancer	Phase III (completed)	SC
	Lymphoma	Phase I (completed)	Intranodal/SC
	Melanoma	Phase I (completed)	IV infusion

Abbreviations: IM= intramuscular, IN= intranasal, ID= intradermal, SC= subcutaneous

Among these nanocarriers, the polymeric nanoparticles, due to their higher mucoadhesive and immune modulation potential, are of particular interest for nasal delivery. Moreover, a large number of polymers/copolymers/polymer blends available helps in designing superlative polymeric vaccine delivery system with controlled release and site specific delivery.

1.5.1 Polymeric nanoparticles in nasal vaccine delivery

In recent time, polymeric nanoparticles have been extensively explored as a particulate nanocarrier system for the delivery of drugs and macromolecules. Various advantages of polymeric nanoparticles like a controlled release, targeted delivery, monodisperse size, high drug payload, excellent biocompatibility make them drug carriers of choice. A number of distinct synthetic, semi-synthetic, natural polymers are used to prepare nanoparticles depending upon nature of drugs, site of action, and duration of action (controlled/sustain release). For vaccine delivery, polymeric nanoparticles are of special importance since they can encapsulate higher amount of antigens, provide sustained release as well as can act as an adjuvant by modulating immune responses. Several polymers, such as poly(ethylene glycol) (PEG)-poly(lactic acid) (PLA) (Kim et al., 1999; Thomas et al., 2011; Vila et al., 2004a), poly(d,l-lactic-co-glycolic acid)(PLGA) (Demento et al., 2012; Lu et al., 2009; Silva et al., 2013; Thomas et al., 2011), poly(g-glutamic acid) (g-PGA) (Akagi et al., 2012; Akagi et al., 2005), PEG (Vila et al., 2004a), polystyrene (Kalkanidis et al., 2006; Minigo et al., 2007), pullulan (Hasegawa et al., 2006; Uenaka et al., 2007), alginate (Li et al., 2013), inulin (Honda-Okubo et al., 2012; Saade et al., 2013), chitosan (Amidi et al., 2006; Feng et al., 2013; Harde et al., 2014; Harde et al., 2015; Thomann-Harwood et al., 2013; Zhao et al., 2013), and semi-synthetic cellulose derivatives have been widely studied for delivery of vaccines through various routes. Antigen delivery by PLA/PLGA based nanoparticles has been extensively investigated for the last two decades and was also encouraged by the institutions such as the World Health Organization for the development of single-dose vaccines (Aguado, 1993; Csaba et al., 2009). Moreover, FDA had already approved products such as Lupron Depot® (TAP Pharmaceutical Products Inc.), Risperdal Consta® (Janssen Pharmaceuticals Inc.) prepared with these polymers for human applications based on well-documented biocompatibility, safety, controlled release capability, and biodegradability. While, most widely investigated natural polysaccharide polymer for vaccine delivery is chitosan owing to its biopharmaceutically relevant characteristics such as mucoadhesiveness, capacity for the transient opening of tight epithelial junctions, biocompatibility and low toxicity (Illum et al., 2001; Issa et al., 2005). These polymers are discussed in detail in section 1.3.1.

1.5.2 Methods of the preparation of polymeric nanoparticles

In the last couple of decades, several methods have been developed to prepare polymeric nanoparticles, which have broadly classified according to whether the particle formation

involves a polymerization of monomer units or arises from a macromolecule or preformed polymer. The monomer polymerization methods are further classified into the emulsion and interfacial polymerization (Pinto Reis et al., 2006). The preparation methods of polymeric nanoparticles from preformed polymers include solvent displacement, emulsion-diffusion, salting out, dialysis, and supercritical fluid technology (Devadasu et al., 2013). The choice of preparation method depends on a number of factors, such as nature of drugs, desired particle size, particle size distribution, site of application, etc. (Bhardwaj et al., 2005; Mora-Huertas et al., 2011; Rao and Geckeler, 2011).

Among the polymerization methods, emulsion polymerization is fastest and easily scalable method. It is sub-classified into two categories based on the continuous phase, aqueous or organic phase method. Continuous organic phase method involves emulsification of monomer into nonsolvent and surfactants or soluble protective polymers are used to prevent aggregation during polymerization (Kreuter, 1991). Poly(acrylamide) nanospheres, PMMA, poly(ethyl cyanoacrylate) (PECA) and poly(butyl cyanoacrylate) nanoparticles were prepared by this method (Ekman and Sjoholm, 1978; Gross-Heitfeld et al., 2014; Lowe and Temple, 1994). In the continuous aqueous phase method, the monomer is dissolved in aqueous phase without the addition of surfactants or emulsifiers and polymerization is initiated by a collision between monomers and initiator molecules, an ion or free radical. When initiated monomer ions or monomer radicals collide with other monomer molecules the chain starts to grow leading to polymerization (Vauthier et al., 2003). Phase separation and formation of solid particles can take place before or after termination of the polymerization reaction (Kreuter, 1982). The single monomers methyl methacrylate (MMA), alkylcyanoacrylate (ACA), dialkylmethylidene malonate were used to prepare different types of polymeric nanoparticles by this method (Alonso et al., 1991; Mbela et al., 1992; Varchi et al., 2013). Another method of polymerization, interfacial polymerization, is a very rapid method and initiated by the ions present in the medium. Poly(alkylcyanoacrylate) (PACA) nanoparticles were prepared by this method. Cyanoacrylate monomer and drug were dissolved in a mixture of an oil and absolute ethanol and were then slowly dropped into an aqueous solution, with or without ethanol or acetone containing a surfactant (Fallouh et al., 1986; Wischke et al., 2013). PACA nanocapsules were formed spontaneously by polymerization of cyanoacrylate after contact with initiating ions present in the water. Advantages of interfacial polymerization method include higher drug encapsulation and in situ polymerization (Couvreur et al., 2002).

In solvent displacement method, two phases are a solvent phase and a nonsolvent phase, which can be both organic, both aqueous, or an organic phase and an aqueous phase. Polymer and

drug are dissolved in the solvent phase, while the nonsolvent phase contains dissolved stabilizer. The solvent phase is added to the nonsolvent phase in a controlled manner to obtain nanoparticles. The organic/non-aqueous solvent is evaporated by drying under vacuum (Devadasu et al., 2013). This method has been used to prepare various polymeric nanoparticles such as PLA (Nemati et al., 1996), PLGA (Barichello et al., 1999), PCL (Molpeceres et al., 1996), and poly(methyl vinyl ether-comaleic anhydride) (PVM/MA) (Irache et al., 2005). The emulsion-diffusion method utilizes three phases, organic, aqueous, and a dilution phase. Polymer and drug are dissolved in the organic phase while the stabilizer in the aqueous phase (Sahana et al., 2008). The organic phase is added to the aqueous phase and subjected to high shear homogenization to obtain an emulsion. The emulsion is then diluted with water to facilitate the diffusion of the organic solvent into the aqueous phase resulting in the formation of nanoparticles. Several kind of nanoparticles including mesotetra(hydroxyphenyl) porphyrin-loaded PLGA (p-THPP) nanoparticles (Vargas et al., 2004), doxorubicin-loaded PLGA nanoparticles (Yoo et al., 1999), plasmid DNA-loaded PLA nanoparticles (Perez et al., 2001), coumarin-loaded PLA nanoparticles (Lu et al., 2005), and cyclosporine (Cy-A)-loaded gelatin nanoparticles (El-Shabouri, 2002) were prepared using this method. In the salting-out method, polymer and drug are dissolved in a completely water-miscible solvent and then separated from aqueous phase via a salting-out effect (Allémann et al., 1992; Ganachaud and Katz, 2005). High amounts of salts are added to the aqueous phase along with the stabilizer before the addition of polymer solution. The oil/water emulsion formed is diluted with a sufficient volume of water or aqueous solution to enhance the diffusion of acetone into the aqueous phase, leading to the formation of nanospheres (Pinto Reis et al., 2006). This method was successfully used to prepare PLA, PMA, and ethylcellulose (EC) nanospheres (Quintanar-Guerrero et al., 1998). In the dialysis method, the organic phase containing polymer is placed in the dialysis membrane which is dialyzed against a nonsolvent in which the organic phase is miscible but the polymer has limited solubility. As the concentration of the nonsolvent increases in the dialysis bag, precipitation of the polymers starts and the nanoparticles are formed (Devadasu et al., 2013). Dialysis method was used to prepare poly(γ-glutamic acid) (γ-PGA) and L-phenylalanine ethylester (L-PAE) nanoparticles (Akagi et al., 2005) and nanoparticles composed of poly(ethylene oxide)-poly (lactide)(PEO–PLA) block copolymer (Lee et al., 2004). Supercritical fluid technology is thought to be safer than other techniques as it does not use organic solvents which might cause toxicity. The polymer and drug dissolved in the supercritical fluid is passed through an orifice into the air or a liquid medium, resulting in

precipitates in nanoscale due to the rapid expansion of the supercritical fluid (Devadasu et al., 2013; Rao and Geckeler, 2011).

Polysaccharide polymeric nanoparticles like alginate, chitosan nanoparticles are prepared by ionic gelation method, first used by Calvo *et al.* (Calvo et al., 1997). The aqueous polymeric solution is added dropwise to the cross-linking agent aqueous solution with continuous stirring to obtain complexes in the nanometer range. The size of nanoparticles depends primarily on polymer solution concentration and polymer to cross-linking agent ratio. Divalent cations are commonly used as cross-linking agents for alginate nanoparticles while sodium tripolyphosphate (TPP) is used for the preparation of chitosan nanoparticles. Chitosan nanoparticles have been extensively explored to encapsulate proteins such as bovine serum albumin, tetanus and diphtheria toxoid (Harde et al., 2014; Illum et al., 2001; Slutter and Jiskoot, 2010; Soppimath et al., 2001), anticancer agents (Janes et al., 2001), insulin (Ma et al., 2005), and nucleic acids (Mansouri et al., 2004; Mao et al., 2001) for various administration routes. In present work, alginate-dextran nanoparticles are proposed to be prepared by ionic gelation method.

1.5.3 Advantages of nanoparticles

Nanoparticles prepared from diverse materials with unique architectures are used as drug delivery systems (DDS) as they offer several advantages over conventional DDS (Parveen et al., 2012). The advantages of NPs as DDS are as mentioned below:

1. Increase the solubility of the drugs: Poorly soluble drugs are formulated as nanocrystals or nanosuspension to improve the aqueous solubility by increasing effective surface area. This also improves the bioavailability and reduce the dose of the drug.
2. Protect the drugs/proteins from degradation: NPs prevents exposure of drug/protein molecules encapsulated inside them to harsh body environments (acidic pH of the stomach) and various enzymes (in GI tract, nasal cavity).
3. Provide controlled release of drug: The drug molecules encapsulated in NPs are released in a controlled manner following degradation of nanoparticle material. Some of the NPs also offer prolonged drug release due to their slow degradation and by controlling drug diffusion through their matrix.
4. Targeted drug delivery: Surface functionalization of NPs with target cell specific ligands helps in target specific delivery of drugs. Folate coated superparamagnetic iron oxide NPs are used to target cancer cells and monitoring the progress of treatment.

5. Decrease the toxic side effects of drugs: Due to improvement in bioavailability, the dose of drugs is reduced and thus the side effects. Moreover, targeted delivery of cytotoxic drugs (anticancer drugs) also reduces toxic side effects on normal cells.
6. Application through various routes of administration: NPs can be formulated in various dosage forms and administered through the desired route of administration.
7. Vaccine adjuvants: In the case of vaccine delivery, NPs also acts as adjuvants depending upon materials used and potentiate the immune response. Higher uptake of nanoparticles by dendritic cells and macrophages improves immune response by specific vaccine antigens.

Taking into consideration several advantages of nanoparticles, we have used this approach for successful delivery of vaccine through nasal route.

1.6 Proteins/vaccine antigens

The details about the model protein and vaccines antigens used in this work are mentioned in following sub-sections.

1.6.1 Bovine serum albumin

Bovine serum albumin (BSA), also known as "Fraction V" is a serum albumin protein obtained from cows. It is called as “Fraction V" as it is the fifth fraction of the original Edwin Cohn purification methodology, which was obtained by the use of differential solubility characteristics of plasma proteins.

BSA is a globular protein with molecular weight of 66,400 Da, isoelectric point 4.7, and stokes radius of 3.48 nm (Axelsson, 1978; Ge et al., 1998). It is a single polypeptide chain consisting of about 583 amino acid residues and no carbohydrates (Figure 5). In the pH range of 5-7, it contains 17 intra-chain disulfide bridges and 1 sulfhydryl group (Hirayama et al., 1990).

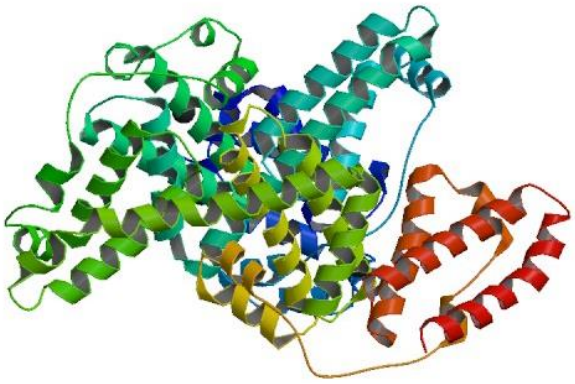

Figure 5 Crystal structure of bovine serum albumin (BSA). (Downloaded from Protein data bank, URL: http://www.rcsb.org/pdb/explore/explore.do?structureId=4OR0 on 26-052016) (Bujacz et al., 2014)

BSA is often used as a protein standard in *in vitro* laboratory experiments and has numerous biochemical applications including ELISAs (Enzyme-Linked Immunosorbent Assay), immunoblots, and immunohistochemistry. It is commonly used as a nutrient source in cell and microbial cultures. It is also used to stabilize some enzymes during the digestion of DNA and to prevent adhesion of the enzyme to reaction tubes, pipet tips, and other vessels. In protein assay methods (Bradford protein assay), BSA is used as a standard protein and concentration of unknown proteins is determined from the BSA calibration curve. Since large quantities of BSA can be readily purified from bovine blood, a byproduct of the cattle industry, it has low price as compared to other proteins and thus widely used.

Due to its cost efficiency and advantageous physicochemical properties, BSA is commonly used as a model protein during development of delivery systems for proteins, peptides and vaccines (Brewer et al., 2005; Goshisht et al., 2015; Lamprecht et al., 1999; Xie and Wang, 2007; Zhang et al., 2004).

In present work, we used BSA as a model protein to develop and thoroughly optimized novel mucoadhesive nanoparticles for nasal delivery of vaccines.

1.6.2 Ovalbumin

Albumin from chicken egg white, popularly known as “ovalbumin” is most important protein found in the chicken egg white portion and constitutes about 60-65% of the total protein (Huntington and Stein, 2001). It is a non-inhibitory member of the serine protease inhibitor (serpin) superfamily (Stein et al., 1991). Ovalbumin (OVA) is a phosphorylated glycoprotein consisting of 385 amino acids with molecular weight of 42.7 kDa (Nisbet et al., 1981). Crystal

structure of uncleaved OVA is presented in Figure 6. The function of ovalbumin is not completely understood until now and it is presumed that it acts as a storage protein in chicken egg (Gettins, 2002).

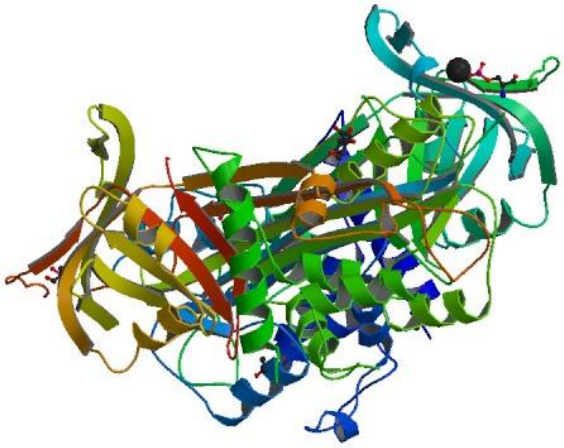

Figure 6 Crystal structure of uncleaved Ovalbumin. (Downloaded from Protein data bank, URL: http://www.rcsb.org/pdb/explore/explore.do?structureId=1OVA on 26-052016) (Stein et al., 1991)

Ovalbumin is widely used as a standard protein to study the structure and properties of other proteins. It is commonly used as a molecular weight marker for calibrating electrophoresis gels. Due to its immunogenic potential, it is widely used as a model protein to develop formulations for vaccine delivery. Several kinds of nanocarriers were developed by using OVA as a model protein and were tested for the successful immunization through various administration routes (Amidi et al., 2006; Bal et al., 2012; Borges et al., 2005; Garinot et al., 2007; Hamdy et al., 2007; Kumar et al., 2015; Mittal et al., 2015; Rahimian et al., 2015; Slutter et al., 2010; Slutter and Jiskoot, 2010).

In present work, OVA was used as a model antigen to study the quality of immune response modulated by the nanoparticles.

1.6.3 Tetanus toxoid

Tetanus toxin is a potent neurotoxin produced by the anaerobic bacterium *Clostridium tetani* (Niemann, 1991). The integral toxin derived from culture supernatants consists of two polypeptide chains with a molecular weight of 150 kDa and connected through an interchain disulfide bond (Craven and Dawson, 1973; Montecucco and Schiavo, 1995). The bigger polypeptide, heavy chain (100 kDa), contains the toxin's binding and translocation domains. While, the smaller polypeptide, light chain (50 kDa), is a protease which cleaves synaptobrevin 2, also known as VAMP 2 (Niemann, 1991). Synaptobrevin 2 is a presynaptic, vesicle

membrane-associated protein that forms a stable complex with two plasma membrane proteins, syntaxin, and SNAP25 in the presence of calcium ions (Montecucco and Schiavo, 1995). This complex formation initiates fusion of transmitter containing vesicles with the plasma membrane to further release neurotransmitters. Tetanus toxin preferentially blocks the release of the inhibitory transmitters, glycine, and GABA, leading to unimpeded muscle contraction and spasm. Furthermore, Seizures may occur, and the autonomic nervous system may also be affected. Extensive immunization programs had reduced the tetanus infection considerably although neonatal tetanus still poses a risk and accounted for nearly 50,000 neonatal deaths around the world every year.

Tetanus toxoid is prepared by formaldehyde inactivation of pure neurotoxin (endotoxin) and mostly adsorbed on the aluminum adjuvants for immunization purposes. The toxoid is standardized for potency in animal tests according to Food and Drug Administration (FDA) regulations. Tetanus toxoid is available alone as well as combined with diphtheria, pertussis antigens for the purpose of effective immunization.

Several attempts were made to improve the immunogenicity of tetanus toxoid through non-parenteral route by encapsulating/ co-delivery of antigens with adjuvants or immunomodulatory particulate systems (nano/microparticles) (Ahire et al., 2007; Harde et al., 2015; Jung et al., 2001; Mitchell et al., 2015; Westerink et al., 2001).

Despite several attempts, the delivery of tetanus vaccine through non-parenteral route is a distant dream. In this work, an attempt was made to formulate tetanus toxoid loaded mucoadhesive immune modulatory nanoparticles for the nasal delivery. The nanocarrier system was developed to provide cost-effective, a patient compliant alternative which could be upscaled to large scale production without need of highly sophisticated equipment and facilities.

1.7 Research objectives

The objective of the proposed work is to explore novel mucoadhesive polymeric nanocarriers with additional adjuvant effect for nasal delivery of vaccines. The research objective will be accomplished by:

1. Preparation and characterization of novel mucoadhesive nanoparticles loaded with model protein, bovine serum albumin (BSA)

2. Preparation, characterization and *in vitro* and *in vivo* evaluation of Tetanus toxoid loaded novel mucoadhesive nanoparticles

3. Mechanistic understanding of immune response modulated by Ovalbumin loaded novel mucoadhesive nanoparticles

2. Materials and Methods

2.1 Materials

2.1.1 Proteins

Albumin from Bovine Serum (A7030, Sigma-Aldrich Chemie GmbH, Steinheim, Germany)
Albumin from Chicken egg white, Ovalbumin (A5503, Sigma-Aldrich Chemie GmbH, Steinheim, Germany)
Tetanus toxoid (Strength: 4300 Lf/mL, Batch no. CPTT- 011/2014), kindly gifted by Biological E Ltd., Hyderabad, India)
Adsorbed Tetanus toxoid formulation (BE tt™) (Kindly gifted by Biological E Ltd., Hyderabad, India)

2.1.2 Polymers

Agar agar (Carl Roth GmbH & Co. KG, Karlsruhe, Germany)
Diethylaminoethyldextran (Carl Roth GmbH & Co. KG, Karlsruhe, Germany)
Mucin from porcine (Carl Roth GmbH & Co. KG, Karlsruhe, Germany)
Sodium Alginate, Protanal® LF120M (FMC Biopolymer, Philadelphia, Pennsylvania, USA)
Sodium Carboxymethyl Cellulose, Cellogen™ HP-SB (Dai-ichi Kogyo Seiyaku Co., Ltd., Kyoto, Japan)
Sodium Hyaluronate (Contipro Pharma, Dolni Dobrouc, Czech Republic)
Sodium Pectinate (Herbstreith & Fox Pektin-Fabriken, Neuenbürg, Germany)

2.1.3 Chemicals

4’,6-diamidino-2-phenylindole (DAPI) dihydrochloride (Sigma-Aldrich, St. Louis, Missouri, USA)
Acetic acid, glacial (Carl Roth GmbH & Co. KG, Karlsruhe, Germany)
Aluminum hydroxide gel, Alu-Gel-S (Serva Electrophoresis GmbH, Heidelberg, Germany)
Ammonium persulfate (Carl Roth GmbH & Co. KG, Karlsruhe, Germany)
Bromophenol blue (Fluka, Neu-Ulm, Germany)
Calcium chloride ($CaCl_2$) (Carl Roth GmbH & Co. KG, Karlsruhe, Germany)
Concanavalin A (HiMedia Laboratories Pvt. Ltd., Mumbai, India)
Coomassie Brilliant Blue (Carl Roth GmbH & Co. KG, Karlsruhe, Germany)
D(+) Glucose, Dextrose (Carl Roth GmbH & Co. KG, Karlsruhe, Germany)
Dimethyl sulfoxide (DMSO) (Carl Roth GmbH & Co. KG, Karlsruhe, Germany)

Disodium ethylenediaminetetraacetic acid (Na_2EDTA) (Carl Roth GmbH & Co. KG, Karlsruhe, Germany)

Disodium hydrogen phosphate (Na_2HPO_4) (Carl Roth GmbH & Co. KG, Karlsruhe, Germany)

Dulbecco's modified Eagle's medium (DMEM) (HiMedia Laboratories Pvt. Ltd., Mumbai, India)

Dulbecco's phosphate buffered saline (10X) (HiMedia Laboratories Pvt. Ltd., Mumbai, India)

Fetal bovine serum (FBS) (HiMedia Laboratories Pvt. Ltd., Mumbai, India)

Fetal Calf serum (FCS) (Biochrom GmbH, Berlin, Germany)

Fluorescein isothiocyanate (FITC) (Sigma-Aldrich, St. Louis, Missouri, USA)

Hydrochloric acid (HCl) (Carl Roth GmbH & Co. KG, Karlsruhe, Germany)

Iscove's Dulbecco modified Eagle medium (DMEM) (Biochrom GmbH, Berlin, Germany)

Isoflurane for anesthesia (Purchased from local pharmacy after completing necessary documentation, Hyderabad, India)

Isoflurane (Essen, Germany)

Lactose (Carl Roth GmbH & Co. KG, Karlsruhe, Germany)

Laemilli Buffer (4X), pH6.8 (In-house)

Tris-HCl pH6.8	0.125M
SDS	2%
Glycerol	10%
β-mercaptoethanol	0.5ml
Coomassie brilliant blue	0.5%
Water	to 10ml

Lipopolysaccharides (LPS) from Escherichia coli (Sigma-Aldrich, St. Louis, Missouri, USA)

Mannitol (Fluka Chemie GmbH, Buchs, Germany)

Monobasic potassium dihydrogen phosphate (KH_2PO_4 (Carl Roth GmbH & Co. KG, Karlsruhe, Germany)

Paraformaldehyde (Sigma-Aldrich, St. Louis, Missouri, USA)

Penicillin (10X) (HiMedia Laboratories Pvt. Ltd., Mumbai, India)

Potassium chloride (KCl) (Carl Roth GmbH & Co. KG, Karlsruhe, Germany)

Poly-acrylamide (Carl Roth GmbH & Co. KG, Karlsruhe, Germany)

Roswell Park Memorial Institute (RPMI) 1640 medium (HiMedia Laboratories Pvt. Ltd., Mumbai, India)

Sodium acetate, trihydrate (Carl Roth GmbH & Co. KG, Karlsruhe, Germany)

Sodium azide (NaN_3) (Sigma-Aldrich Chemie GmbH, Steinheim, Germany)

Sodium bicarbonate ($NaHCO_3$) (Carl Roth GmbH & Co. KG, Karlsruhe, Germany)

Sodium Chloride (NaCl) (Carl Roth GmbH & Co. KG, Karlsruhe, Germany)

Sodium dodecyl sulfate (SDS) (Carl Roth GmbH & Co. KG, Karlsruhe, Germany)

Sodium hydroxide (NaOH) (Carl Roth GmbH & Co. KG, Karlsruhe, Germany)

Sodium dihydrogen phosphate, NaH_2PO_4 (Merck KGaA, Darmstadt, Germany)

Spectra/Por® dialysis membrane (MWCO 6-8,000; The Spectrum Companies, USA)

D-Sucrose (Carl Roth GmbH & Co. KG, Karlsruhe, Germany)

SyPRO Ruby© Protein stain (Thermo Fischer Scientific, Darmstadt, Germany)

N,N,N',N'-tetramethylethylenediamine (TEMED) (Carl Roth GmbH & Co. KG, Karlsruhe, Germany)

D(+)-Trehalose dihydrate (Carl Roth GmbH & Co. KG, Karlsruhe, Germany)

Tris-HCl (Carl Roth GmbH & Co. KG, Karlsruhe, Germany)

Tris-Glycine-SDS Buffer (10X) (In-house):

Tris-base	250mM
Glycine	1.92M
SDS	1%

Triton X-100 (Sigma-Aldrich, St. Louis, Missouri, USA)

Trypsin-EDTA (Biochrom GmbH, Berlin, Germany)

2.1.4 Reagents and kits

3-(4,5-dimethylthiazol-2-yl)-2,5-diphenyltetrazolium bromide (MTT) (Sigma-Aldrich, St. Louis, Missouri, USA)

3,3′,5,5′-Tetramethylbenzidine (TMB) Liquid Substrate System for ELISA (Sigma-Aldrich, St. Louis, Missouri, USA)

Anti-Mouse IgA (α-chain specific) −Peroxidase antibody produced in goat (Sigma-Aldrich, St. Louis, Missouri, USA)

Anti-Mouse IgG (γ-chain specific) −Peroxidase antibody produced in goat (Sigma-Aldrich, St. Louis, Missouri, USA)

Cytotoxicity Detection Kit (LDH) (Roche Diagnostics GmbH, Mannheim, Germany)

Mouse IgG ELISA quantitation set (Bethyl Laboratories Inc., Hamburg, Germany)

Mouse Interferon- γ ELISA MAX™ (BioLegend®, San Diego, CA, USA)

Mouse Interleukin- 2 ELISA MAX™ (BioLegend®, San Diego, CA, USA)

Pierce™ BCA Protein Assay Kit (Thermo Fischer Scientific, Darmstadt, Germany)

IL-17a ELISA kit (eBioscience, California, USA)

IFN- γ ELISA kit (eBioscience, California, USA)

IL-6 ELISA kit (eBioscience, California, USA)

IL-10 ELISA kit (eBioscience, California, USA)

2.1.5 Instruments

Agilent 8453 UV-visible Spectroscopy System (Agilent Technologies, Deutschland GmbH, Waldbronn, Germany) with UV-ChemStation analysis software

Axioscope optical light microscope (Carl Zeiss Jena GmbH, Jena, Germany) with image analysis software (EasyMeasure, Inteq Informationstechnik GmbH, Berlin, Germany)

Bandelin LS4 with Sonopuls HD 200 probe sonicator (Bandelin Electronic GmbH & Co. KG, Berlin, Germany)

Bandelin Sonorex RK 255H (Bandelin Electronic GmbH & Co. KG, Berlin, Germany)

BD LSRFortessa™ cell analyzer with BD FACSDiva™ v8.0 software (BD Biosciences, San Jose, California, USA)

Bio-Tek® ELISA plate washer (Bio-Tek® Instruments GmbH, Bad Friedrichshall, Germany)

CelCulture® CO_2 Incubator (Esco Micro Pte. Ltd., Singapore)

Christ Gamma 2-20 freeze dryer with Christ K 50 cooling unit (Martin Christ Gefriertrocknungsanlagen GmbH, Osterode am Harz, Germany)

Circular Dichroism J-715 (JASCO Corp., Japan)

Excalibur 3100 FTIR spectrophotometer (Varian Inc., Palo Alto, USA) with single reflection diamond crystal (ATR) (Pike MIRacle, Pike 62 Technologies, Madison, USA) and Resolution Pro 4.0 software

GFL freezer (GFL Gesellschaft für Labortechnik mbH, Burgwedel, Germany)

Gel Doc™ XR+ Molecular Imager (Bio-Rad, California, USA)

GENios Plus Multi-mode microplate reader (Tecan Deutschland GmbH, Crailsheim, Germany)

Heraeus™ Biofuge™ Stratos™ centrifuge (Thermo Electron Corporation, Osterode, Germany)

Horizontal shaker (GFL 3033, Gesellschaft für Labortechnik GmbH & Co. KG, Burgwedel, Germany)

Invitrogen™ PowerEase® 500 Power Supply with XCell SureLock™ Electrophoresis Cell (Life Technologies Corp., USA)

Isoflurane anesthesia (E-Z Anesthesia® system, Palmer, USA)

Megafuge 3.0R centrifuge (Kendro Laboratory Products GmbH, Osterode, Germany)

Metrohm pH meter (Metrohm Ltd., Herisau, Switzerland)

Mettler Toledo MX5 microbalance (Mettler Toledo, Greifensee, Switzerland)

Milli Q® (Millipore Corporation, California, USA)

Olympus IX53 inverted microscope (Olympus Corporation, Tokyo, Japan)

Orion Sage M362® syringe pump (Sage Instruments, Freedom, California, USA)

Sanyo Gallenkamp climate chamber (Thermotec Weilburg GmbH & Co. KG, Weilburg, Germany)

Semi-dry blotting apparatus (Biorad, California, USA)

SpectraMax® M4 Multi-mode microplate reader (Molecular Devices, Sunnyvale, California, USA) with software SoftMax® Pro 6.3 (Molecular Devices, Sunnyvale, California, USA)

Texture analyzer (TA.XT, Stable Microsystems, Germany)

Vacuum oven (Heraeus VT 5042 EKP, Hanau, Germany) coupled with a chemistry hybrid vacuum pump (Vacuubrand GmbH, Wertheim, Germany)

Variomag multipoint magnetic stirrer (H+P Labortechnik AG, Oberschleissheim, Germany)

Vilber Lormount Imaging detection system (Vilber Lourmat, France)

Zetasizer Nano ZS with Zetasizer software version 7.11 (Malvern Instruments, Malvern, UK)

2.1.6 Cell lines and animals

Human macrophage cell line (THP-1) (Leibniz-Institut DSMZ Cat. Nr. ACC-16, Braunschweig, Germany)

Human nasal septum epithelial (RPMI 2650) (National Centre for Cell Science (NCCS), Pune, India)

Murine macrophage (RAW 264.7) (National Centre for Cell Science (NCCS), Pune, India)

BALB/c mice, albino mice (National Institute of Nutrition, Hyderabad, India)

C57BL/6 mice, Black 6 mice (Universitätklinikum Essen, Essen, Germany)

2.1.7 FACS antibodies

CD11b-Qdot (eBioscience, California, USA)

CD11c-PE-Cy7 (eBioscience, California, USA)

CD8a-Pacific Blue (eBioscience, California, USA)

CD4-Per-CP (eBioscience, California, USA)

CD3-Per-CP (eBioscience, California, USA)

CD80-FITC (eBioscience, California, USA)

CD86-PE (eBioscience, California, USA)

CD69-PE (eBioscience, California, USA)

MHCII-APC (eBioscience, California, USA)

B220-APC (eBioscience, California, USA)

2.1.8 Others

ELISA plates, 96 well, high binding (HiMedia Laboratories Pvt. Ltd., Mumbai, India)

Nunc Immuno™ Maxisorb F 96-well solid plates (Sigma Aldrich Chemie GmbH, Steinheim, Germany)

40-µm cell strainer (HiMedia Laboratories Pvt. Ltd., Mumbai, India)

Coated sterile 12 well plates (Sigma-Aldrich, St. Louis, Missouri, USA)

Corning cell culture flask, T75 flask (Corning, India)

Falcon™ tubes, sterile conical 15 ml and 50 ml (HiMedia Laboratories Pvt. Ltd., Mumbai, India)

2.2 Methods

2.2.1 Preparation of polymeric nanoparticles

The polymeric nanoparticles were prepared by ionic gelation method (Avadi et al., 2010; Bodmeier et al., 1989; Calvo et al., 1997; Fan et al., 2012; Shu and Zhu, 2002). The polyanionic polymers sodium alginate (ALG), sodium carboxymethylcellulose (CMC), sodium hyaluronate (HA) and sodium pectinate (PCT) were screened as a mucoadhesive component of nanocarrier system (nanoparticles) while polycationic polymer, diethylaminoethyldextran (DEAE) was used as an immune stimulant (adjuvant) component. For the preparation and optimization of nanoparticle system, bovine serum albumin (BSA) (MW 66.4 kDa) was used as model protein. Nanoparticles were prepared with different combinations of different mucoadhesive polymers with BSA and DEAE. Figure 7 is a schematic presentation of the preparation method of BSA loaded polymeric nanoparticles.

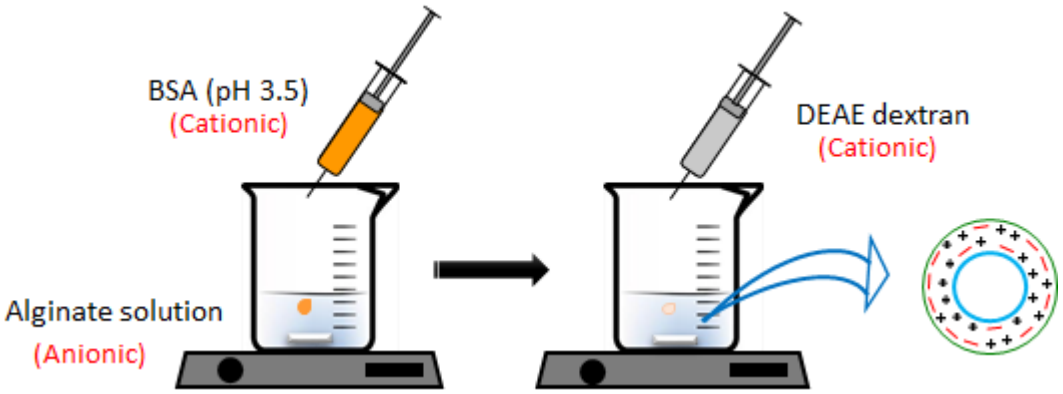

Figure 7 Schematic presentation of preparation of BSA loaded nanoparticles.

Briefly, mucoadhesive polymer, BSA, and DEAE solutions were prepared with concentration 1 mg/ml in different beakers. Since, BSA at pH < 4.7 (isoelectric point) acquires a positive charge, it interacts strongly with anionic mucoadhesive polymers. Therefore, the pH of BSA solution was lowered to 3.5 using 0.1 N HCl (Benichou et al., 2002; Brewer et al., 2005; Peng et al., 2004). The BSA solution was added dropwise (Orion Sage M362® syringe pump (Sage Instruments, USA)) into polyanionic mucoadhesive polymer (ALG/CMC/HA/PCT) solution under continuous stirring (Variomag Multipoint, H+P Labortechnik AG, Germany) using Omnifix® 10 ml syringe (B. Braun melsungen AG, Germany) and 20G Sterican® hypodermic needle (B. Braun melsungen AG, Germany). Finally, DEAE solution was added dropwise to the BSA-mucoadhesive polymer complex under continuous stirring. The particles that

precipitated out in the solution were characterized for particle size, polydispersity index (PDI), zeta potential and encapsulation/association efficiency. On the basis of the results, one mucoadhesive polymer was selected for further optimization. The method was optimized to achieve lower particle size (< 200 nm), low PDI (< 0.2), optimal zeta potential (around -30 mV) and maximum encapsulation efficiency. Throughout the studies, Milli Q® (Millipore Corporation, USA) water was used to ensure that no other ions play a role in the ionic interactions between BSA and polymers.

2.2.2 Optimization of polymeric nanoparticles

The nanoparticles were further optimized with respect to BSA solution pH, BSA loading, and BSA/polymer solution addition rate. To study the effect of BSA solution pH on particle size and encapsulation efficiency (% EE), the pH was adjusted to 3, 3.5, 4.7, 5.0 and 6.0 using 0.1 N HCl. Rest of the parameters like 50% drug loading (with respect to total weight) and addition rate of 1 ml/min were kept constant. Similarly, for evaluating the effect of BSA loading and BSA/polymer solution addition rate, the BSA loading (20%, 30%, 40%, and 50% with respect to total weight) and addition rate (0.6, 0.8, 1.0 and 1.2 ml/min) were changed severally while other parameters were kept constant.

2.2.3 Improvement of BSA encapsulation by dialysis of polymers

To improve encapsulation efficiency of BSA, ALG solution was dialyzed against Milli Q® water using Spectra/Por® dialysis membrane (MWCO 6000-8000). Briefly, ALG solution (1 mg/ml) was prepared in Milli Q® water and filled in previously activated Spectra/Por® dialysis membrane. This membrane was then inserted in the beaker containing 2 L Milli Q® water. Nanoparticles were prepared using the same method followed by measurement of particle size, zeta potential, encapsulation efficiency and turbidity (% Transmittance).

2.2.4 Characterization of nanoparticles

2.2.4.1 Morphology, surface charge, and encapsulation efficiency

For characterization of nanoparticles, particle size, zeta potential and polydispersity index (PDI) were measured using Zetasizer Nano ZS instrument (Malvern Instruments, UK). For encapsulation efficiency (%EE) assessment, 1 ml of nanoparticle dispersion was centrifuged at 28000×g (17000 rpm) for 45 min and 500 µl supernatant containing unencapsulated BSA was

sampled for the analysis (Anal et al., 2006). The protein content was analyzed by using BCA protein assay kit (Thermo Fischer Scientific, Darmstadt, Germany) and %EE was calculated using following formula:

$$\%Encapsulation\ Efficiency = \frac{Total\ BSA - Free\ BSA}{Total\ BSA} \times 100$$

2.2.4.2 Fourier transform infrared (FTIR) analysis

Ionic interaction between oppositely charged polymers and BSA was confirmed by Fourier transformer infrared (FTIR) spectroscopy (Fu et al., 1999; Peng et al., 2004; Shang et al., 2007). Nanoparticles were freeze-dried and placed on a horizontal ATR accessory with a single reflection diamond crystal (Pike MIRacle, Pike Technologies, Madison, USA). FTIR analysis was performed with an Excalibur 3100 FTIR spectrophotometer (Varian Inc., Palo Alto, USA). Average of 64 scans at 4 cm^{-1} resolution (sensitivity of 8) was collected as a spectrum and further smoothing and corrections were performed using Resolution Pro 4.0 software (Varian software).

2.2.5 In-process stability of BSA

2.2.5.1 Structural integrity evaluation using gel electrophoresis (SDS-PAGE)

The structural integrity of BSA extracted from nanoparticles was assessed by sodium dodecyl polyacrylamide gel electrophoresis (SDS-PAGE, Invitrogen, USA) (Harde et al., 2015; Peng et al., 2004). In a gel casting cassette, 12% w/v separating SDS-polyacrylamide gel and 4% w/v stacking gel was cast along with a well comb and was allowed to solidify. During this time, BSA (standard) and extracted BSA from nanoparticles were mixed with Laemilli buffer and heated at 95 °C for 5 min. to denature the protein. The assembly was then placed in an ice tray and the cell was filled with Tris-Glycine running buffer. In each well 30 µl of the sample (protein ladder and BSA) was added and subjected to electrophoresis with a constant current of 10 mA for stacking gel and 20 mA for separating gel. The protein separation was monitored by Coomassie brilliant blue loading dye until the dye ran out of the gel. The gel was then removed and stained with SyPRO Ruby© protein stain for 1 hour followed by 3 washing (10% methanol, 7% acetic acid) for 15 min each to destain the gel and bands were visualized using an ultraviolet filter in Vilber Lourmat Imaging detection system (Vilber Lourmat, France).

2.2.5.2 Conformational stability

Conformational stability of BSA was assessed by Circular Dichroism (CD) spectroscopy (JASCO Corp., J-715 Rev. 1.00, Japan) (Siddhapura et al., 2016; Xie and Wang, 2007). Briefly, BSA was separated from nanoparticles by centrifugation at 28000×g and concentration was measured using BCA protein assay kit. Standard BSA solution was prepared with equal concentration as of BSA extracted from nanoparticles and subjected to CD spectroscopic measurements in the far UV region of 250-190 nm at data pitch 0.5 nm and a scan rate of 20 nm/min. An average of three accumulations was taken for each sample and a baseline correction was performed with Milli Q® water to obtain CD spectrum (Iovescu et al., 2015).

2.2.6 *In vitro* BSA release from nanoparticles

The release of BSA from nanoparticles over a period of 8 hours was carried out in phosphate buffer pH 6.0 as well as in simulated nasal electrolyte solution (SNES) pH 6.0. For release study, 200 µl BSA-NP suspension was placed in 800 µl pre-incubated (37°C) phosphate buffer/SNES in a microcentrifuge tube and placed in Horizontal shaker (GFL 3033, Gesellschaft für Labortechnik GmbH & Co. KG, Burgwedel, Germany) at 37°C and 80 rpm. These experiments were performed in triplicate and samples were centrifuged at each time point and the supernatant was analyzed for released BSA with Agilent 8453 UV-visible Spectroscopy System (Agilent Technologies, Deutschland GmbH, Waldbronn, Germany) (Baudner et al., 2003). A set of (n=3) blank nanoparticles with same polymer concentration was placed in phosphate buffer/SNES and the supernatant collected after centrifugation was analyzed and used as blank (Harde et al., 2015).

2.2.7 *In vitro* mucoadhesion measurement

2.2.7.1 Assessment of in vitro mucoadhesion using Texture Analyzer

The study was performed using Texture analyzer (TA.XT, Stable Microsystems, Germany) and following the previously developed protocol with some modifications in the setup (Bertram and Bodmeier, 2006; Nakamura et al., 1996; Wong et al., 1999). Mucin suspension was prepared by addition of mucin (from porcine) in distilled water (4% w/v) and stirring overnight. In another beaker, 2% w/v agar gel was prepared by heating agar in distilled water followed by addition of equal volume of mucin suspension (Final concentration: mucin 2% w/v and agar 1% w/v). The hot mixture was then cast in Petri plates (diameter= 5 cm) and allowed to cool

in refrigerator to form a gel. Mucin-agar gel cast in Petri plates was then equilibrated to room temperature and humidity above 75% (saturated KBr solution) for 1 hour before starting the experiment. The assembly of *in vitro* mucoadhesion test is presented schematically in Figure ***8***. A both-sided tape (area= 1.96 cm^2) was stuck on the surface of probe adapter. Approximately 10 mg of sample was spread evenly on another side of tape and adapter was fixed to the probe. The sample was kept in contact with mucin-agar gel for 5 min (contact force= 1 g) and then detachment force was measured by applying trigger force of 5 g (0.05 N).

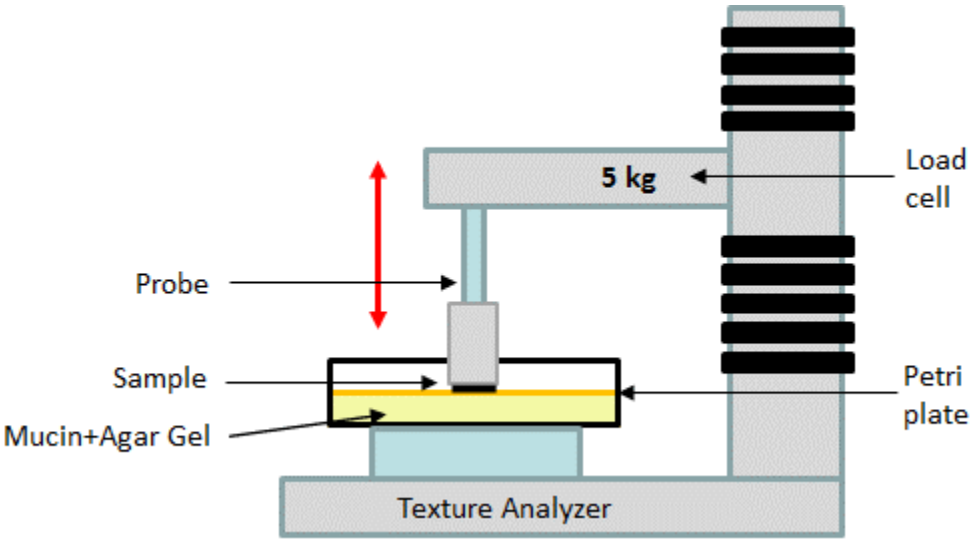

Figure 8 Schematic presentation of texture analyzer setup to evaluate the mucoadhesive potential of polymers and nanoparticles.

2.2.7.2 In vitro mucoadhesion as a function of zeta (ζ) potential

Changes in net surface charge (zeta (ζ) potential) was evaluated using Zetasizer Nano ZS instrument (Malvern Instruments, UK) to further confirm the mucoadhesive potential as a function of interactions between mucin and BSA-NP as well as polymers. The 1% w/v mucin suspension was prepared by hydrating mucin (from porcine) in phosphate buffer pH 6.0 overnight with continuous stirring. The mucin suspension was then sonicated for 1 min. using Bandelin LS4 with Sonopuls HD 200 probe sonicator (Bandelin Electronic GmbH & Co. KG, Berlin, Germany) and was then filtered subsequently through Whatman™ Grade GF/C (1.2 µm) and Grade GF/F (0.6-0.8 µm) glass microfiber filters (GE Healthcare, UK) (Shen et al., 2009). The obtained mucin suspension was incubated at 37°C for 3-4 hours before starting the experiment. Polymer solutions (ALG, DEAE) and BSA solution were prepared (1% w/v) followed by preparation of BSA nanoparticles using optimized method. The polymers and BSA-NP were mixed with mucin suspension in 1:1 ratio (Mucin: polymer/NP samples = 10:1)

and incubated at 37°C for 1 hour, cooled down to room temperature followed by measurement of zeta potential using Zetasizer Nano ZS instrument (Shen et al., 2009; Takeuchi et al., 2005).

2.2.8 *In vitro* cytotoxicity study

Human macrophage-like cells THP-1 (DSMZ Cat. Nr. ACC-16) were used for this experiment. The cells were grown in Iscove's Dulbecco modified Eagle medium (DMEM), supplemented with 10% Fetal Calf serum (FCS) under standard tissue culture conditions of 37°C, 5% CO_2. The cells were regularly passaged with 1% trypsin-EDTA. Each well was seeded with 10,000 cells and 200 µl of different polymers and nanoparticle samples (prepared in medium) were added in different concentrations viz. 20, 50 and 100 µg/ml. As a negative control, Iscove's DMEM medium was added to the control wells. A 1% v/v Triton X-100 in DMEM medium was used as a positive control and considered that it released 100% LDH for further calculations. Less than 10% cell death was considered as a non-toxic effect. The 96 well plate containing THP-1 cells and samples were incubated in tissue culture incubator at 37°C, 5% CO_2 for 24 hours. In principle, following the cell membrane disruption by the toxic materials, lactase dehydrogenase (LDH) is released in the extracellular fluid (medium). This released LDH was quantified using commercial LDH kit (Roche, Germany) by following Manufacturer's protocol. (das Neves et al., 2012; Fischer et al., 2003; Rahimi et al., 2010).

2.2.9 Freeze-drying of nanoparticle formulation

To improve the stability of the formulation, nanoparticles were freeze-dried (Christ Gamma 2-20, Germany) and the effect of cryoprotectants was studied. Different sugars like sucrose, dextrose, trehalose, mannitol and lactose were used as cryoprotectant with a concentration of 5% w/v for initial screening of sugars. The sugars were added to nanoparticles dispersion just before freezing at -80°C (GFL freezer, Germany) for 2 hours. The conditions for freeze-drying were as follows: condenser temperature -90°C, the temperature of shelves -40°C and pressure P = 0.133 mbar. For primary drying temperature was increased from -40°C to -5°C, over the time period of 24 hours (P = 0.133 mbar). Final drying was carried out with a temperature increment of -5°C to 10°C with P = 0.025 mbar for 6 hours. Further optimization of the process was carried out with Sucrose as cryoprotectant with different concentrations between 2.5 to 15% w/v (Jain et al., 2014; Shaikh et al., 2009; Wendorf et al., 2006).

2.2.10 Stability study of freeze-dried BSA loaded nanoparticle formulation

BSA loaded nanoparticles were prepared by the optimized method as mention in section 2.2.2 and lyophilized with sucrose (10% w/v) as per method mentioned in section 2.2.9. These sample vials were sealed and stability study was performed according to ICH guidelines. The samples were kept for stability study at three different stability conditions: 1) Real time (2-8°C), 2) 25°C/60% RH and 3) 40°C/75% RH. At each time point, samples were redispersed with Milli Q® water followed by particle size, PDI, and zeta potential determination with Zetasizer (Malvern Instruments, UK). Structural integrity and conformational stability of BSA were also checked using gel electrophoresis (SDS-PAGE) and CD spectroscopy techniques respectively (Abdelwahed et al., 2006a; Harde et al., 2014; Shaikh et al., 2009).

2.2.11 Preparation and optimization of Tetanus toxoid loaded nanoparticles

Tetanus toxoid antigen (TT) (4300 Lf/mL) was kindly provided by Biological E Ltd. Hyderabad, India. All the studies involving TT were performed at BITS Pilani, Hyderabad, India. Tetanus toxoid loaded nanoparticles were prepared using method optimized for BSA as model protein (section 2.2.1-2.2.3). To remove buffer ions from TT solution, the TT solution was dialyzed before starting the nanoparticles preparation. The strength of the buffered TT solution was 4300 Lf/ml and thus diluted appropriately with Milli Q® water immediately after dialysis. As TT has two peptide chains with different isoelectric points (pI), it started to precipitates at pH below 5.2 (visual observation). The preparation method was further modified and optimized to avoid any aggregation or degradation of TT. Dialyzed TT solution was added dropwise to the dialyzed ALG polymer solution and the pH of the resultant mixture was adjusted to 4.5 with 0.1 N HCl. Finally, the DEAE polymer solution was added dropwise to the ALG-TT mixture to obtain TT loaded nanoparticles. Effect of ALG-TT solution pH on particle size, PDI, zeta potential and %EE was also studied. The nanoparticles were characterized for particle size, PDI, zeta potential and %EE as mentioned in section 2.2.4.1.

2.2.12 Structural integrity evaluation of Tetanus toxoid using gel electrophoresis (SDS-PAGE)

In-process stability was assessed by running extracted TT on the sodium dodecyl polyacrylamide gel (SDS-PAGE). A similar method was followed as mentioned in section 2.2.5.1.

2.2.13 *In vitro* TT release from nanoparticles

In vitro release of TT from nanoparticles was measured in phosphate buffer pH 6.0 over the period of 8 hours. For the release study, the same method was followed as mentioned in section 2.2.6. At each time point, samples were withdrawn and centrifuged to measure released TT in supernatant followed by calculating percentage release.

2.2.14 *In vitro* proliferation assay

The proliferation of human nasal epithelial cells (RPMI 2650) in the presence of TT loaded nanoparticles was assessed using MTT (3-[4,5-dimethylthiazol-2-yl]-3,5-diphenyl tetrazolium bromide dye) assay (He et al., 2010; Lemarchand et al., 2006). Briefly, 10,000 nasal epithelial cells (RPMI 2650) were seeded to each well of 96 well plate and incubated at 37°C, 5% CO_2 (ESCO, Singapore). After 24 hours, the supernatant media was removed and control, as well as samples diluted in cell culture media (DMEM), supplemented with 10% FBS, were added to each well and incubated at 37°C, 5% CO_2 (CelCulture®, ESCO, Singapore) for 48 hours. After an incubation period of 48 hours, 10 µl of MTT (10 mg/mL) was added to each well and incubated for another 4 hours followed by removal of all media and addition of 100 µl DMSO to dissolve formed formazan crystals. The purple color developed due to solubilization of formazan crystals was quantified at 570 nm spectrophotometrically (SpectraMax M4, Molecular Devices, US).

2.2.15 *In vitro* macrophage uptake study

In vitro macrophage uptake was performed on murine macrophage cell line (RAW 264.7) using fluorescent dye fluorescein isothiocyanate (FITC) labeled nanoparticles (Jain et al., 2014; Shukla et al., 2005). DEAE dextran was labeled with FITC dye by dropwise addition of FITC into DEAE solution (in 0.1 M sodium carbonate buffer, pH 9.0) with continuous stirring. The incubation of FITC in DEAE was performed for 24 hours at room temperature. Later, the DEAE-FITC conjugate was dialyzed (Spectra/Por®, The Spectrum Companies, USA, MWCO: 6-8 kDa,) to remove unconjugated FITC. Complete removal of free FITC was confirmed by thin layer chromatography using 5:4:1 of chloroform: methanol: water as the mobile phase (Labala et al., 2015). Nanoparticles were prepared using the FITC labeled DEAE as per optimized method.

For *in vitro* uptake study, 50,000 cells were seeded into each well of 12 well, coated plate (Thermo Fischer Scientific, India) and incubated for 24 hours at 37°C, 5% CO_2 (CelCulture®, ESCO, Singapore). Cells were treated with FITC-nanoparticles (200 µg/ml in RPMI 1640 medium) and incubated for 5, 15, 30 and 60 min. After each time point, NPs were removed and plates washed carefully with sterile phosphate buffered saline (PBS) followed by fixation with 4% paraformaldehyde. The cells were then treated with 0.1% w/v Triton X-100 to permeate cell membrane and then treated with DAPI dye to stain the nucleus. The cells were washed with PBS and visualized under a fluorescence microscope (Olympus IX53, Japan).

2.2.16 *In vivo* immunization study of Tetanus toxoid loaded nanoparticles

In vivo immunization study was performed on 6-8 weeks old male Balb/c mice in collaboration with BITS Pilani, Hyderabad, India. All animal experiments were performed after approval from Institutional Animal Ethics Committee of BITS Pilani, Hyderabad, India and performed according to CPCSEA, India guidelines.

Animals were divided into 5 groups containing 6 animals per group. Animals were anesthetized with a mixture of Isoflurane and Oxygen (E-Z Anesthesia® system, Palmer, USA) before each dosing and bleeding time points. The first group was kept as control (untreated) while other groups were treated with intranasal administration of TT nanoparticles, blank nanoparticles, free TT and last group was treated with *i.m.* injection of marketed TT vaccine formulation (BE tt™). Prior to the nasal dosing, mice were anesthetized and 10 µl of formulations were administered into each nostril using 1-20 µl micropipette while 20 µl of the marketed formulation was administered through *i.m.* route using 1 ml insulin syringe. All treatment groups were immunized with TT dose equivalent to 1 Lf on day 1 followed by booster doses on day 7 and 14 (Jung et al., 2001; Vila et al., 2004b).

2.2.17 Collection of samples and tissues for analysis

Blood samples were collected on day 0 (pre-immunization), 7 and 14 prior to dosing and remaining were collected on day 21, 28 and 35 (post-booster) by retro-orbital puncture using heparinized capillaries. The blood samples were centrifuged at 6000 rpm for 5 min (Rotary incubator, REMI, India) in 0.5 M EDTA as anticoagulant to separate serum. The serum samples were stored at -20°C until further analysis for serum IgG using commercial ELISA kits.

On day 35, after collection of blood samples, mice were sacrificed by spinal dislocation and nasal lavage as well as spleens were collected aseptically. For nasal lavage collection, 500 µl of ice-cold PBS (pH 7.4) was forced through trachea and nasal washing/lavage was collected from nostrils. The same buffer was used for two more washing and the final lavage collected was stored at -20°C until further analysis of sIgA.

The spleen removed from each mouse was cut into two parts, one part was used to determine cytokines (IL-2 and IFN-γ) while another part was used to prepare the splenocytes cell suspension for stimulation assay.

2.2.18 Determination of serum IgG levels

Serum samples were analyzed for immunoglobulin IgG levels by using goat anti-mouse IgG (γ-chain specific)-peroxidase antibody ELISA kit (Sigma-Aldrich, USA) (Boonyo et al., 2007; Borges et al., 2008b; Jain et al., 2014). Briefly, 96 well flat bottom high binding ELISA (HiMedia Laboratories Pvt. Ltd., India) plates were coated overnight with 100 µl of 1 Lf/ml TT solution (in carbonate buffer, pH 9.5) and kept in the refrigerator overnight. The coating solution was then discarded and plates were washed three times with phosphate-buffered saline (PBS) containing 0.05% v/v Tween® 20. The plates were blocked with 1% w/v BSA in PBS for 1 hour to avoid non-specific binding. The plates were then washed three times with PBS containing 0.05% v/v Tween® 20. The 100 µl of diluted serum samples (in PBS) and PBS as blank were added to the wells and incubated at 37°C for 2 hours. The plates were again washed three times with PBS containing 0.05% v/v Tween® 20 followed by addition of 100 µl Goat anti-mouse IgG HRP conjugate detection antibody (1:15000 dilution) and incubated for 45 min. The plates were again washed three times with PBS containing 0.05% v/v Tween® 20 and 100 µl of 3,3′,5,5′-Tetramethylbenzidine (TMB) liquid substrate was added to each well and incubated for 15 min. The color developed was stopped by adding 2 N H_2SO_4 and the intensity of the color was measured at 450 nm on SpectraMax® M4 Multi-mode microplate reader (Molecular Devices, California, USA).

2.2.19 Determination of mucosal immune response (sIgA)

Nasal secretions/washings were collected from each mouse to measure secretory IgA (sIgA) antibodies titer using goat anti-mouse IgA (α-chain specific)-peroxidase antibody ELISA kit (Sigma-Aldrich, USA) (Borges et al., 2008a; Harde et al., 2015). Similar procedure was

followed for determination of sIgA as mentioned in section 2.2.18 except the addition of goat anti-mouse IgA (α-chain specific)-peroxidase antibody (1:10000 dilution) instead of goat anti-mouse IgG HRP conjugate detection antibody.

2.2.20 Cytokine analysis from spleen homogenate

On day 35, all animals were sacrificed and spleens were separated aseptically and kept in 2 ml sterile ice-cold PBS. A portion of spleen from each mouse was homogenized in sterile phosphate buffer pH 7.4 (containing 0.001% v/v Protease inhibitor) and centrifuged to remove tissue debris. The cytokine (IL-2 and IFN-γ) levels were analyzed in the supernatant using commercially available ELISA kits by following manufacturer's protocol (BioLegend®, California, USA) (Harde et al., 2014).

2.2.21 Preparation of splenocytes suspension

To prepare splenocyte cell suspension, the spleen from each mouse was smashed and strained through 40-micron cell strainer. The cell suspension was then centrifuged at 1500 rpm for 5 min. (Rotary incubator, REMI, India) and the supernatant was discarded. To the splenocyte pellet, 2 ml RBC lysis buffer was added and incubated for 5 min. followed by centrifugation and removal of supernatant. To this pellet, 5 ml RPMI 1640 medium was added to re-suspend the cells followed by centrifugation at 1500 rpm for 5 min. The supernatant was discarded and the pellet was resuspended in 2 ml RPMI 1640 medium containing 1% v/v fetal bovine serum (FBS) and 1% v/v Penicillin. The splenocyte cell suspension was used for *in vitro* T cell stimulation assay.

2.2.22 Cytokine production by splenocytes

The splenocytes were counted and 50,000 cells were seeded per well of 96 well assay plate and stimulated with 1 µg/ml Concanavalin A (ConA) and incubated for 72 hours at 37°C, 5% CO_2 (CelCulture®, ESCO, Singapore) (Borges et al., 2007). The plates were centrifuged and the supernatant was analyzed for the production of IL-2 and IFN-γ using ELISA kits (BioLegend®, California, USA).

2.2.23 Preparation and characterization of Ovalbumin loaded nanoparticles

Detailed study of interactions between vaccine adjuvants/formulation components and the immune system is necessary to assess the efficacy and probable side effects. To understand the mechanism by which developed nanoparticles modulate immune system Ovalbumin (OVA) loaded nanoparticles were prepared with the previously optimized method. Briefly, 1 mg/ml solutions of OVA, ALG and DEAE were prepared separately. The pH of OVA solution was adjusted to 4.0 using 0.1 N HCl and was added dropwise to dialyzed ALG solution with continuous stirring. Later DEAE solution was added to this OVA-ALG complex which then precipitated out as ionic complexes in the nanometer range (50% OVA loading). The nanoparticles were prepared with 50% w/w OVA loading to achieve 20 µg of OVA dose in 20 µl of the formulation. Blank nanoparticles were prepared by adding DEAE solution to dialyzed ALG solution and Milli Q® water was added to keep the concentration of polymers same as in OVA NP formulation.

2.2.24 Adsorption of Ovalbumin on aluminum hydroxide gel

Soluble antigens especially subunit vaccines are poor immune stimulants and thus, there is a need to administer them in combination with some immune stimulants/adjuvants. Most of the vaccine formulations available in the market are adsorbed on Aluminum salts (aluminum hydroxide, aluminum sulfate), which acts as an adjuvant. OVA was adsorbed on Sterile Aluminum hydroxide gel suspension (Alu-Gel-S, Serva Electrophoresis GmbH, Germany) to make it potent immune stimulant and used as a positive control/standard when administered by intramuscular route. The efficacy of OVA nanoparticles was compared with the intranasal administration of adsorbed.

For adsorption of OVA to Alu-Gel-S, 400 µl of the gel was suspended in 1.6 ml sterile Milli Q® water (final concentration- 1.26 mg/ml) and 2 mg OVA was added with stirring at 300 rpm for 2 hours. Adsorption efficiency was checked by centrifugation of suspension at 10,000 rpm for 10 min. and analyzing OVA in the supernatant by BCA protein assay.

2.2.25 *In vivo* immunization study of Ovalbumin loaded nanoparticles

Animal experiments were authorized by the Nordrhein Westfalen Landesamt für Natur, Umwelt und Verbraucherschutz (Recklinghausen, Germany), and in accordance with the German law for animal protection and were performed at Institute of Immunology, Medical

Faculty, University of Duisburg-Essen, Essen, Germany. Immunization study was performed as per the protocol developed earlier and samples were collected as per previously developed protocols/methods. Briefly, *in vivo* immunization of 6-8 weeks old female C57BL/6 mice was performed with OVA-loaded nanoparticles (OVA_NP *i.n.*), blank nanoparticles (BNP *i.n.*), OVA adsorbed on aluminum hydroxide gel (OVA_Ads *i.n.*) through intranasal and OVA_Ads *i.m.* through intramuscular route. The control group received 20 µl PBS (Phosphate buffered saline) through intranasal route. All treatment groups were immunized with OVA dose equivalent to 20 µg on day 0 followed by booster doses on day 7 and 14.

2.2.26 Collection of blood samples

Blood samples were collected on day 0 (pre-immunization), 7 and 14 prior to dosing and remaining were collected on day 21, 28 and 35 (post-booster) by retro-orbital puncture using heparinized capillaries. The blood samples were collected in EDTA/sodium heparin coated tubes and centrifuged at 6000 rpm for 5 min (Hettich Lab Technologies, Germany) to separate serum. The collected serum was then stored at -20°C until further analysis for serum IgG using commercial ELISA kits.

2.2.27 Determination of serum IgG levels

Serum samples were analyzed for immunoglobulin IgG levels by using mouse IgG ELISA quantitation set (Bethyl Laboratories Inc., Hamburg, Germany) (Boonyo et al., 2007; Borges et al., 2008b; Jain et al., 2014) and following the protocol as described in section 2.2.18.

2.2.28 Fluorescence-activated cell sorting (FACS) analysis of blood

Apart from the analysis of serum immunoglobulins, flow cytometric analysis of different cell populations was performed by tagging cells with labeled anti-epitope antibodies and counting the cells using BD LSRFortessa™ cell analyzer with BD FACSDiva™ v8.0 software (BD Biosciences, California, USA) (Khairnar et al., 2015). Flow cytometry (FACS) is used to measure characteristics of individual particles flowing in a stream of fluid (scattering of light) as well as to sort the cell, which is labeled with fluorescent antibodies (emitted light). In present work, the components of the immune system activated in blood and spleen were analyzed by this highly sophisticated technique. The cells were labeled with different fluorescently marketed antibodies and cell surface expression markers. These markers help to differentiate

types of cells like T cells and B cells and differentiate them from their activated forms. Briefly, the blood samples were collected at different time points was labeled with anti-mouse Epitope-specific antibodies mentioned above for 30 minutes at 4°C. Erythrocytes were lysed with Erythrocyte Lysis Buffer (BD Biosciences California, USA) for 7 minutes and the cell population was counted with BD LSRFortessa™ cell analyzer & BD FACSDiva™ v8.0 software (BD Biosciences, California, USA). The anti-epitope antibodies used for flow cytometry were: CD11b-Qdot, CD11c-PE-Cy7, CD8a-Pacific Blue, CD4-Per-CP, CD3-Per-CP, CD80-FITC, CD86-PE, CD69-PE, MHCII-APC, B220-APC (all purchased from eBioscience, California, USA). For each sample, 30,000 counts were measured and an average was expressed as Cell population (% of total Leucocytes).

2.2.29 Fluorescence-activated cell sorting (FACS) analysis of spleen

Flow cytometry analysis of splenocyte was performed to quantify different cells populations in spleen, which are essential components of the adaptive immune system (Borges et al., 2007; Nembrini et al., 2011). The splenocytes were collected as per protocol mentioned in section 2.2.21 and samples were further processed for FACS analysis as per protocol mentioned in the section 2.2.28. For each sample, 50,000 counts were measured and an average was expressed as cell population (% of total Lymphocytes).

2.2.30 *Ex vivo* intracellular cytokine staining (ICS) assay

Intracellular cytokine staining (ICS) assay of splenocytes was performed to evaluate the production of different cytokines by T cells after stimulations (Priebe et al., 2008). The splenocytes were suspended in DMEM medium containing 2% v/v FCS and 1% v/v antibiotics Penicillin G, streptomycin and Glutamine (PSG) was seeded in the high binding 96 well round bottom plate (200,000 cells/well) and stimulated with and without phorbol 12-myristate 13-acetate (PMA) (20 ng/ml) plus Ionomycin (1 µg/ml) for 6 hours. An inhibitor of protein transport, Brefeldin-A (BFA) was added after 1 hour of stimulation to retain cytokines inside the cell and incubated at 37°C, 5% CO_2 (Thermo Scientific, Germany). After 6 hours of incubation, the cells were washed and stained with anti-CD8 PE-Cy7-A antibody (eBioscience, California, USA) for 30 minutes at 4°C. After staining, the cells were washed and fixed with 2% w/v formalin and permeabilized with 1% w/v saponin solution. The cell suspension was then stained with anti-IFN-γ (APC-A), anti-IL-10 (APC-Alexa 700-A) and anti-IL-17a (PE-A)

antibodies (all from eBioscience, California, USA) separately and was analyzed by BD LSRFortessa™ cell analyzer & BD FACSDiva™ v8.0 software (BD Biosciences, California, USA). For each sample, 50,000 counts were measured and an average was expressed as Cell population (% of total Lymphocytes).

2.2.31 Cytokine production by splenocytes

In vitro splenocyte stimulation with OVA was performed to analyze the production of OVA-specific cytokines. Briefly, 200,000 splenocytes were seeded into each well of 96 well round bottom plate and stimulated with OVA (10 µg/well) and incubated for 72 hours at 37°C, 5% CO_2 (Thermo Scientific, Germany). The plates were then centrifuged and supernatant of splenocyte culture was analyzed for the production of IFN-γ, IL-6, IL-10 and IL-17a using ELISA kits and strictly following manufacturer's protocol (eBioscience, California, USA) (Slutter and Jiskoot, 2010).

2.2.32 Data presentation and statistical analysis

All *in vitro* experiments were performed in triplicate and data presented as the sample mean ± standard deviation (SD). All *in vitro* cell culture related experiments were performed in triplicate and data presented as the sample mean ± standard error of mean (SEM). *In vivo* experiments were performed with at least 5 animals per treatment group and data presented as the sample mean ± standard error of mean (SEM). The statistical analysis was performed using GraphPad Prism 5.0, CA, USA, and Microsoft® Excel programmes. In general, *in vitro* results were analyzed using Student's t-test for unpaired data and with paired t-test for paired data. All *in vivo* data were analyzed by either unpaired t-test, Student's t-test, one-way Analysis of Variance (ANOVA) with Dunnett's multiple comparison test or Two-way ANOVA with Bonferroni post-test depending on the type of data. For all statistical tests $p<0.05$ was considered as statistically significant.

3. Results and Discussion

3.1 Preparation and characterization of novel mucoadhesive nanoparticles loaded with model protein bovine serum albumin (BSA)

3.1.1 Preparation of polymeric nanoparticles

Polymeric nanoparticles were prepared by ionic gelation method. Ionic gelation is based on the principle of interaction between oppositely charged polymers or oppositely charged polymer with cross-linking agents. The most commonly used cross-linking agent is sodium tripolyphosphate (TPP) for cationic polymers such as Chitosan (Bodmeier et al., 1989; Fan et al., 2012; Harde et al., 2014; Shu and Zhu, 2002). TPP is a small, chemical agent with a limited number of interactive sites. Conversely, polyanionic mucoadhesive polymers like alginate, carboxymethylcellulose, pectinate and hyaluronate have many negatively charged interactive sites leading to robust nanoparticles in combination with polycationic polymers. In the last couple of decades, some polymeric nanoparticles were prepared with polyanionic polymers in combination with chitosan and some other polycationic polymers for the delivery of biological molecules (Avadi et al., 2010; Douglas and Tabrizian, 2005; Rajaonarivony et al., 1993; Sarmento et al., 2006; Takahashi et al., 1990). Moreover, preparing polymeric nanoparticles with the ionic gelation method have several advantages over other methods such as it is a "green method" (absence of organic solvents during preparation), cost effective, provides higher stability, controlled release as well as protection of three dimensional conformation of biologicals (proteins/peptides) (Fan et al., 2012).

In present work, mucoadhesive polymers as the polyanionic component, and diethylaminoethyldextran (DEAE) as an immune modulatory polycationic component were used to encapsulate bovine serum albumin (BSA). Different polyanionic mucoadhesive polymers such as sodium salts of alginic acid (ALG), carboxymethylcellulose (CMC), hyaluronic acid (HA) and pectin (PCT) were screened to obtain higher encapsulation of BSA.

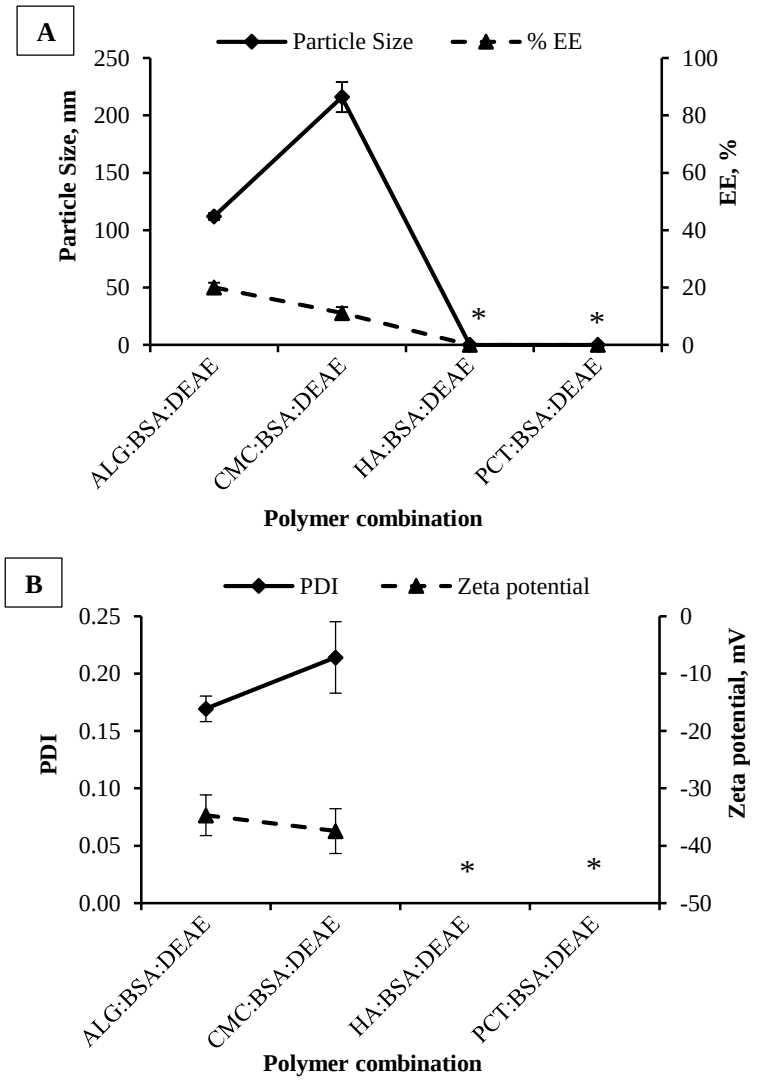

Figure 9 Effect of the combination of different mucoadhesive polymers with DEAE dextran on A) particle size and encapsulation efficiency and B) PDI and zeta potential of BSA loaded nanoparticles. (BSA loading = 30% w/v; *= aggregation, not determined; n=3; mean±SD)

ALG as a mucoadhesive polymer produced nanoparticles with maximum encapsulation of BSA (%EE = 20%), lowest particle size (~about 100 nm), narrow PDI (< 0.2), and optimal zeta potential (-34.7 mV) (Figure 9). In the case of HA and PCT, their combinations with DEAE and BSA lead to aggregation while CMC produced nanoparticles with higher particle size and lower encapsulation of BSA. The aggregation of HA-BSA and PCT-BSA complexes might be due to the neutralization of negative surface charges of polymers. This decrease in net negative surface charges of polymers led to a decrease in hydrophilicity and solubility of polymers and thus aggregation. In addition, higher viscosity of HA and PCT polymer solutions altered the kinetics of interactions between DEAE and HA/PCT polymers leading to aggregation as well (Benichou et al., 2002; Oyarzun-Ampuero et al., 2009; Oyarzun-Ampuero et al., 2013; Santander-Ortega et al., 2011). The presence of excessive sodium ions in polymer solutions might have led to the aggregation by reducing the electrostatic repulsion between particles as

explained by DLVO theory of colloid stability (Molina-Bolivar et al., 1999; Verwey and Overbeek, 1999).

Based on these results, ALG was selected as a mucoadhesive polymer of choice for further optimization of the nanoparticulate system.

3.1.2 Optimization of polymeric nanoparticles

The method of preparation of polymeric nanoparticles was further optimized with respect to the pH of BSA solution, BSA loading and polymer addition rate to improve encapsulation of BSA without affecting particle size and stability of nanoparticles and stability of BSA.

Proteins are amphoteric molecules and possess an equal number of positive and negative charges at specific pH called the isoelectric point (pI). At pH<pI, proteins are protonated and possess net positive charge while at pH>pI, the proteins are negatively charged (Benichou et al., 2002; Schmitt et al., 1998). The effect of BSA solution pH on BSA-polymers association was studied at, below and above the isoelectric of BSA (pI of BSA ~4.7).

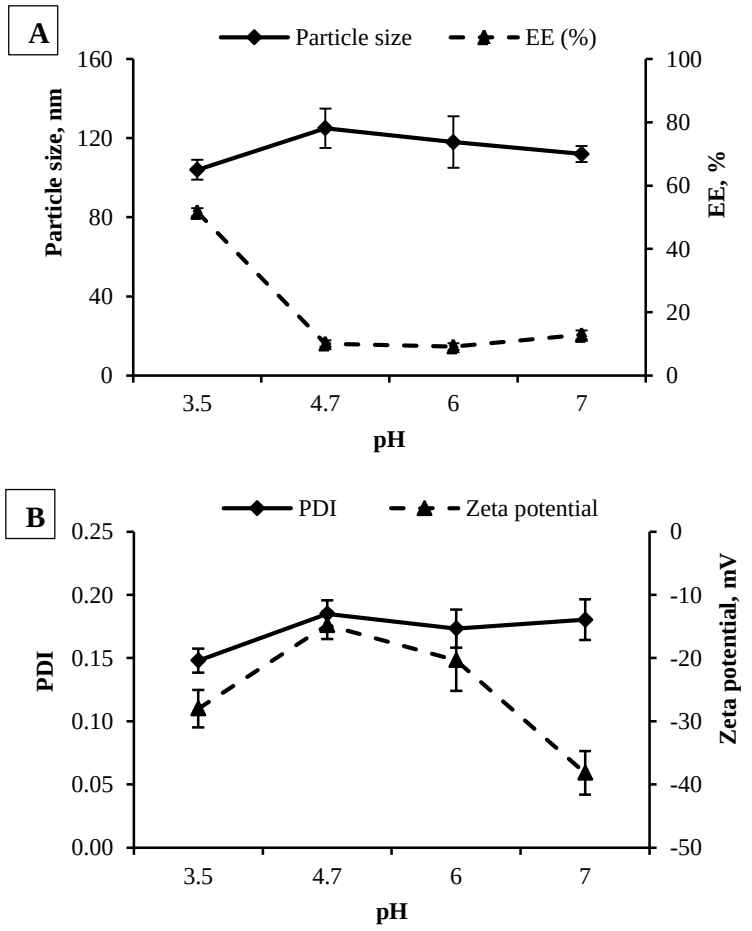

Figure 10 Effect of BSA solution pH on the A) particle size and encapsulation efficiency and B) PDI and zeta potential of BSA loaded nanoparticles. (BSA loading = 50% w/w, addition rate = 1.0 ml/min). (n=3, mean±SD)

Maximum BSA encapsulation was achieved at pH 3.5 with least particle size and optimal zeta potential (Figure 10A). The stronger interaction between protonated BSA at pH 3.5 and negatively charged ALG was predominantly electrostatic. In addition, the positively charged patches of amino acids (arginine, histidine, and lysine) in BSA structure augmented the interaction between ALG and BSA (Menchicchi et al., 2015). At pH below 3.5, the ALG polymer became highly protonated and hydrophobic attractive forces predominated over electrostatic repulsive forces. This led to coiling of ALG polymer and precipitation of ALG-BSA complex as aggregates (Menchicchi et al., 2015).

The encapsulation efficiency of BSA significantly decreased ($p<0.001$) with an increase in pH as the BSA acquired net negative surface charge and electrostatic repulsive forces overtook the attractive forces. BSA molecule has 60 surface lysine amino groups which are protonated even at physiological pH (Benichou et al., 2002; Brewer et al., 2005; Schmitt et al., 1998). They interacted with negatively charged ALG polymer and thus notable encapsulation of BSA (~13%) was observed even at pH 7.0. Decrease in zeta potential (-38 to -15 mV) of ALG-BSA-DEAE complex with a change in pH from 7.0 to 4.7 indicated neutralization of net negative surface charges of ALG (Figure 10B). At pH 3.5, the zeta potential dropped again to more negative value (-28 mV), which might be due to an excess of ALG molecules on NP surface or the attachment of some free ALG molecules on the surface of positively charged BSA and DEAE molecules after the complex formation.

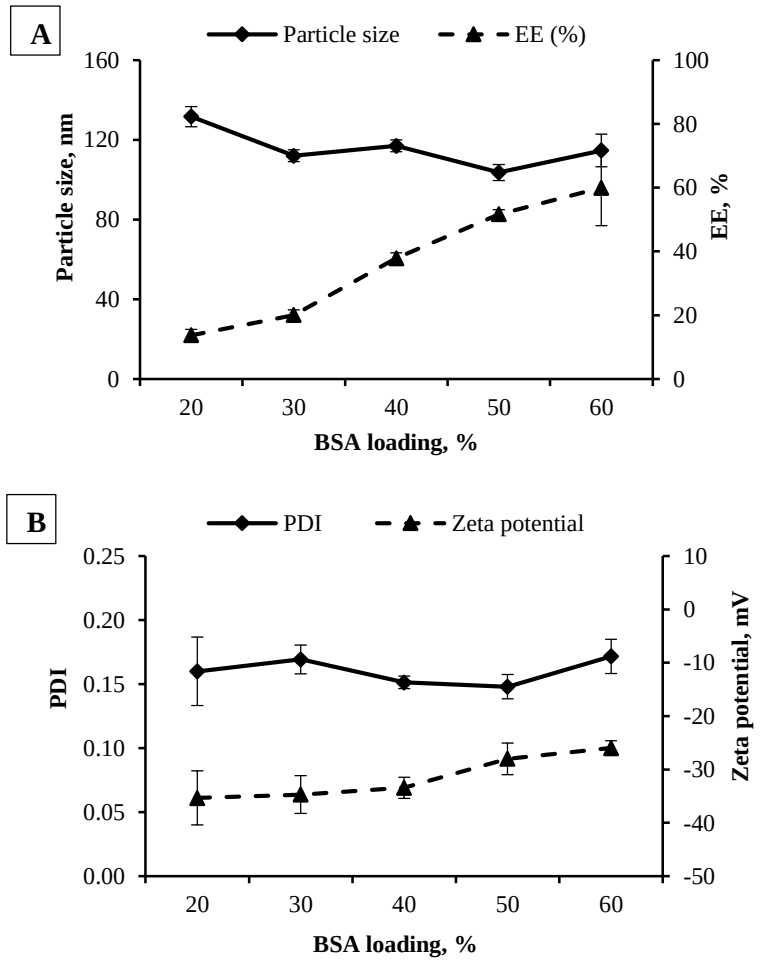

Figure 11 Effect of BSA loading on the A) particle size and encapsulation efficiency and B) PDI and zeta potential of BSA loaded nanoparticles. (BSA solution pH = 3.5, addition rate = 1.0 ml/min). (n=3, mean±SD)

The %EE of BSA increased with increase in BSA loading (Figure 11A). The association between ALG and BSA depends on the number of ionic groups available on the surface of both ALG and BSA for interaction. Moreover, the association of proteins with the polymers also depends on flexibility/structure of the proteins. The BSA is a globular protein and thus, it can interact with the polymers through the ionic sites/groups available on its surface only. The linear polymers offer the higher stoichiometric association with proteins because of a maximum number of active sites/ionic groups can interactive with the active sites on protein surface (Menchicchi et al., 2015). The BSA loading (by weight of total solids) was increased by keeping the polymer solution concentration constant and increasing the BSA solution concentration. Thus increasing in BSA loading increased BSA encapsulation until a sufficient number of interactive sites (ionic groups) on ALG were available. There was non-significant increment in %EE above 50% w/w BSA loading due to the saturation of binding sites on the

polymers. These results were in agreement with previously published work by Amadi *et. al.*, Gan *et. al.* and Xu *et.al.* (Amidi et al., 2006; Gan and Wang, 2007; Xu et al., 2003).

After the addition of BSA (pH 3.5) into the ALG polymer solution, the pH of the resultant mixture increased above the isoelectric point of BSA (4.7) and thus BSA acquired a partial negative charge. The unsaturated/available negatively charged sites of ALG as well as some negatively charged amino acids of BSA then interacted with added polycationic polymer DEAE to form an ionic complex in the size range of 100-200 nm. This interaction also reduced the net negative surface charge of BSA-ALG complex and the effect was more pronounced with an increase in BSA loading (Figure 11B**)**.

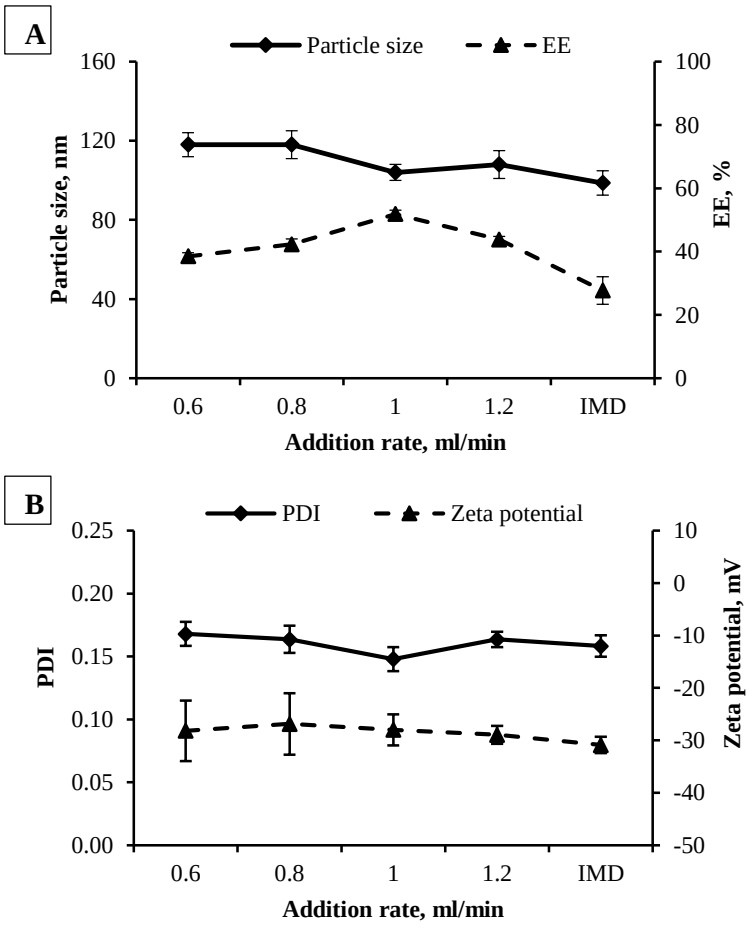

Figure 12 Effect of BSA and DEAE solution addition rate on A) particle size and encapsulation efficiency and B) PDI and zeta potential of BSA loaded nanoparticles. (IMD = immediate addition, BSA loading = 50% w/w, BSA solution pH = 3.5). (n=3, mean±SD)

In the case of ionic gelation method, the cross-linking is instantaneous due to the strong attractive forces between oppositely charged molecules. In the tested conditions, polymer/BSA addition rate has no significant effect on nanoparticles characteristics (particle size, PDI, zeta

potential) and BSA encapsulation (Figure 12). The difference in addition rate was kept small taking into consideration small batch sizes. For bigger batch sizes, the addition rates and thus differences in them might need to change which in turn will need further optimization. Thus, a small difference in addition rates has no significant effect on the encapsulation of BSA. However, the instant addition of BSA and DEAE solutions sequentially to the ALG solution led to decrease in the encapsulation of BSA and particles size. This might be due to the competition between protonated BSA and polycationic DEAE to complex with the polyanionic ALG polymer, when added straightaway. Furthermore, due to the instantaneous addition, there was insufficient time for the interaction between BSA and ALG.

3.1.3 Improvement of BSA encapsulation by dialysis of polymers

It is well documented that the subunit vaccine antigens, which are not adsorbed on the adjuvants, exist as free soluble parts and failed to stimulate the immune system (Csaba et al., 2009; Zinkernagel, 2000). Hence, it is important to adsorb maximum amount of antigen on the adjuvant and in turn reduce the dose as well as improve the efficacy of the vaccine. In addition, the controlled release of antigen from adjuvant depot assures long-term stimulation of immune system and thus long-term protection (Cox and Coulter, 1997; Kataoka and Fujihashi, 2009). An attempt was made to achieve maximum BSA encapsulation in order to reduce the volume of the formulation to be administered in the nasal cavity.

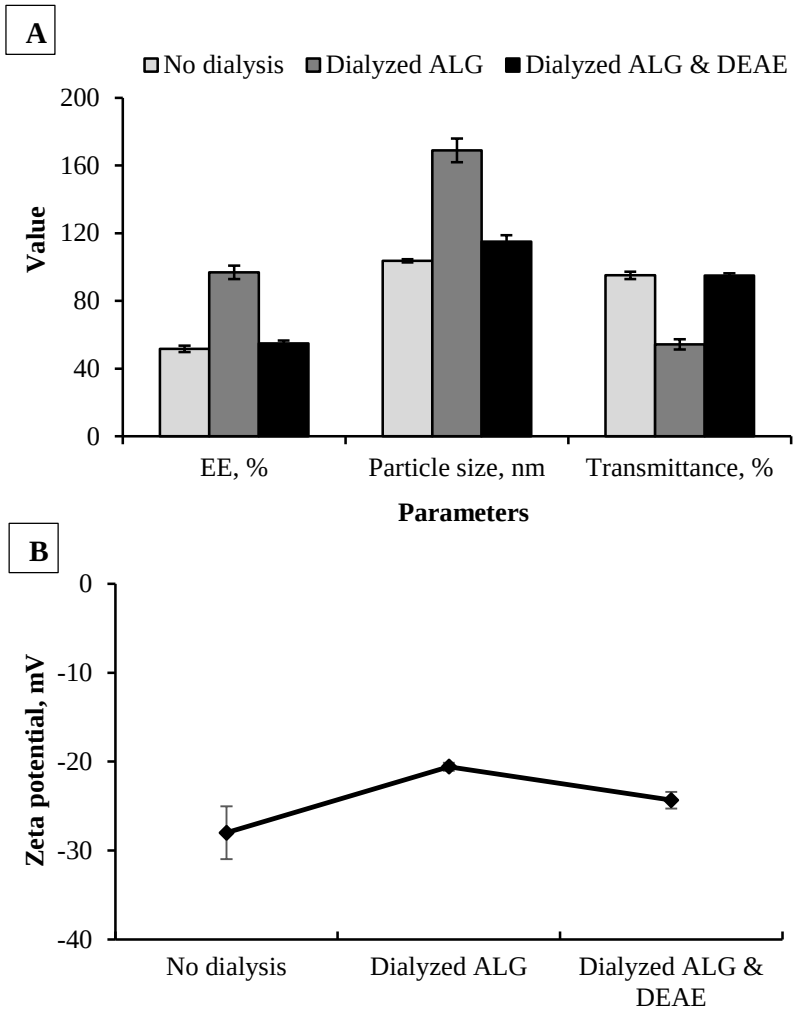

Figure 13 Effect of polymer dialysis on the A) encapsulation efficiency of BSA, particle size and % Transmittance (turbidity) and B) zeta potential of ALG-DEAE nanoparticles. (BSA loading 50% w/w, n=3, mean±SD)

As sodium ions from ALG polymer solution had very small size and higher charge density than BSA molecule, they compete with the protein molecules. To avoid the effect of sodium ions, ALG polymer solution was dialyzed against ultrapure Milli Q® water. As a result, the BSA encapsulation increased significantly (Figure 13A). The higher association between the BSA and the polymers was also confirmed by assessment of net surface charge (zeta potential) of the nanoparticle system (Figure 13B). The dialysis of ALG led to the higher association of BSA and DEAE to ALG, which also resulted in the dropping down of zeta potential from -28 mV to -20.57 mV. Additionally, DEAE polymer solution was also dialyzed to remove chloride ions which might have an effect on the interaction between BSA-ALG complex and DEAE polymer. No significant effect on BSA encapsulation or particle size was observed when both ALG and DEAE polymers were dialyzed as compared to non-dialyzed polymers. This might

be due to the stronger interaction between dialyzed ALG and dialyzed DEAE, expelling more BSA into the solution. In addition, when only ALG was dialyzed, particle size was increased due to higher encapsulation of BSA. The increase in the turbidity of the solution when measured as a function of % transmittance further confirmed the formation of larger particles encapsulating more BSA. Higher the turbidity of the solution lower is the amount of light transmitted through the sample, lower the % transmittance. Thus, dialysis of ALG polymer led to a significant increase in % EE with an increase in particle size as well as solution turbidity (lower % transmittance).

3.1.4 Fourier transform infrared (FTIR) analysis

The interactions between oppositely charged polymers and BSA was studied by Fourier transform infrared (FTIR) spectroscopy.

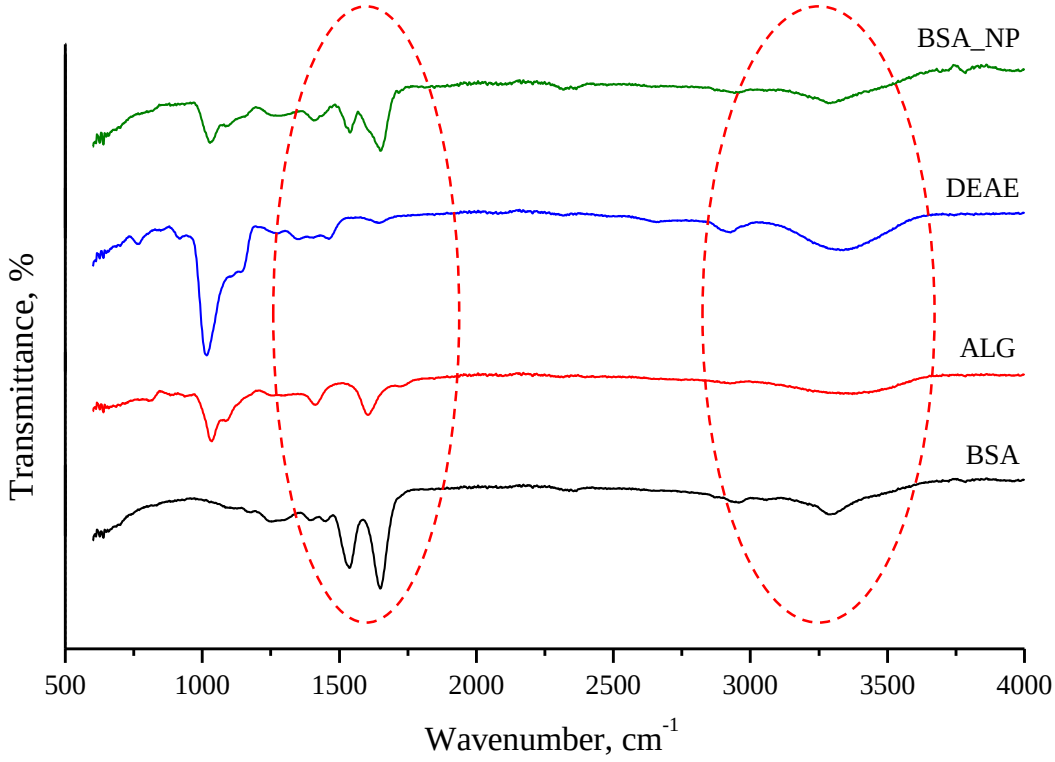

Figure 14 Overlay of FTIR spectra's of BSA, ALG, DEAE, and BSA-nanoparticles demonstrated the interaction of alginate, BSA, and DEAE-dextran to form nanoparticles. Dotted oval shapes represent regions of interactions.

The overlay of FTIR spectra (Figure 14) indicated the interactions between amide -NH of BSA and -COOH of alginate, as well as a quaternary amino group of DEAE, lead to the formation of a complex in the nanometer range. Amide-I C=O peak of BSA at 1651 cm^{-1} was broadened

and shifted to 1649 cm^{-1} in the BSA-loaded nanoparticles. The spectra also illustrated that this broadened peak partially merged into the amide-II peak of BSA at 1539 cm^{-1}. The asymmetric $-COO^-$ stretching peak of ALG at 1608 cm^{-1} broadened in the nanoparticles. Symmetric $-COO^-$ stretching peak of ALG at 1413 cm^{-1} also shifted to 1409 cm^{-1} in the nanoparticles.
The -NH stretch peak of BSA at 3296 cm^{-1} and of DEAE at 3325 cm^{-1} broadened and shifted to 3288 cm^{-1}. The -OH stretching peak from carboxylic group of BSA at 2927 cm^{-1} and of ALG at 2924 cm^{-1} was broadened with very weak intensity in BSA nanoparticles due to the hydrogen bonding. All these shifts in the wavenumbers as well as broadening of the peaks suggested the ionic interactions as well as other interactions like hydrogen bonding between polymers, resulted in the formation of nanoparticles (Borges et al., 2005; Li et al., 2007; Ribeiro et al., 2005; Sarmento et al., 2006; Shang et al., 2007; Takahashi et al., 1990).

3.1.5 In-process stability of BSA

During formulation development, proteins may break down or form larger aggregates by hydrophobic interactions or may undergo conformational changes and lose their activity (Braun and Alsenz, 1997; Cleland et al., 1993; Shire et al., 2004). These fragments or aggregates acts as either a foreign antigen and may lead to severe allergic reactions or result in loss of activity of biological molecules (Dalum et al., 1997; Kimchi-Sarfaty et al., 2013). Therefore, it is very important to ensure their structural integrity and conformational stability is maintained and it is also recommended in the FDA guidelines for Therapeutic protein products (Adm et al., 2013).

3.1.5.1 Structural integrity evaluation using gel electrophoresis (SDS-PAGE)

The structural integrity of the BSA extracted from the nanoparticles was evaluated by sodium dodecyl sulfate-polyacrylamide gel electrophoresis (SDS-PAGE).

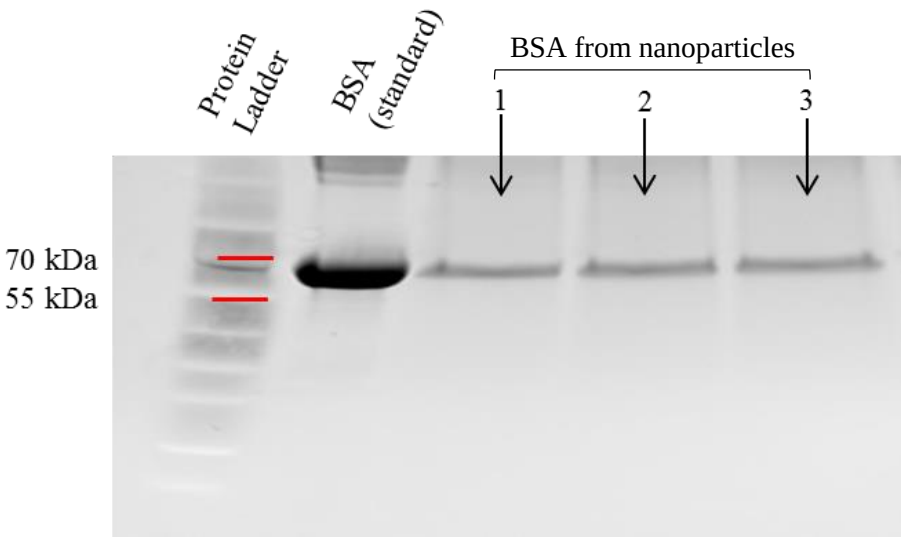

Figure 15 Gel electrophoretic analysis (SDS-PAGE) of BSA extracted from nanoparticles confirmed the structural integrity.

The appearance of the band at around 66 kDa identical to standard BSA and absence of any other bands confirmed the structural integrity of the BSA molecules (Figure 15). Changes in BSA solution pH, stirring at higher speed had no effect on the structural integrity of BSA. Moreover, the encapsulation of BSA in the nanoparticles did not affect its structural integrity.

3.1.5.2 Conformational stability

Circular dichroism (CD) is a very sensitive technique, used to analyze the conformational changes in proteins induced by certain processes or interactions with other chemicals/biologicals molecules. A typical CD spectrum of BSA is characterized by two negative bands at 208 nm and 222 nm, which are confined to the $\pi \rightarrow \pi^*$ and $n \rightarrow \pi^*$ transitions, respectively (Ali et al., 2015; Price, 2000; Yang and Gao, 2002), the so-called negative Cotton effect in the peptide bond of α-helix (Greenfield, 1982; Staprans and Watanabe, 1970).

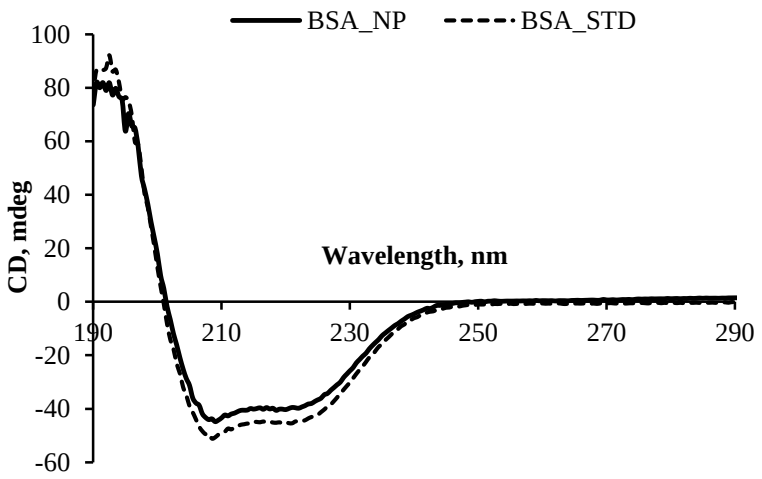

Figure 16 Overlay of CD spectra of BSA standard (BSA_STD) and BSA extracted from nanoparticles (BSA_NP) obtained to assess the conformational stability of protein.

The characteristic α-helix minima at 208 and 222 nm in the individual CD spectrum of standard BSA (BSA_STD) and BSA extracted from the nanoparticles (BSA_NP) confirmed the conformational stability of the BSA (Figure 16). The superimposable CD spectra of BSA extracted from nanoparticles with the BSA_STD indicated no loss in the secondary structure of BSA due to various formulation process related factors.

3.1.6 *In vitro* BSA release from nanoparticles

In general, the drug molecules located/adsorbed on the surface of particles lead to the initial burst effect (Zarate et al., 2011). In previous work by Almeida *et. al.*, it was observed that at lower pH, the ALG matrix contracts and thus retain more drug inside which in turn reduced the drug release (Almeida and Almeida, 2004). On the other hand, the presence of small counter-ions with higher charge density like PO_4^{3-} and Na^+ increase the release of drug/protein from the alginate matrix (Ramdas et al., 1999).

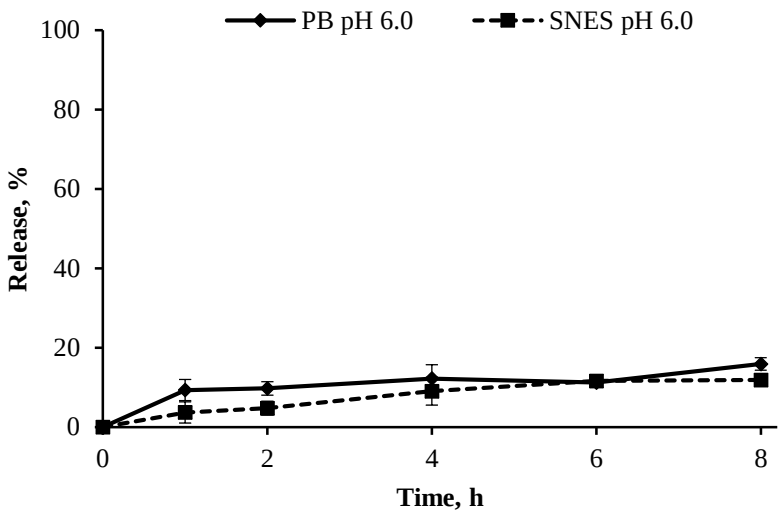

Figure 17 *In vitro* release of BSA from polymeric nanoparticles in phosphate buffer pH 6.0 and simulated nasal electrolyte solution (SNES) pH 6.0. (n=3, mean±SD)

BSA release from the nanoparticles was slow and controlled (~15% released in 8 hours) without any burst effect (Figure 17). The BSA was strongly associated with ALG and DEAE by ionic as well as other interactions and thus, the release was significantly slow. A sufficient number of small ions (like PO_4^{3-}, K^+, Cl^- and Na^+) present in the buffer/release medium acted as counter ions to break ionic bonds between BSA and ALG/DEAE and released BSA in the medium.

Similar findings were reported in the literature for alginate matrix systems with the additional coating of polycationic polymers. The cationic polymer coating significantly reduced the erosion of ALG matrix and thus retained more drug/protein inside the matrix (Hassan, 1991; Ramdas et al., 1999; Xu et al., 2003; Zarate et al., 2011).

Prolonged release of subunit vaccine antigen assures continuous and efficient stimulation of the immune system. In addition, the maximum amount of antigen should be associated with the nanoparticles until it reaches the macrophages, where they are engulfed and processed to present to components of immune system. The higher release would have lowered the amount of antigen reaching the macrophages. In addition, the protein/vaccine antigen released into the nasal cavity would have degraded by enzymes. Altogether it would have led to the failure of the delivery system. The controlled release profile achieved by encapsulating BSA in the nanoparticles and mucoadhesive property imparted by ALG polymer will ensure maximum uptake and availability of BSA/vaccine antigen to modulate desired immune response.

The release profile of BSA in phosphate buffer pH 6.0 and SNES pH 6.0 was comparable since the ionic strength of these two release media was similar (~0.2 M).

3.1.7 *In vitro* mucoadhesion measurement

3.1.7.1 Assessment of in vitro mucoadhesion using Texture Analyzer

Mucoadhesion as a function of detachment force between polymers/nanoparticles and mucin-agar gel was measured using a Texture analyzer.

The alginate is a known mucoadhesive polymer and it interacts with mucin by forming hydrogen bonding with a sialic acid hydroxyl group (–OH). ALG also interacts electrostatically with positive patches (arginine, histidine, and lysine) in the mucin protein backbone. At pH 6.0, DEAE dextran through its positively charged quaternary amino group interacts with negatively charged mucin by electrostatic interactions. In addition to hydrogen bonding and electrostatic interactions, the proteins can also interacts with sulfur-containing amino acids (cysteine, methionine) of mucin by forming disulfide bonds (Bernkop-Schnurch et al., 2001; Gåserød et al., 1998; Menchicchi et al., 2015; Serp et al., 2000; Shilpa et al., 2003; Taylor Nordgård and Draget, 2011).

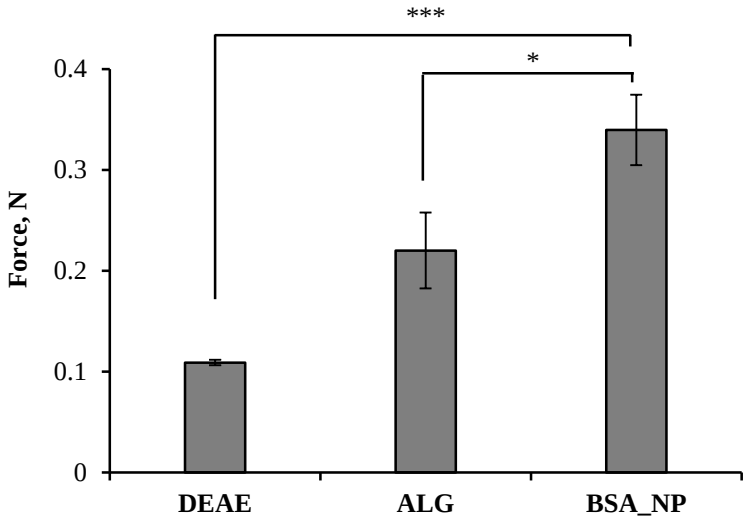

Figure 18 Detachment force (N) between DEAE/ALG/BSA_NP and the mucin-agar gel was measured to assess mucoadhesive potential. (n=3, mean±SD, *$p<0.05$, ***$p<0.001$).

The detachment force was significantly higher for the BSA_NP as compared to ALG ($p<0.05$) and DEAE ($p<0.001$) (Figure 18). The BSA_NP was a combination of ALG, DEAE, and BSA. The higher detachment force required for the BSA_NP was due to strong interactions with the mucin particles. As mentioned above the interactions involved could be electrostatic, hydrogen bonding, hydrophobic interactions. The surface bound BSA molecules, if any, could have also interacted by forming disulfide bonds with the amino acids (cysteine, methionine) of mucin proteins. These all interactions led to the higher mucoadhesive potential than polymers alone.

3.1.7.2 In vitro mucoadhesion as a function of zeta (ζ) potential

Since there are electrostatic interactions involved between mucin and polymer/protein molecules, the measurement of net surface charge could be a handy tool to determine the extent of the mucoadhesive potential of polymers or protein-polymer complex (nanoparticles). The zeta potential of mucin-polymers/mucin-nanoparticles mixture was measured and compared with the zeta potential of mucin suspension.

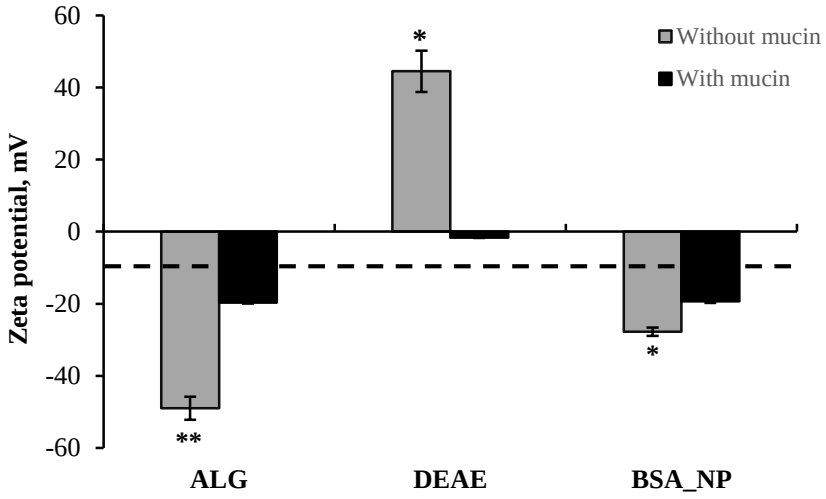

Figure 19 Mucoadhesive potential of ALG, DEAE and BSA nanoparticles was measured as a function of the change in zeta potential. Dotted line represents zeta potential of 1% w/v mucin suspension. (n=3, mean±SD, *$p<0.05$, **$p<0.01$)

There was a significant change in the zeta potential of mucin particles (-8.39±0.14 mV) after interaction with ALG ($p<0.01$), DEAE ($p<0.05$) and BSA_NP ($p<0.05$) (Figure 19). The change in mucin surface charge was due to the various interactions with ALG, DEAE, and BSA_NP as mentioned in the section 3.1.7.1. In BSA-loaded nanoparticles, due to the interactions between BSA and polymers, less number of active sites/ionic groups were available to interact. On the other hand, the uncoiling along with higher flexibility in aqueous solution contributed to stronger interactions between ALG/DEAE and mucin particles. This might have led to the contradictory results of mucoadhesive potential as compared to those obtained with the texture analyzer.

3.1.8 *In vitro* cytotoxicity study

To assess the biocompatibility of nanoparticles and polymers as a function of cell membrane integrity, the lactate dehydrogenase (LDH) assay was performed. The harmful interactions of

polymers/nanoparticles may lead to cell membrane disruption and cell death. The cell membrane disruption leads to increased level of the lactate dehydrogenase (LDH) enzyme in extracellular fluid, which can be quantified by LDH assay (Lemarchand et al., 2006).

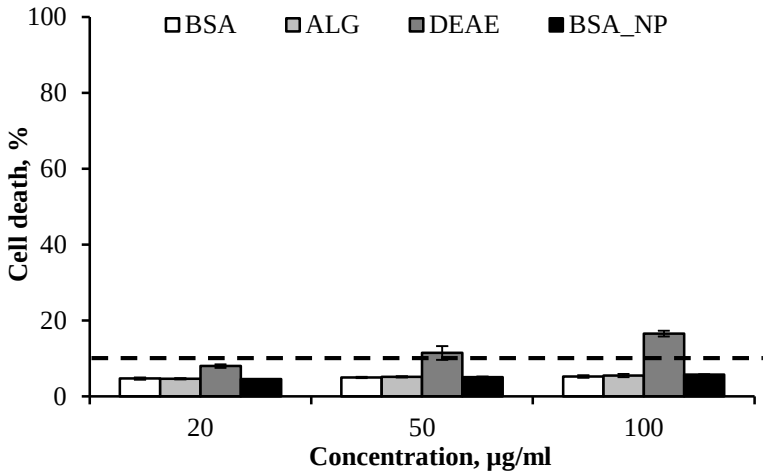

Figure 20 Percentage cell death after 24 hours of THP-1 cells incubation with different concentrations of polymers and BSA nanoparticles. 1% v/v Triton-X 100 was used as positive control, considering it causes 100% cell death. Dotted line represents cytotoxicity limit (> 10% cell death). (n=3, mean±SEM)

The nanoparticles, as well as ALG and BSA, showed no toxic effect while DEAE showed toxic effects on THP-1 cells (Figure 20). The DEAE dextran is a known cytotoxic polymer at a higher dose and thus at 50 and 100 µg/ml showed toxicity (> 10% cell death) (Fischer et al., 2003). Due to interactions with ALG and BSA, the quaternary ammonium groups of DEAE were not available to interact with the cell membrane and thus no toxic effect of BSA nanoparticles was observed.

3.1.9 Freeze-drying of nanoparticle formulation

When colloidal nanoparticles are stored as aqueous suspensions for a longer period of time, the physical and chemical stability are compromised (Abdelwahed et al., 2006b; Chacon et al., 1999). The freeze drying of the formulation or drug products, especially biologics, is extremely important considering the solution state stability of drug substance in addition to possible interactions of drug/biologics with excipients where solvents/dispersant medium plays catalytic function. Freeze-drying imparts additional stability to the formulation as well as ease in transport, storage of the finished products. It is also an important technique to improve the long-term stability of colloidal submicronic systems.

The freeze-drying process generates a lot of stress especially of freezing and dehydration which could destabilize the colloidal nanoparticle suspensions. The crystallization of water during freezing also generate mechanical stress, which further tend to destabilize the nanoparticles suspension. The addition of stabilizers, which acts as a cryoprotectant (against freezing stress) and/or lyoprotectant (against drying stress), protects the colloidal nanoparticles suspensions from those shocks. Furthermore, the concentration of these stabilizers, as well as the ratio of stabilizers to nanoparticles (w/w), is crucial to ensure efficient freeze-drying (De Jaeghere et al., 1999; Schwarz and Mehnert, 1997). Thus, it is necessary to optimize the process of freeze-drying thoroughly with respect to the type and concentration of cryoprotectants.

BSA-loaded polymeric nanoparticles were freeze-dried and the process was optimized to obtain stable freeze-dried formulation.

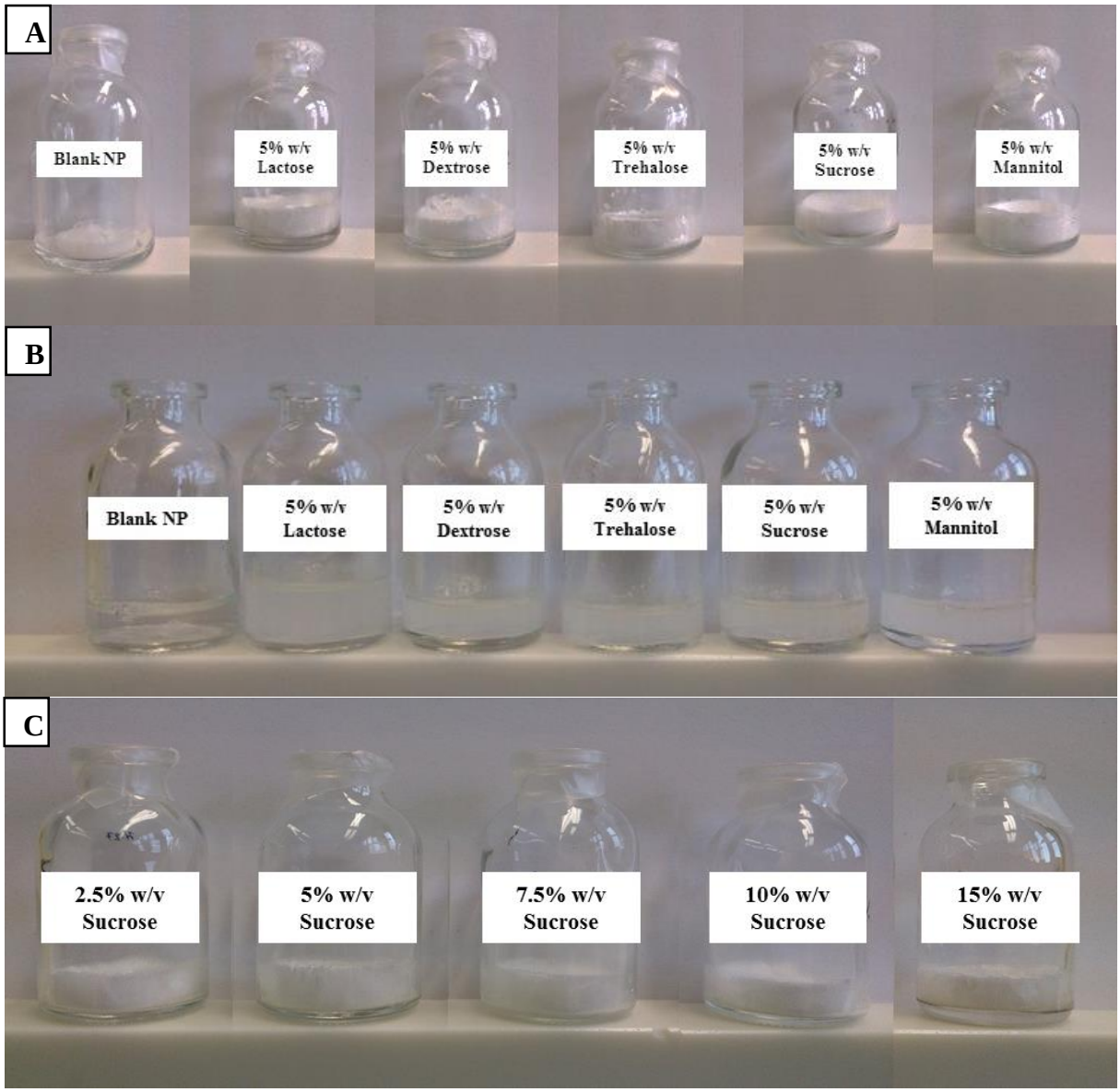

Figure 21 Photographs of freeze-dried nanoparticles formulations and redispersed nanoparticles suspension with Milli Q® water. A) effect of different cryoprotectants like lactose, dextrose, trehalose, sucrose and mannitol (5% w/v) on cake morphology, B) redispersibility of freeze-dried nanoparticles stabilized with different cryoprotectants and C) effect of different concentrations (2.5-15% w/v of nanoparticle suspension) of sucrose on cake morphology.

As shown in Figure 21A, all of the nanoparticle formulations containing cryoprotectants formed intact porous cake while nanoparticle formulation without any cryoprotectants (Blank-NP) formed a collapsed cake. The redispersibility index (Ri) which is a ratio of particle size after redispersion of freeze-dried cake to initial particle size is the measure of the efficiency of the freeze-drying process and it should be closer to 1. The particle size of the redispersed nanoparticles in Milli Q® water was significantly affected by the type of cryoprotectant used (Figure 21B, Table 6). Lactose at the concentration of 5% w/v led to about 8-fold increase in

particle size while 5% w/v sucrose stabilized nanoparticles with 1.8-fold increment in the particle size after redispersion, being the lowest among the group.

Table 6 Effect of different cryoprotectants at 5% w/v concentration on the redispersibility index (Ri) of the freeze-dried nanoparticles. (* = Not-redispersible). (n=3, mean±SD)

Sample	Particle size (nm)±SD	Ri	PDI±SD
Initial	132±1	-	0.147±0.019
NP+Lactose	1034±35	7.772	0.418±0.042
NP+Dextrose	247±4	1.86	0.163±0.011
NP+Trehalose	274±18	2.058	0.208±0.033
NP+Sucrose	**236±7**	**1.772**	**0.133±0.003**
NP+Mannitol	259±1	1.945	0.241±0.008
Without cryoprotectant	*	*	*

Table 7 Effect of concentration of sucrose (% w/v) on the redispersibility index (Ri) of the freeze-dried nanoparticles. (n=3, mean±SD)

Sample	Particle size (nm)±SD	Ri	PDI±SD
Initial (0% w/v)	124±2	-	0.158±0.010
2.5% (w/v) Sucrose	255±7	2.051	0.168±0.017
5% (w/v) Sucrose	236±7	1.772	0.133±0.003
7.5% (w/v) Sucrose	176±10	1.418	0.112±0.008
10% (w/v) Sucrose	**173±11**	**1.389**	**0.110±0.007**
15% (w/v) Sucrose	175±9	1.408	0.182±0.008

The freeze-drying process was further optimized using different concentrations of sucrose as a cryoprotectant. Sucrose in a concentration range of 2.5 to 15% w/v formed a porous intact mass of freeze-dried nanoparticles and the minimum redispersibility index (Ri) was obtained at 10% w/v sucrose concentration (Table 7). Sucrose formed a three-dimensional amorphous structure around the nanoparticles and thus prevented nanoparticles aggregation. At 10% w/v concentration, sucrose already reached the limit of stabilization (minimum Ri) and was selected as an optimum concentration for freeze-drying of formulations for stability study.

3.1.10 Stability study of lyophilized BSA loaded nanoparticle formulation

Stability study of a pharmaceutical formulation is necessary to claim a shelf life of the formulation and propose storage condition. Stability study of freeze-dried BSA loaded nanoparticles was performed according to the International Conference on Harmonization (ICH) guidelines (CPMP/ICH/2736/99).

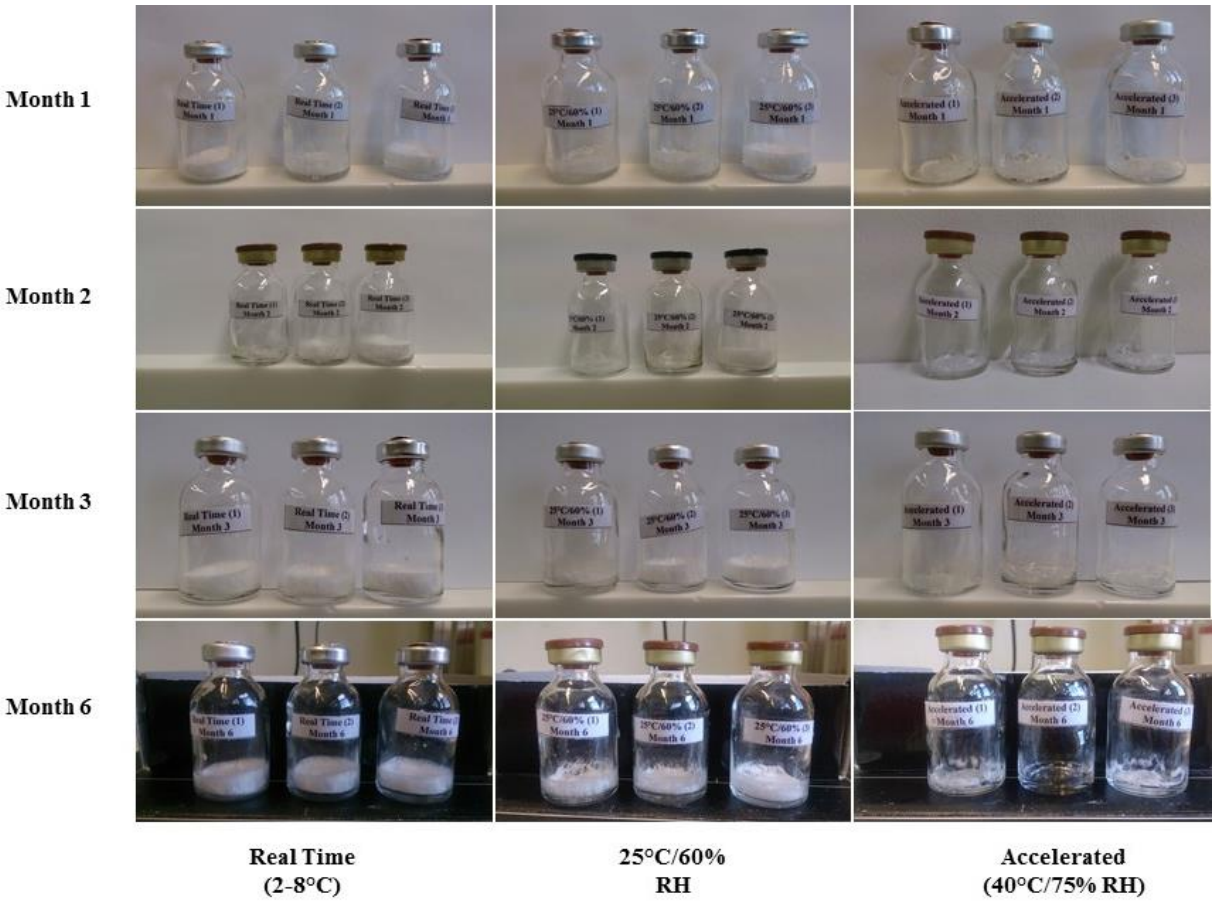

Figure 22 Photographs of freeze-dried nanoparticle formulations (cake morphology) kept at different storage conditions. (n=3)

The freeze-dried nanoparticles stored at 2-8°C and 25°C/60% RH conditions showed no significant change in morphology of freeze-dried cake while samples stored at 40°C/75% RH condition were melted and took a long time to redispersed in Milli Q® water (Figure 22). Furthermore, no significant differences in the particle size, PDI and zeta potential of nanoparticles stored at 2-8°C and 25°C/60% RH conditions was observed (Table 8). Controversially, freeze-dried nanoparticles stored at 40°C/75% RH condition showed a significant increase in the particle size and PDI over the period of 6 months, indicating aggregation after melting of the freeze-dried cake. Due to the strong interference of sucrose in

the BCA protein assay, the encapsulation efficiency, recovery, and BSA release study after redispersion could not be performed.

To confirm the physical integrity and conformational stability of the encapsulated BSA, its gel electrophoresis (SDS-PAGE) and CD spectra were obtained, respectively (Figure 23). The structural integrity of BSA was conserved in the freeze-dried nanoparticles stored at tested stability conditions (Figure 23A). There was no aggregation (size > 66 kDa) or fragmentation (size < 66 kDa) in the BSA molecule and its conformational stability was also maintained at tested storage conditions and duration considered. There was no effect of the melting of the freeze-dried cake in the samples stored at 40°C/75% RH on two negative bands at 208 and 222 nm which is characteristics for the α- helix of the proteins (Figure 23B). The CD spectra of the BSA stored at 40°C/75% RH showed a slight shift from other two spectra, might be due to the difference in concentration of BSA extracted from the redispersed nanoparticles.

Table 8 Properties of the freeze-dried nanoparticles kept at different storage conditions for a different period. (n=3, mean±SD)

Condition →	2-8°C			25°C/60% RH			40°C/75% RH		
Timepoint ↓	Size (nm)	PDI	Zeta Potential (mV)	Size (nm)	PDI	Zeta Potential (mV)	Size (nm)	PDI	Zeta Potential (mV)
Initial	224±25	0.183±0.012	-24.48±2.68	224±25	0.183±0.012	-24.48±2.68	224±25	0.183±0.012	-24.48±2.68
Month 1	247±21	0.198±0.02	-22.89±0.96	221±15	0.176±0.030	-22.44±0.48	330±16	0.297±0.040	-22.37±0.78
Month 2	251±32	0.204±0.035	-24.53±097	242±22	0.192±0.031	-24.96±2.22	356±13	0.465±0.030	-25.75±0.88
Month 3	258±21	0.201±0.017	-23.63±1.11	236±15	0.195±0.032	-24.77±1.27	481±23	0.37±0.049	-24.68±1.20
Month 6	243±31	0.203±0.026	-25.14±2.41	235±31	0.210±0.035	-29.75±4.73	521±31	0.479±0.063	-27.27±2.23

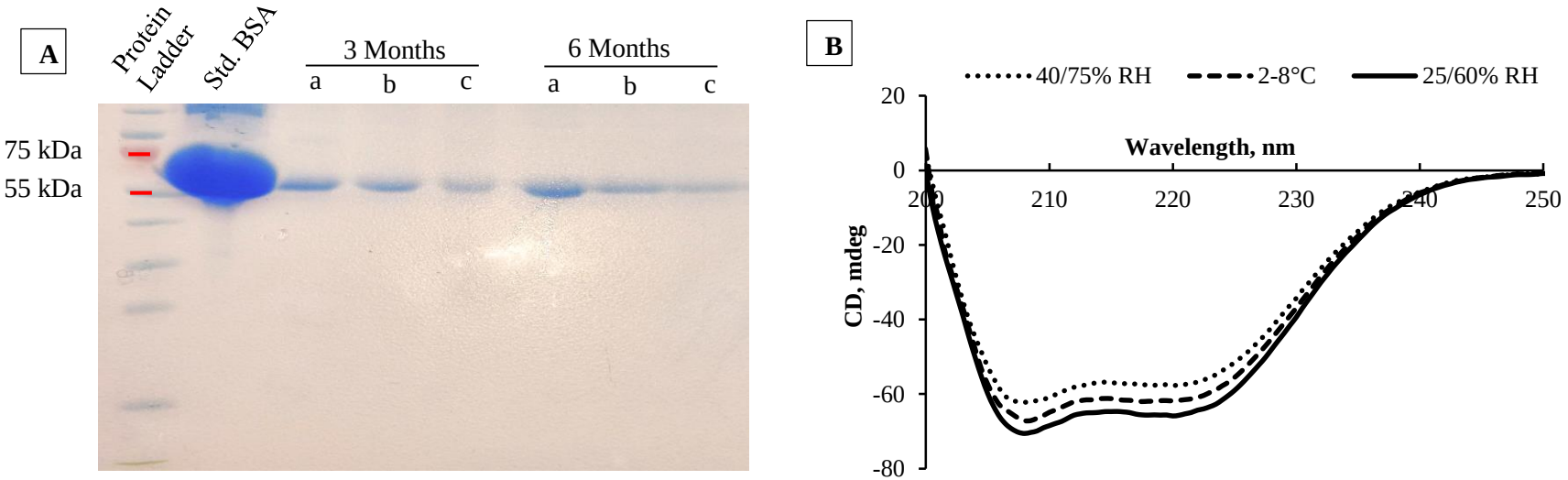

Figure 23 Structural integrity and conformational stability of BSA extracted from stability samples evaluated using (A) Electrophoresis technique (SDS-PAGE) and (B) CD spectroscopy, respectively. Stability conditions: a) 2-8°C, b) 25°C/60% RH, c) 40°C/75% RH.

From the stability study, it could have been concluded that BSA molecule was stable in the samples stored at 40°C/75% RH, although significant changes in the cake morphology, particle size and PDI of nanoparticles occurred. Thus, the best-suited storage conditions for the BSA-loaded, freeze-dried nanoparticles are at refrigerated conditions (2-8°C) or at room temperature conditions (25°C).

3.2 Preparation, characterization and *in vitro* and *in vivo* evaluation of Tetanus toxoid loaded novel mucoadhesive nanoparticles

3.2.1 Preparation and optimization of Tetanus toxoid loaded nanoparticles

Tetanus toxoid (TT) is a two-chain protein and have a higher isoelectric point (pI 6.0) as compared to BSA (pI 4.7). Due to two different isoelectric points of two peptide chains i.e. light (pI 4.8) and heavy (pI 7.2), the stability of TT is compromised significantly with change in pH (Craven and Dawson, 1973; Montecucco and Schiavo, 1995; Weller et al., 1989). The preparation method optimized for the BSA-loaded nanoparticles was implemented to prepare tetanus toxoid (TT) loaded nanoparticles (section 2.2.1-2.2.3). Reduction in pH below 5.0 unit led to the aggregation of TT which was detected by the development of turbidity in TT solution. The aggregation was reversible and after increasing pH above 5.25±0.1 units, the solution became clear again. Based on the observations, the method was modified to avoid the aggregation of TT and achieve higher encapsulation of it. The TT solution was dialyzed for 2 hours against Milli Q® water, pH adjusted to 5.3±0.05 followed by preparation of nanoparticles as per optimized method. The nanoparticles obtained were around 150 nm in size with a zeta potential of -24.0 mV and encapsulation efficiency of around 54%. To increase the TT encapsulation, the method was further modified. The pH of the ALG-TT solution mixture was changed and its effect on characteristics of the nanoparticles was studied.

Table 9 Effect of pH on the particle size, PDI, zeta potential and encapsulation efficiency (%EE) of TT loaded nanoparticles. (*= Aggregates observed, # = not determined). (n=3, mean±SD)

pH	Particle size (nm)	PDI	Zeta Potential (mV)	% EE
4.0	*	#	#	#
4.5	**142±9**	**0.154±0.002**	**-25.68±3.22**	**78.50±5.44**
5.0	121±5	0.141±0.012	-31.02±3.41	29.45±1.02
6.0	145±12	0.180±0.050	-36.51±2.23	19.36±1.30

Optimization of the method with respect to the pH of ALG-TT mixture showed maximum encapsulation at pH 4.5. At pH 4.0, aggregates were formed which might be due to the instability of TT at acidic pH (Table 9).

With the increase in pH, the encapsulation efficiency of nanoparticles further decreased due to the deprotonation of TT. This eventually led to stronger repulsive forces between polyanionic

ALG polymer and neutral/negatively charged TT. The stronger attractive forces between polyanionic ALG and polycationic DEAE as well as the bigger size of TT as compared to BSA also contributed to lower encapsulation efficiency of nanoparticles for TT with an increase in pH (above 4.5). No further optimization was performed, as the encapsulation efficiency of 78% was sufficient to compare the efficacy with marketed formulation (BE tt™).

3.2.2 Structural integrity evaluation of Tetanus toxoid using gel electrophoresis (SDS-PAGE)

The in-process stability assessment for the biologicals is very important as their pharmacological activity depends on structural integrity as well as conformational stability. Fragmentation of the vaccine antigen during formulation does not only lead to a loss in activity but may cause severe allergic reactions. The allergic reactions/side effects are due to the generation of new protein fragments/peptides which acts as allergens and trigger stronger immune responses (Adm et al., 2013; Dalum et al., 1997; Kimchi-Sarfaty et al., 2013).

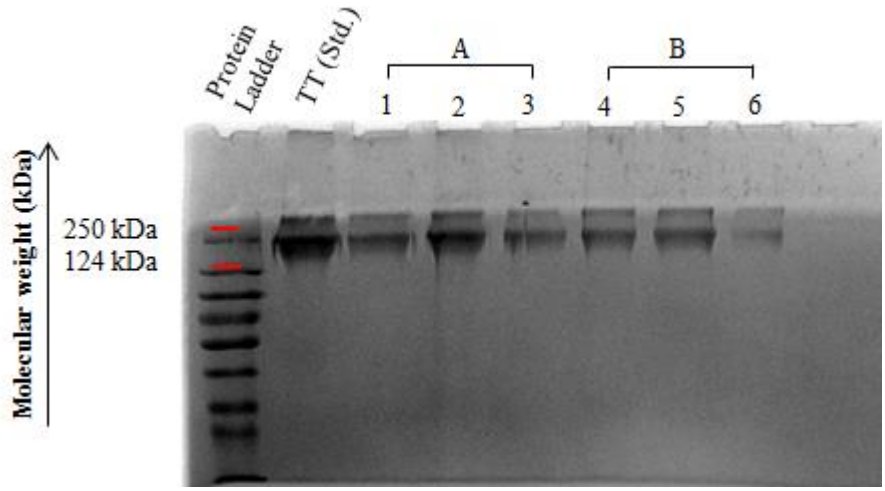

Figure 24 Polyacrylamide gel (SDS-PAGE) electrophoresis confirmed the structural integrity of TT. A) TT extracted from nanoparticles B) Free TT from release study.

The single protein band observed below 250 kDa mark in all samples confirmed the structural integrity of the TT encapsulated in the nanoparticles (Figure 24). The TT released in the phosphate buffer pH 6.0 (incubated at 37°C for 8 hours) also maintained the structural integrity (Figure 24B). The association of TT with the ALG and DEAE polymers further prevented it from aggregation (no protein bands at or above 250 kDa) which might have occurred due to the changes in pH as well as the absence of stabilizing buffer ions.

3.2.3 *In vitro* TT release from nanoparticles

As mentioned and explained thoroughly in the section 3.1.6, the release of drug/proteins from ionically crosslinked matrices depends on the concentration of small ions (PO_4^{3-}, Cl^-, K^+ and Na^+), which possess high charge density (Ramdas et al., 1999).

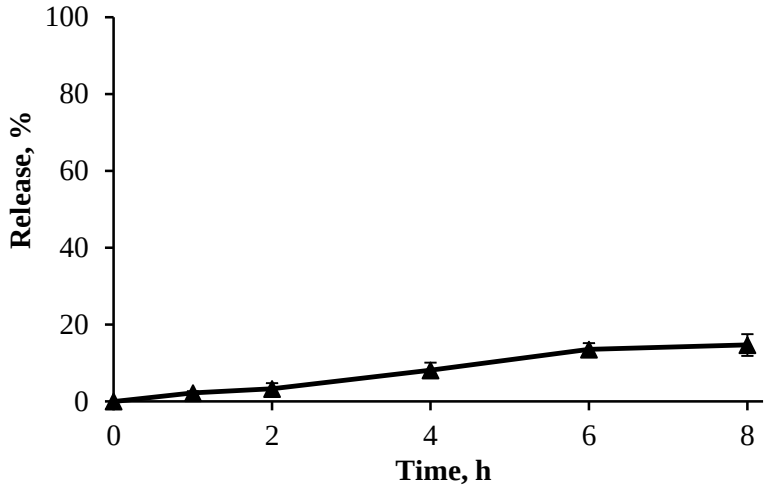

Figure 25 *In vitro* release of TT from polymeric nanoparticles in pH 6.0 phosphate buffer (50% TT loading). (n=3, mean±SD)

The release of TT from the nanoparticles was very slow and controlled without any burst effect over the period of 8 hours (Figure 25). The ions like K^+, Cl^- and Na^+ present in the buffer/release medium have small sizes and thus high charge density, which competes for the ionic sites on the polymers. These small ions with higher charge density displaced the TT from the ALG-TT-DEAE complex and released it in the medium. The stronger interactions between ALG, TT and DEAE resulted in the slower release of TT from the nanoparticles (~15% released in 8 hours). The release profile for TT nanoparticles was similar to the release profile of BSA nanoparticles and there was no effect of bigger size and structural difference of TT on release profile. The controlled release of TT/vaccine antigen is highly desired as it retains a higher amount of TT inside nanoparticles and thus will protect it from enzymatic degradation in the nasal cavity. Moreover, the controlled release will present the TT to components of the immune system for a longer duration, thereby ensuring long-term protection from infection. Furthermore, the released TT/vaccine antigen would also have cleared out of the nasal cavity by the nasal mucociliary clearance.

3.2.4 *In vitro* proliferation assay

To assess the effect of nanoparticles (with or without TT) on the metabolic activity of human nasal epithelial cells (RPMI 2650), *in vitro* proliferation (MTT) assay was performed. The inhibition of metabolic activity depends on the polymer/excipient structural characteristics, concentration as well as the time of incubation. In general increase in concentration and incubation time reduces the metabolic activity of the cells. The dose of TT is 5 Lf unit which corresponds to around 18 µg of protein content. Thus, the Blank_NP and TT_NP with three different concentrations viz. 20, 50 and 100 µg/ml were tested for an incubation period of 48 hours.

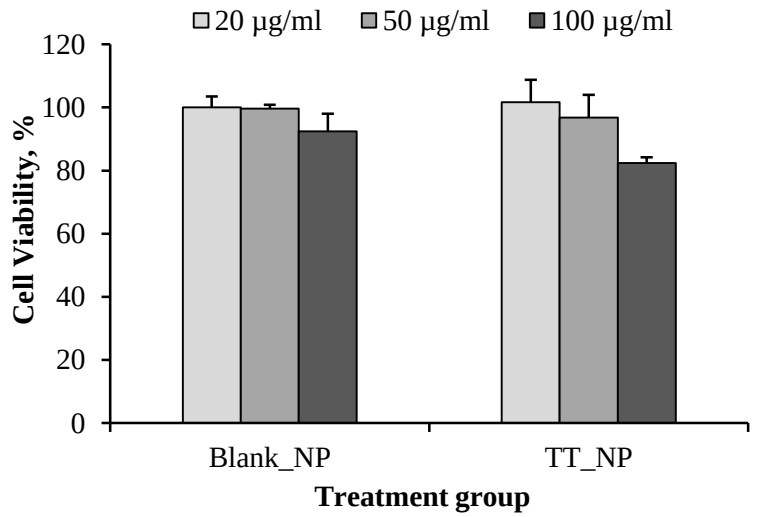

Figure 26 Percentage cell viability 48 hours after incubation of human nasal epithelial cells with different concentrations of Blank_NP and TT_NP. 1% v/v Triton-X 100 was used as positive control, considering it causes 100% cell death. (n=6, mean±SEM).

At lower concentrations i.e. 20 and 50 µg/ml, there was no significant effect on the metabolic activity of the human nasal epithelial cells (Figure 26). Contrary, both Blank_NP and TT_NP affected the metabolic activity of cells at higher concentration i.e. 100 µg/ml. A significant effect of TT_NP (at 100 µg/ml) on metabolic activity could be due to the higher concentration of DEAE which was present on the surface of nanoparticles. The presence of TT in TT_NP could have increased the number of free quaternary ammonium groups of DEAE on the surface of nanoparticles and thus led to higher toxicity as compared to blank nanoparticles. The higher ratio of nanoparticles to cells (at 100 µg/ml) could have also increased the uptake of nanoparticles and consequently higher effect on the metabolic activity of the cells (Fischer et al., 2003; Morgan et al., 1989; Tang et al., 2014). The results were in accordance with the

findings of Fischer *et. al.* in which the high molecular weight (500 kDa) DEAE-dextran polymer solution (1 mg/ml) showed severe toxicity in L929 cells when incubated for 12 to 24 hours (Fischer et al., 2003). As the DEAE was complexed with nanoparticles, the less number of free quaternary amino groups were available to interact as compared to DEAE polymer alone and thus showed less toxicity in RPMI 2650 cells.

3.2.5 *In vitro* macrophage uptake study

In general, the macrophages recognize nano/mico-particles as foreign objects and rapidly internalize them to eliminate from the body. This is a part of our body's defense mechanism. Once crossed the nasal epithelial membrane, nanoparticles are rapidly engulfed by macrophages, which process them further through phagocytosis. During phagocytosis, acidic pH and several enzymes inside macrophages breaks down the nanoparticles and the antigenic components/proteins are processed and presented to the components of the immune system (CD4 and CD8 cells). Internalization of the nanoparticles inside the macrophages generally occurs within first 30 to 60 min. of incubation (Cannon and Swanson, 1992; Davda and Labhasetwar, 2002; Lemarchand et al., 2006).

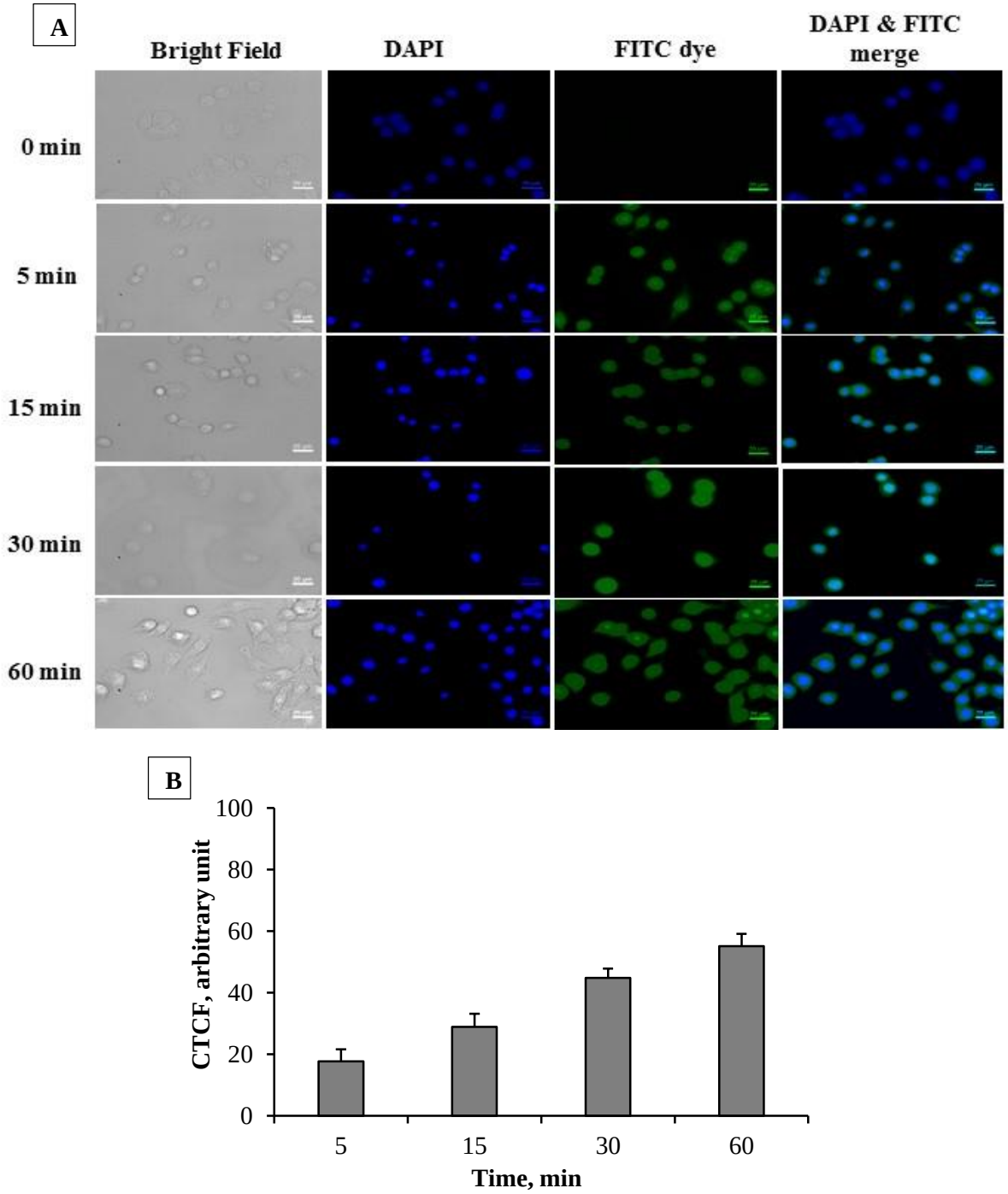

Figure 27 A) *In vitro* uptake of FITC-labeled nanoparticles in murine macrophage cell line (RAW 264.7) at different incubation time. B) Fluorescence intensity of labeled nanoparticles was quantified using ImageJ software and presented as CTCF (an arbitrary unit) vs time. (n=6, mean±SD)

The uptake of FITC labeled nanoparticles was time dependent and observed as early as 5 min. after incubation at 37°C (Figure 27). The fluorescence intensity, as measured by fluorescence microscope, increased with time, specifically in the cytoplasm region (Figure 27A). The overlay of DAPI dye stained nucleus images with and FITC labeled nanoparticles images showed the intensity of FITC in cell cytoplasm increased with the time. The quantification of

fluorescence intensity using ImageJ software showed a significant increase in uptake at 60 min. (Figure 27B). The nanoparticle uptake at 60 min. increased by 3-folds as compared to uptake after 5 min. of incubation.

Although, it is well documented that the uptake of positively charged nanoparticles is higher due to the better interaction with negatively charged cell surfaces, no significant effect on the uptake of negatively charged polymeric nanoparticles was observed. The nanoparticles might have attached to the cells surfaces and entered by other mechanisms like specific receptors mediated internalization.

3.2.6 *In vivo* immunization study of Tetanus toxoid loaded nanoparticles

The humoral immune response produced against tetanus toxoid was measured by analyzing the TT-specific antibodies in serum collected at different time points.

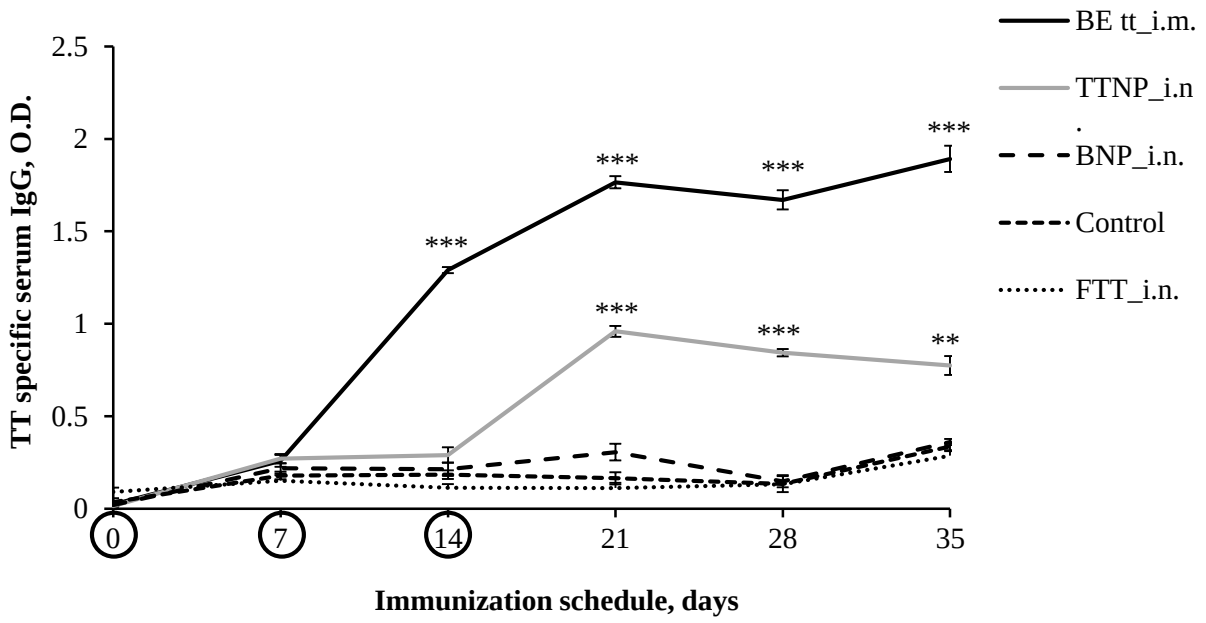

Figure 28 TT-specific serum IgG antibody levels were measured in the mice immunized with intranasal administration of FTT_*i.n.*, BNP_*i.n.*, TTNP_*i.n.* and intramuscular administration of marketed TT formulation (BE tt_*i.m.*). The circles on X-axis represent the day of dosing. (n=5, mean±SEM, ***p<0.01*, ****p<0.001*)

TT-specific serum IgG antibody levels determined after intranasal (*i.n.*) and intramuscular (*i.m.*) administration of BNP, TTNP, FTT and marketed formulation is presented in Figure 28. The TT-specific serum IgG levels were significantly higher for TTNP_*i.n.* and the marketed TT formulation (BE tt™) as compared to FTT administered by *i.n.* route (*p<0.001*). Controlled release and higher uptake of TT, as well as adjuvant effect imparted by nanoparticles, produced

higher serum IgG levels for TTNP administered through *i.n.* route. The lower TT-specific serum IgG levels for TTNP_*i.n.* compared to the marketed TT formulation might be due to the restricted volume of the nasal cavity of mice and mucociliary clearance, which washed away part of the TTNP_*i.n.* formulation before its absorption.

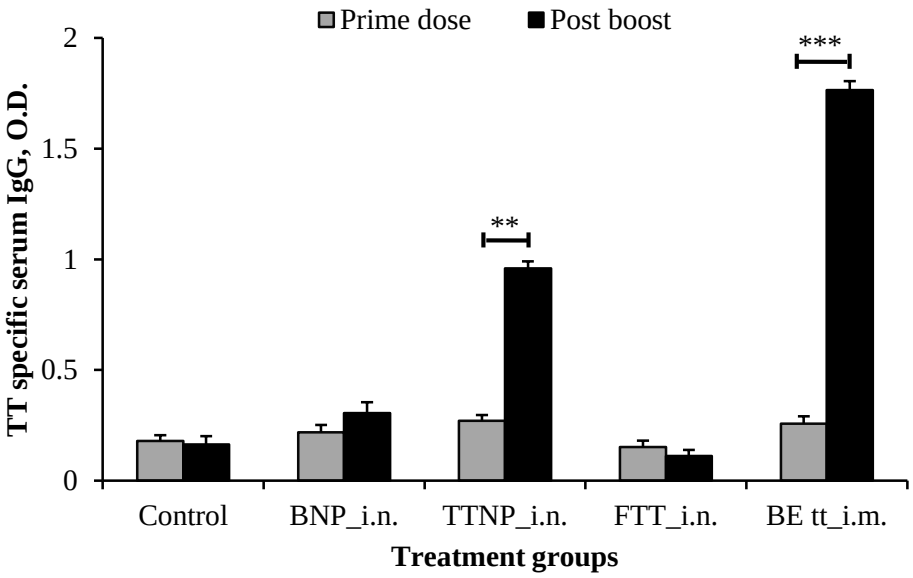

Figure 29 TT-specific serum IgG antibody response after the prime dose (day 7) compared with the post booster (day 21). (n=5, mean±SEM, ***p<0.01*, ****p<0.001*)

The TTNP_*i.n.* (*p<0.01*) and BE tt_*i.m.* formulations significantly increased TT-specific serum IgG a week after 2nd booster dose (day 21) as compared to a week after prime dose (day 7) (Figure 29). Due to the weak potential in eliciting an immune response, BNP_*i.n.* and FTT_*i.n.* formulations did no show improvement in TT-specific serum IgG level even a week after 2nd booster dose.

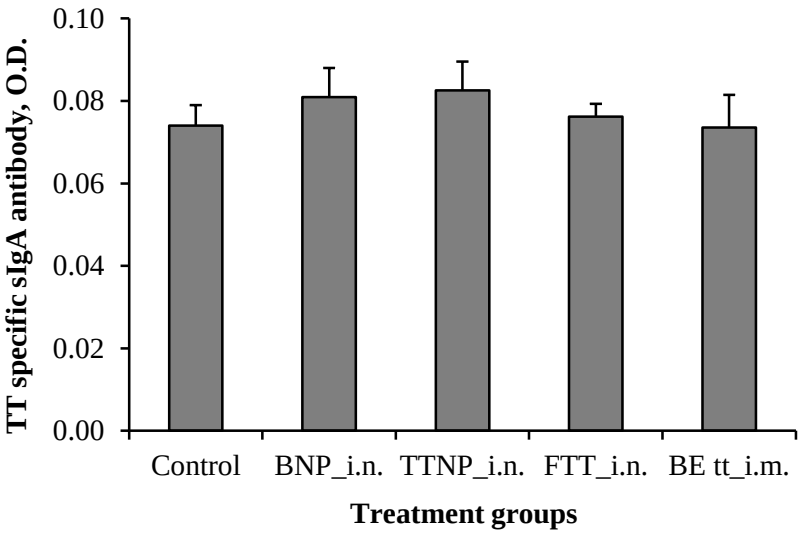

Figure 30 Estimation of TT-specific mucosal secretory IgA (sIgA) antibody response from the nasal lavage of the treated animals. (n=5, mean±SEM)

The nasal associated lymphoid tissues (NALT) upon activation by invading organisms produce the secretory IgA (sIgA) locally. Nasal administration of BNP, TTNP, and FTT formulations did not evoke a significant mucosal immune response as measured by sIgA levels in the nasal secretions (Figure 30).

The measurement of sIgA secreted in the nasal cavity is a difficult task. The complex and time-consuming nasal washing procedure as well as presence of proteolytic enzymes often resulted in the variable results (Ambrose et al., 2012; Jung et al., 2001). In addition, the sIgA produced in the nasal cavity further migrate and stimulate the immune components in the serum and at other mucosal surfaces. The low TT-specific sIgA antibody levels detected in nasal washings might be attributed to one or more of the above-mentioned factors.

3.2.7 Cytokine analysis from spleen homogenate

The quality of adaptive immune response was studied in spleen homogenate of immunized mice by analyzing cytokine levels.

After activation by antigen-MHC II complex, the $CD4^+$ T cells secretes cytokines as an effector T helper (Th) cells. The T helper responses can be divided into two major lineages viz. Th1 and Th2 depending upon their selective secretion of different cytokines. IFN-γ and IL-2 are the Th1 type cytokines, which provide cell-mediated immunity while IL-4, IL-5, IL-6, and IL-10 are Th2 type cytokines secreted by $CD4^+$ T cells (Broere et al., 2011; Nordly et al., 2009). Adjuvants added in the vaccine formulations manipulate Th cell responses by either producing

a danger signal or sustaining the release of antigen for sufficient period. Adjuvants activate the Th1 or Th2 pathway depending upon their nature, thereby augmenting the efficacy of the vaccine antigens. Th1 lineage facilitates cellular immune response (IFN-γ and IL-2) along with activation of cytotoxic T-lymphocytes (CTL) response and enhanced phagocytosis. Th2 lineage secretes cytokines (IL-4, IL-5, IL-6, and IL-10) to eliminate predominantly extracellular pathogens and support the production of circulating antibodies (Luckheeram et al., 2012; Nordly et al., 2009).

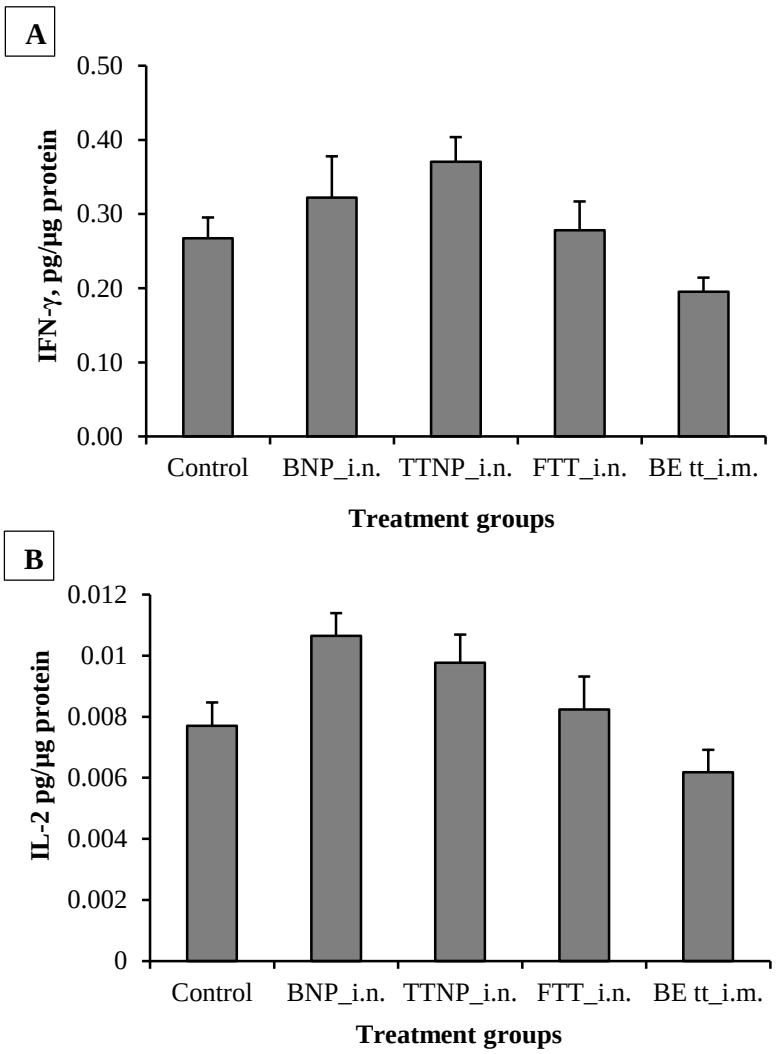

Figure 31 Estimation of the Th1 type cytokine levels in the spleen homogenate of treated mice. (A) IFN-γ and (B) IL-2. (n=5, mean±SEM)

Slightly higher but the non-significant difference was observed for both IFN-γ and IL-2 levels in BNP_*i.n.*, TTNP_*i.n.* and BE tt_*i.m.* treatment groups as compared to the control and FTT_*i.n.* (Figure 31). The reason behind this might be the immune homeostasis, which

downregulates the secretion of cytokines and chemokines after complete elimination of processed antigen or infectious agents. The regulatory T cells (Treg), as part of immune homeostasis, suppress the effector T cells (CD4 and CD8) and reduce secretion of cytokines (Broere et al., 2011; Vignali et al., 2008). Another reason could be the time of sample collection. The spleen samples were collected 3 weeks after the last dosing and thus the levels of the produced cytokines dropped down to the normal. By this time, the immune system could have eliminated the antigens and in turn ending the active secretion of cytokines.

3.2.8 Cytokine production by splenocytes

To assess the cytokine production by the splenocytes after immunization study, the splenocytes were stimulated with Concanavalin A (ConA), a strong T cell stimulant. The cytokines, IFN-γ and IL-2 levels were measured to ensure the long-term efficacy of TTNP formulation.

After the first exposure of pathogens/antigen to the immune system, the memory T- and B-cells are produced to store the memory of immune response generated against a specific pathogen. The subsequent exposure to pathogens/antigen produces a rapid immune response by speedy activation and proliferation of memory T- and B-cells. These memory cells secrete specific cytokines to further activate the specific pathways of the immune system (section 3.2.7).

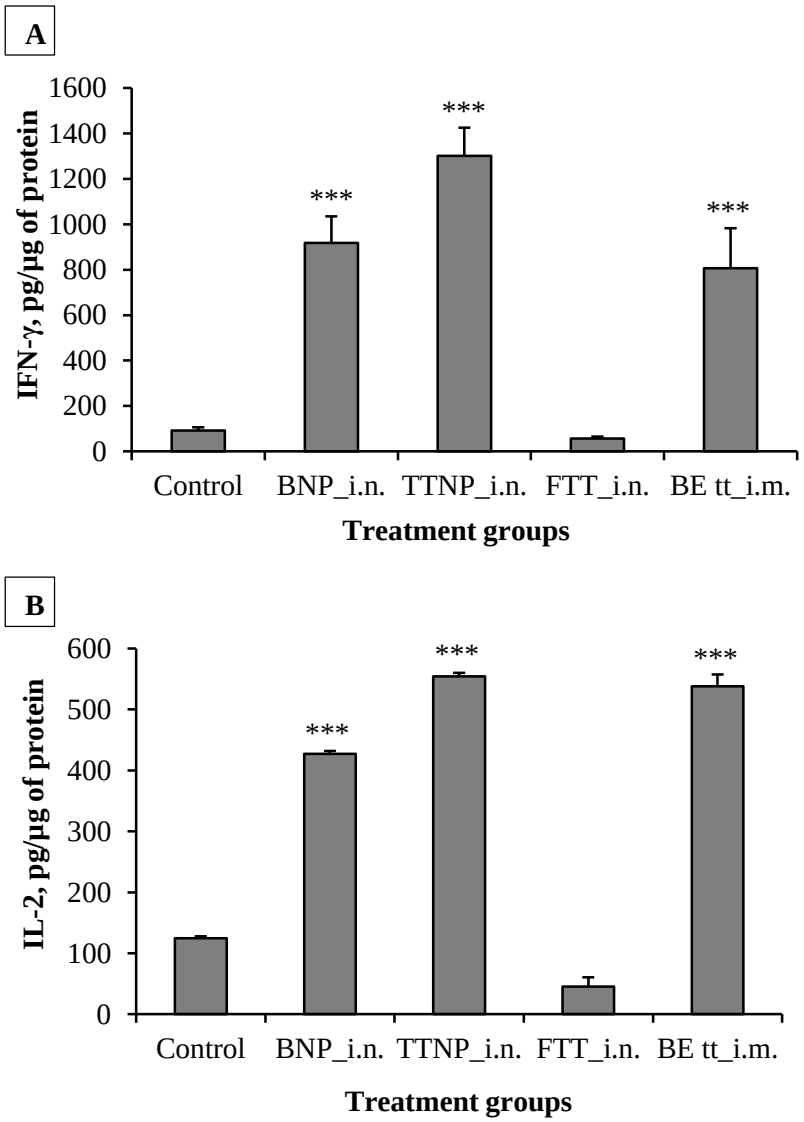

Figure 32 Estimation of (A) IFN-γ and (B) IL-2 cytokine production by splenocytes after stimulation with ConA. (n=4, mean±SEM, ****p<0.001* vs FTT_*i.n.*).

Significant upregulation in IFN-γ and the IL-2 level was observed in TTNP_*i.n.* and BE tt_*i.m.* treatment groups as compared to the control and FTT_*i.n.* groups (*p<0.001*) (Figure 32). Higher production of IFN-γ and IL-2 after stimulation with ConA in BNP_*i.n.*, TTNP_*i.n.* and BE tt_*i.m.* group indicated the strong Th1 immune response. Significantly higher production of both IFN-γ and IL-2 cytokines in animals treated with blank nanoparticles (BNP_*i.n.*) further strengthen our hypothesis of additional adjuvant effect elicited by nanoparticles itself. Moreover, higher TT-specific serum IgG levels for TTNP_*i.n.* and BE tt_*i.m.* treatment groups confirmed the activation of Th2 immune response.

The protection offered by the intranasal administration of TT loaded nanoparticles was comparable to the intramuscular administration of the marketed TT formulation, BE tt™.
Thus, a mixed Th1/Th2 response observed for the TTNP_*i.n.* the formulation will ensure the success of the immunization through nasal route.

3.3 Mechanistic understanding of immune response modulated by Ovalbumin loaded novel mucoadhesive nanoparticles

Ideally, a vaccine should stimulate both humoral and cellular arms of the immune system to assure maximum protection (Chadwick et al., 2010; Srivastava and Singh, 2005). It is therefore expected that newly developed vaccine/vaccine formulations should be evaluated for the stimulation of humoral and cellular responses. The efficacy of the most vaccine formulations is evaluated by determining antigen-specific serum immunoglobulin G (IgG) antibody levels and performance of "challenge test" in mice or guinea pigs. But there is more to the antibody-mediated (B cell response) protection which ensures long-term vaccine efficacy. The T cell mediated responses are essential to produce high-affinity antibody and generate an immune memory. However, the conventional development of vaccines pays very little or no attention to the mechanism with which they activate immune system (Siegrist, 2008). Thus, a rational development of vaccine antigen or vaccine formulation, based on the systematic study of their impact on the immune effectors, has emerged recently.

In present work, the influence of the Ovalbumin (OVA) loaded nanoparticles on various components of the immune system has been studied. The humoral immune response was measured during and after the immunization study by evaluating serum IgG antibody levels. To determine the adaptive immune response generated after immunization, populations of activated immune cells (T- and B-cells) in blood and spleen were analyzed. Furthermore, the spleen cells (splenocytes) were re-stimulated *ex vivo* and levels of different cytokines secreted by CD4 T-helper cells were determined to establish the type of immune response generated (Th1, Th2 or Th17).

3.3.1 Preparation and characterization of Ovalbumin loaded nanoparticles

Ovalbumin loaded nanoparticles (OVA NP) were prepared by optimized ionotropic gelation method (Avadi et al., 2010; Calvo et al., 1997; Fan et al., 2012; Shu and Zhu, 2002) described in section 3.1.1-3.1.3. The OVA NP had average particle size of 206±11 nm, a narrow size distribution with PDI 0.052±0.007, the zeta potential of -15.57±1.01 mV and encapsulation efficiency of 86%.

3.3.2 Adsorption of Ovalbumin on Aluminium hydroxide gel

The adsorption efficiency of Sterile Aluminum hydroxide gel suspension (Alu-Gel-S) for OVA at pH 6.0 was above 97% due to strong ionic interactions between negatively charged OVA and positively charged alumina gel at this pH. The adsorbed OVA (OVA_Ads) was used as positive control for the immunization study because of stronger immune stimulation potential of alum adjuvants. All the formulations were prepared freshly before each dosing and used within 24 hours after preparation.

3.3.3 *In vivo* immunization study of Ovalbumin loaded nanoparticles

The serum immunoglobulin analysis was performed to measure the humoral immune response produced by different treatments. The antigen-specific IgG antibodies secreted in blood following immunization are quantified and considered as the most important parameter to claim protective efficacy of the vaccine formulation (Siegrist, 2008). C57BL/6J mice were immunized with intranasal administration of PBS (Control), blank nanoparticles (BNP *i.n.*), OVA nanoparticles (OVA NP *i.n.*), OVA adsorbed on alum adjuvant (OVA_Ads *i.n.*) and intramuscular administration of OVA adsorbed on alum adjuvant (OVA_Ads *i.m.*).

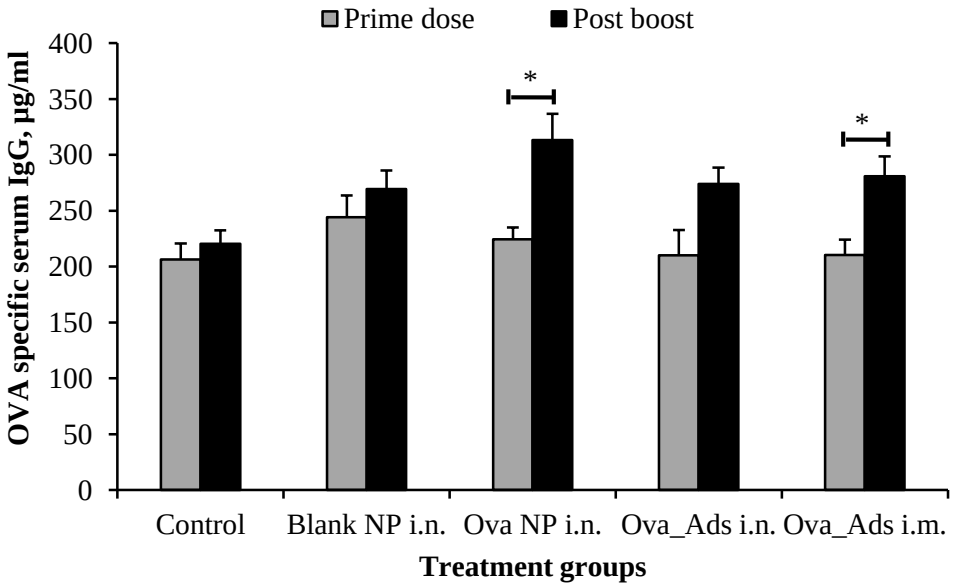

Figure 33 OVA-specific serum IgG levels analyzed pre and post booster dose in C57BL/6J mice immunized with different formulations intranasally/intramuscularly. (n=4, mean±SEM, *$p<0.05$)

OVA-specific serum IgG antibody analysis showed a significant increase ($p<0.05$) in the mice treated with OVA NP *i.n.* after 2nd booster dose (Figure 33). While, mice treated with BNP *i.n.*

and OVA_Ads *i.n.* did not show significant improvement in serum IgG levels even after 2nd booster, indicating poor stimulation of immune system. Mice treated with OVA_Ads *i.m.* also produced significantly higher serum IgG levels after 2nd booster dose indicating higher efficacy through intramuscular route. Non-significant differences in serum IgG levels in OVA NP *i.n.* and OVA_Ads *i.m.* treatment groups indicated comparable efficacy.

Higher uptake and better presentation of OVA to CD4 T immune cells might have produced higher levels of OVA-specific IgG in OVA NP *i.n.* treatment group. Moreover, OVA NP *i.n.* treatment group showed better efficacy than OVA_Ads *i.m.* treatment group.

3.3.4 Fluorescence-activated cell sorting (FACS) analysis of blood

To determine the adaptive immune response generated after immunization, the blood samples were analyzed for activated immune cell population.

Different markers present on the surface of innate immune cells are upregulated after immune activation. Among the variety of immune cells, dendritic cells, macrophages, and B cells are of higher importance. DCs are the most "professional" antigen presenting cells (APC) as they are highly specialized in internalizing and processing antigens (Gonzalez et al., 2009).

CD11b molecules are expressed on the surface of activated macrophages while CD11c are expressed on mature dendritic cells. Similarly, CD69 co-stimulatory molecules are expressed by T cells while MHCII is mainly expressed by APCs. The upregulation of MHCII on activated dendritic cells (APCs) activates naïve CD4 T cells which further activates plasma B cells to produce antigen-specific antibodies (IgG, IgA).

A detailed analysis of the activated DCs and macrophage cells along with upregulation of co-stimulatory molecules helps in determining immune stimulation potential of vaccine antigen/vaccine formulation of interest. To monitor the upregulation of dendritic cells and macrophages and their respective activation markers, blood samples were treated with fluorescent labeled anti-epitope antibodies and the intensity of fluorescent dye was analyzed by flow cytometry.

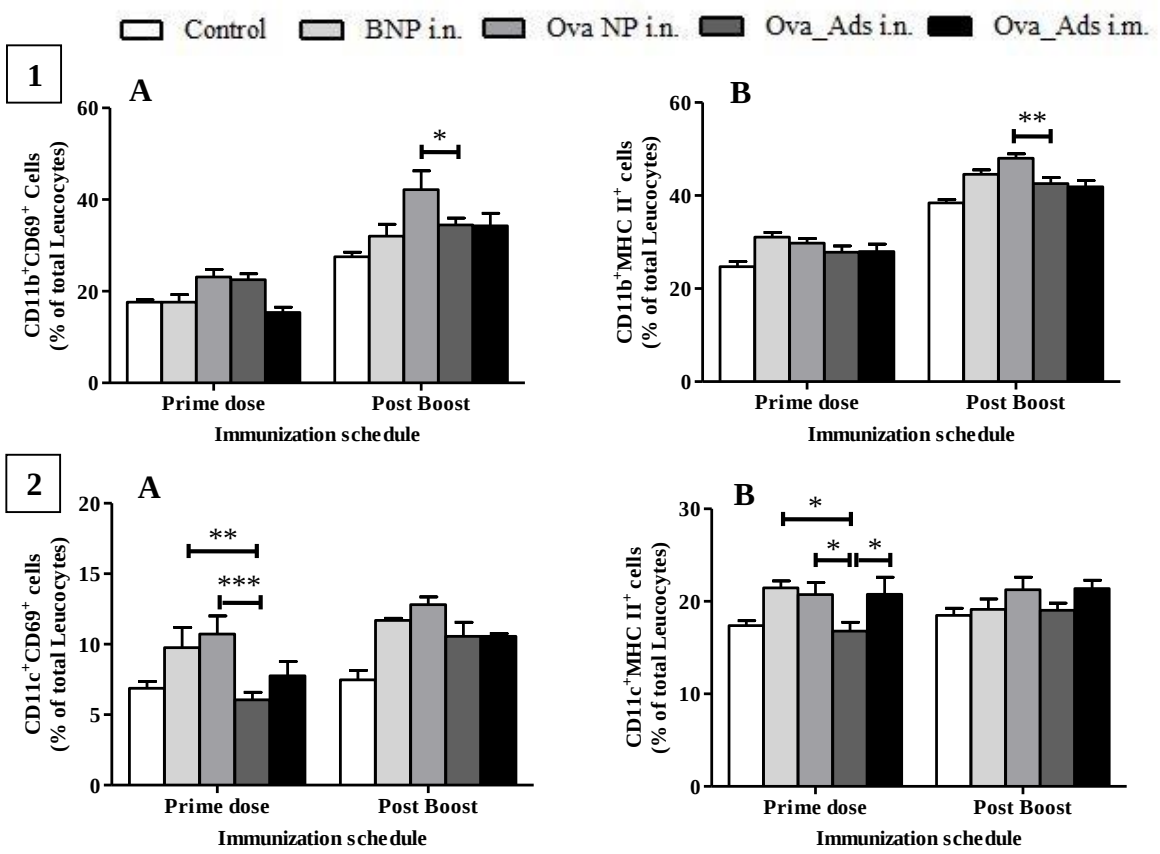

Figure 34 Activation levels of 1) macrophages ($CD11b^+$) and 2) dendritic cells ($CD11c^+$) in blood was measured using two different activation markers A) CD69 and B) MHCII on day 7 and 21 of immunization. (n=4, mean±SEM, *$p<0.05$, **$p<0.01$, ***$p<0.001$ vs. OVA_Ads *i.n.*).

Significantly higher populations of activated monocytes ($CD11b^+$) and dendritic cells ($CD11c^+$) were observed in OVA NP *i.n.* treatment group compared to OVA Ads *i.n.* group when analyzed a week after prime dose (day 7) and 2nd booster (day 21), respectively (Figure 34). Early activation of macrophages increases phagocytic activity, which is an innate immune response to invading pathogens. The higher upregulation of CD69 and MHCII co-stimulatory molecules on dendritic cells and macrophages suggested higher stimulation of T-lymphocytes which further helped in activation of adaptive immune responses. These results are in agreement with the serum antibody results (section 3.3.3) since higher antibody secretions detected in the mice immunized with OVA NP *i.n.* was the result of better activation of the adaptive immune system.

Moreover, a significant increase in the population of activated dendritic cells (**$p<0.01$ for CD69 and *$p<0.05$ for MHCII) in mice treated with blank nanoparticles (BNP *i.n*) confirmed the immune adjuvant potential of nanoparticles.

3.3.5 Fluorescence-activated cell sorting (FACS) analysis of spleen

The spleen is one of the most important organ in the context of the human immune system. The dendritic cells matured at the site of infection migrates to the lymph nodes and spleen. These matured dendritic cells (APCs) present the processed antigen to the T- or B-lymphocytes with the help of co-stimulatory molecules (MHCI or II, CD69) and activate them to generate an adaptive immune response.

The migration of activated APCs was monitored in the blood (section 3.3.4) while the secondary responses were evaluated by studying activation of other immune components in the spleen. In this study, expression of co-stimulatory molecules (CD69, MHCII, CD80, and CD86) on different splenic cell population ($CD11c^+$, $CD4^+$, and $B220^+$) was studied after completion of immunization study (3 weeks after 2^{nd} booster).

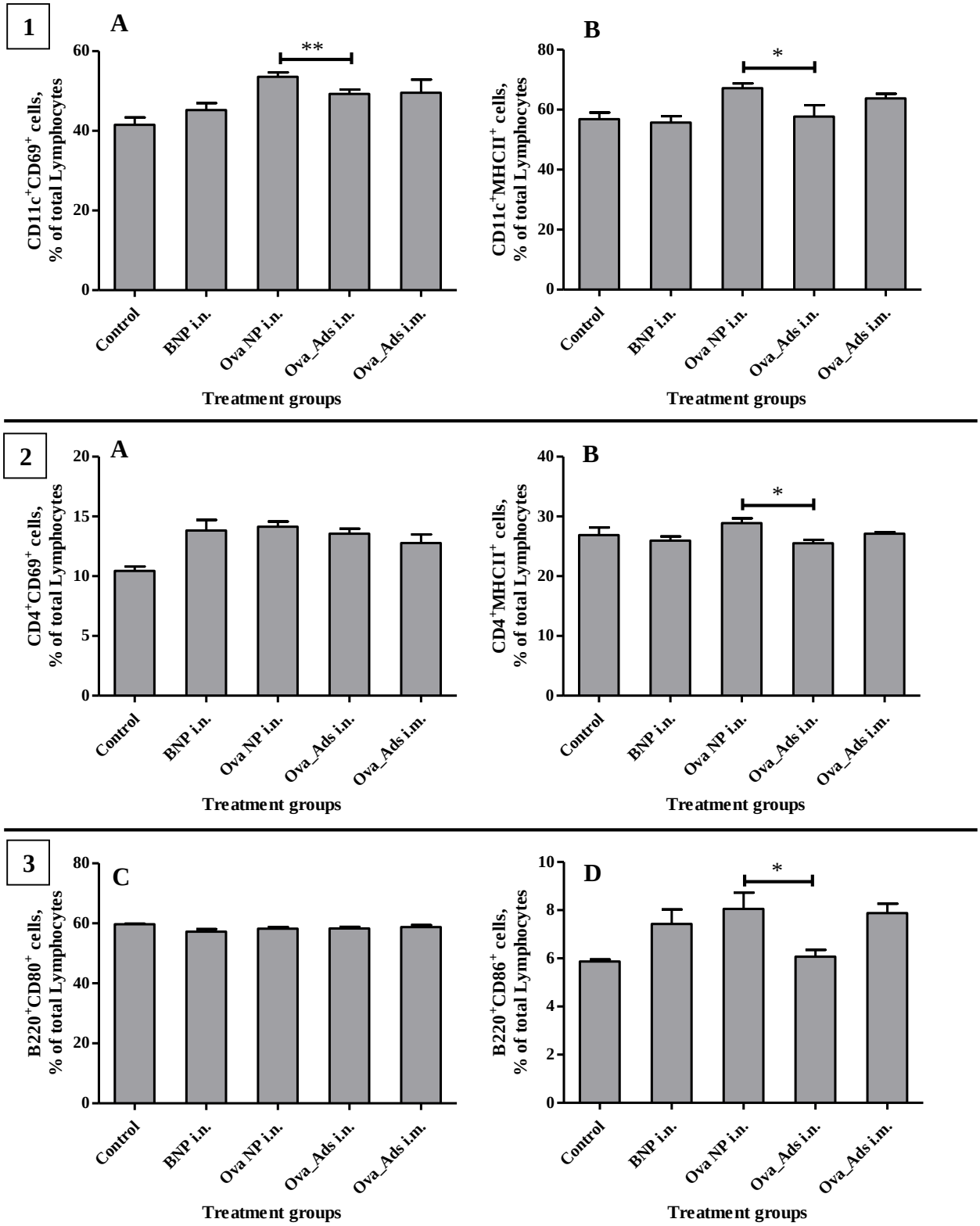

Figure 35 Expression levels of A) CD69 and B) MHCII co-stimulatory molecules on 1) $CD11c^+$, 2) $CD4^+$ cells and C) CD80 and D) CD86 co-stimulatory molecules on 3) $B220^+$ cells population was measured in splenocytes. (n=4, mean±SEM, *$p<0.05$, **$p<0.01$ vs. OVA_Ads *i.n.*)

Similar to the observations with blood sample flow cytometric analysis, $CD11c^+$ cells (dendritic cells) showed significantly higher upregulation in $CD69^+$ ($p<0.01$) and $MHCII^+$ ($p<0.05$) co-stimulatory molecules in OVA NP *i.n.* group compared to OVA Ads *i.n.*

group (Figure 35). Likewise, OVA NP *i.n.* treated mice showed significantly higher upregulation of $MHCII^+$ ($p<0.05$) co-stimulatory molecules of CD4 T cells compared to OVA_Ads *i.n.* group (Figure 35). The results indicated a better uptake and presentation of antigen (OVA) by DCs to the $CD4^+$ T cells resulting in further stimulation of adaptive immune responses. No significant difference in upregulation of $CD69^+$ co-stimulatory molecule of CD4 T cells was observed among all treatment groups.

Further, OVA NP *i.n.* treatment also showed significantly higher upregulation in $CD86^+$ co-stimulatory molecules of B-lymphocytes ($B220^+$), indicating the higher IgG antibody production as compared to OVA_Ads *i.n.* group.

3.3.6 *Ex vivo* intracellular cytokine staining (ICS) assay

Following the promising results from immunization study and flow cytometric analysis of activated immune cells, T cell specific cytokine production by splenocytes was estimated.

Since effector T cell (CD4 and CD8) responses are short-lived, they produce memory T cells (CD4 and CD8) to preserve the antigen-specific information. Upon re-exposure to processed antigen, memory T cells rapidly differentiate into effector CD4 and CD8 T cells to generate an antigen-specific immune response. Type of infectious organisms (virus/bacteria/extracellular pathogens) determines the stimulation of specific memory T cells (CD4 or CD8 or both) (Badovinac and Harty, 2000). Moreover, the production of the memory T cells depends on the magnitude of initial T cell responses which are dependent on the amount of antigen processed and presented to T cells.

Thus, to evaluate the magnitude of initial immune response generated by different formulations, splenocytes were restimulated to analyze the type and amount of cytokines secreted *ex vivo*.

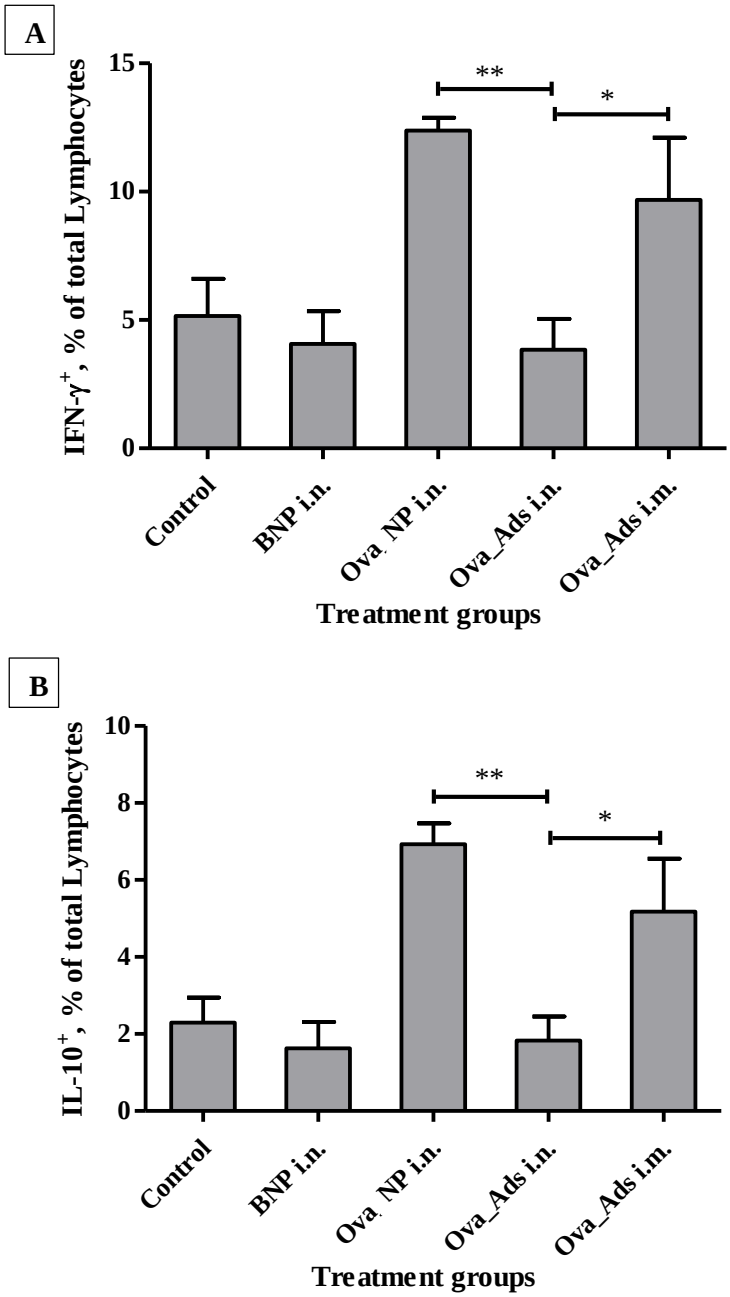

Figure 36 Population of **A)** Th1 (IFN-γ) and **B)** Th2 (IL-10) type cytokine secreting splenocytes was checked in mice treated with BNP, OVA NP, OVA_Ads intranasally and OVA_Ads intramuscularly by intracellular cytokine staining (ICS). (n=4, mean±SEM, **p<0.05*, ***p<0.01*, vs. OVA_Ads *i.n.*)

Significant increase in IFN-γ (*p<0.001*) and IL-10 (*p<0.01*) cytokine-secreting T cell population was observed in OVA NP *i.n.* group as compared to OVA_Ads *i.n.* group (Figure 36). IFN-γ is a Th1 type cytokine while IL-10 is Th2 type cytokine, both secreted by effector $CD4^+$ and/or $CD8^+$ T cells after stimulation with APCs (Kallas et al., 1999; Teixeira et al., 2005). IFN-γ activates mononuclear phagocytes, including macrophages, microglial cells, thereby enhancing antigen phagocytic activity (Murray et al., 1985). IL-10 is an anti-

inflammatory cytokine secreted after clearance of pathogens. It helps in immune homeostasis through the inhibition of Th1 type of CD4 T cells as well as other immune cells of the innate immunity (Couper et al., 2008; Luckheeram et al., 2012). The stimulant combination (PMA and Ionomycin) used in the study was more specific to CD8 memory T cells stimulation. The $CD8^+$ T cell specific IFN-γ and IL-10 cytokine secretion were higher than CD4 T cell cytokines (data not shown).

Higher levels of IFN-γ and IL-10 in OVA NP *i.n.* group suggested a mixed Th1-Th2 type immune responses, thereby activating both cellular and humoral components of the immune system.

3.3.7 Cytokine production by splenocytes

As discussed in section 3.3.6, the CD4/CD8 effector T cells upon activation secrete specific cytokines which further guide the cellular and humoral immune responses. The activation of CD4 T cells triggers their differentiation into two distinct and mutually exclusive immune pathways, Th1 and Th2 (Kapsenberg, 2003). Th1 pathway produces IFN-γ, TNF-α, and IL-12 cytokines which eliminate intracellular viruses and infected cells and provides adaptive cellular immunity (O'Garra and Robinson, 2004). Th2 type pathway produces IL-4, IL-5, IL-6, IL-10 and IL-13 cytokines which eliminate extracellular pathogens and bacteria by promoting adaptive humoral (antibody) immunity (Luckheeram et al., 2012).

Another less understood T helper pathway, Th17, produces IL-17a, IL-17F, IL-21 and IL-22 cytokines which support response against extracellular bacteria and fungi and also involved in autoimmunity (Annunziato et al., 2007; Komiyama et al., 2006; Weaver et al., 2006). IL-17a is also helping in the induction of Th1 and Th2 type cellular responses (Nakae et al., 2002). Moreover, IFN-γ and IL-6 are pro-inflammatory cytokines and are responsible for proliferation and differentiation of B cells into plasma cells (Duque and Descoteaux, 2014).

Splenocytes collected at the end of the immunization study were stimulated in presence or absence of OVA to analyze the secretion of OVA-specific cytokines. The cytokines representing Th1, Th2 and Th17 type immune pathways were determined to understand the mechanism of immune stimulation by OVA nanoparticles.

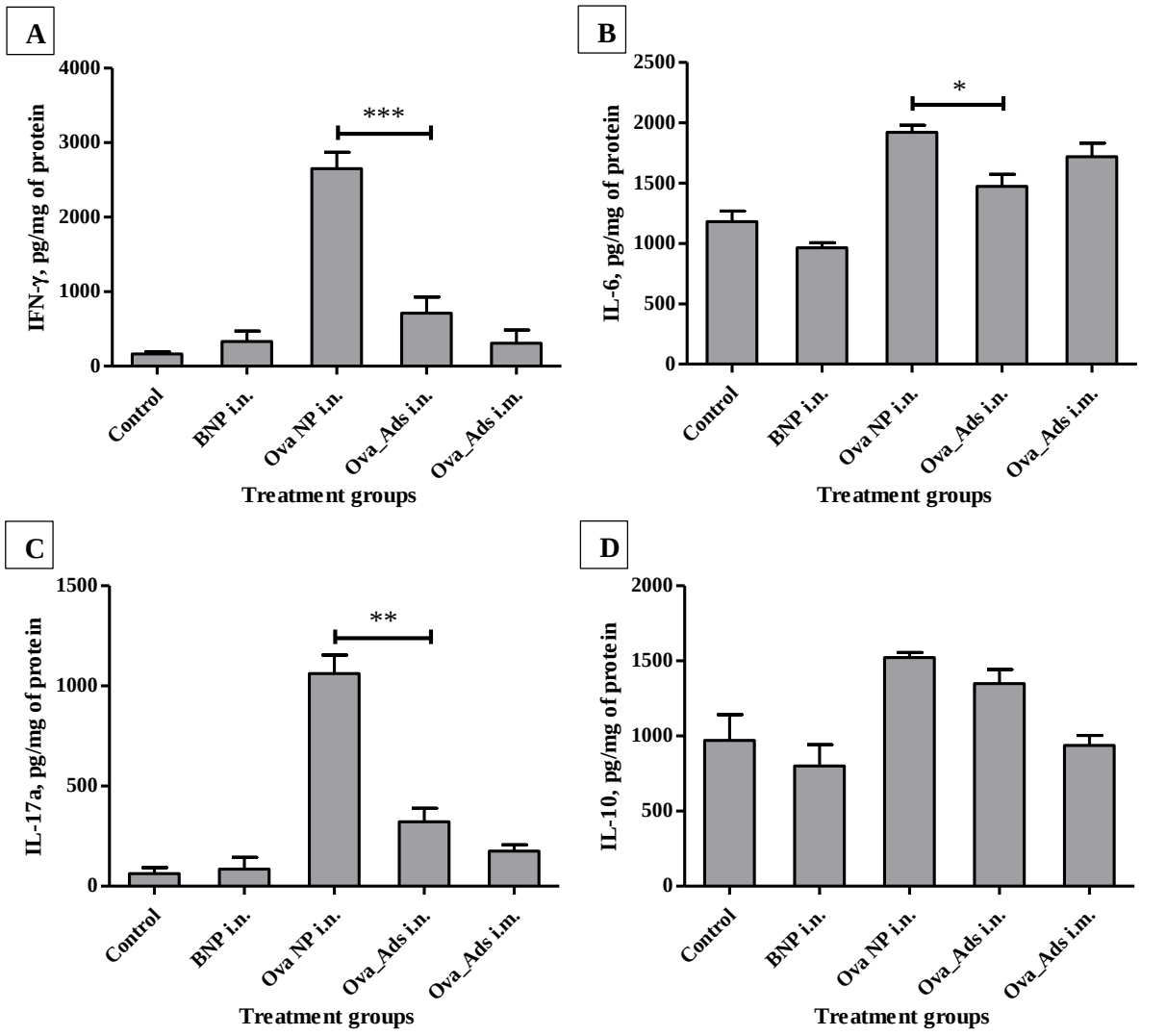

Figure 37 Th1, Th2 and Th17 type cytokine secretion after re-stimulating splenocytes with OVA for 72 hours. A) IFN-γ, B) IL-6, C) IL-17a, D) IL-10. (n=4, mean±SEM, *$p<0.05$, **$p<0.01$, ***$p<0.001$ vs. OVA_Ads *i.n.*)

Significant increase in IFN-γ ($p<0.001$), IL-6 ($p<0.05$) and IL-17a ($p<0.01$) levels were observed in mice treated with OVA NP *i.n.* as compared to mice treated with OVA_Ads *i.n.* as well as a control group (Figure 37). No significant difference was observed in the anti-inflammatory IL-10 cytokine levels, indicating no sign of inflammation.

Higher secretion of IFN-γ indicated activation of Th1 type immune response which further activates cellular immune response of adaptive immunity. Significantly higher levels of IL-6, a Th2 type cytokine observed was probably due to its role in activation of IL-17a cytokine, as well as its role in the recruitment of neutrophils at the site of infection (Hunter and Jones, 2015; Zhou et al., 2007). IL-6 also helps in the transition of immune response from an innate to an adaptive response (Jones, 2005). The Th2 type immune response activates the humoral immunity and stimulates plasma B cells to produce antigen-specific antibodies.

In conclusion, a mixed Th1, Th2 and Th17 type of immune response elicited by OVA-loaded polymeric nanoparticles activated all components of the immune system which in turn ensured better protection and thus success of the delivery system.

4. Summary

The introduction of vaccination/immunization significantly reduced the burden caused by infectious diseases. Vaccination completely eradicated smallpox while poliomyelitis (Polio) is near to complete eradication. In recent years, vaccine technology has experienced a tremendous leap. Yet, vaccines for many life-threatening infections like human immunodeficiency virus (HIV) and some recent viral originated infections are not available to date. Moreover, the vaccines which are available on the market are ineffective in severely immune-compromised individuals due to poor or lacking immune components in their body. For such individuals, the vaccine antigens are administered along with adjuvants which provide an initial trigger for the immune response. Most of the marketed vaccines use aluminum salts as adjuvants. Although aluminum salts have a proven safety record as adjuvants, sometimes they cause severe allergic reactions.

Most of the vaccines are administered via a parenteral route. This causes pain and local irritation reactions in many individuals and thus leading to inconveniences for patients. From the past few years, the scientific community has placed emphasis on formulating vaccines for the oral or nasal route. In recent years, nanoparticles were explored as potential vaccine delivery carriers with little success. As most of the nanoparticles alone are not capable of eliciting an immune response, there is a need to add an adjuvant in the nanoparticle formulation. This further increases the cost of the formulation and it might compromise the stability of nanoparticle suspensions.

The objective of the present work was to prepare nanoparticles which will improve nasal uptake of antigen and trigger the initial cascade of the immune response. Novel polymeric nanoparticles with additional adjuvant effect were developed by combining a mucoadhesive polymer and an immune stimulant polymer. The work was divided into three parts which focus on **a)** development and characterization of novel mucoadhesive polymeric nanoparticles, **b)** *in vitro* and *in vivo* assessment of tetanus toxoid loaded mucoadhesive polymeric nanoparticles and **c)** mechanistic understanding of immune response modulated by mucoadhesive polymeric nanoparticles.

a) Preparation and characterization of novel mucoadhesive nanoparticles loaded with the model protein bovine serum albumin:

Nanoparticles loaded with the model protein bovine serum albumin (BSA) were prepared by ionic gelation method. Different polyanionic mucoadhesive polymers like sodium alginate (ALG), sodium carboxymethylcellulose (CMC), sodium hyaluronate (HA) and sodium

pectinate (PCT) were screened to obtain stable nanoparticles with low particle size and high encapsulation of BSA. Diethylaminoethyldextran (DEAE), an immune stimulant polymer, was incorporated into the nanoparticles to achieve immune modulation. ALG as a mucoadhesive polymer produced nanoparticles with maximum encapsulation of BSA (20%), the smallest particle size (~100 nm), lowest polydispersity index (PDI) and optimal zeta potential (-34.7 mV). To achieve higher BSA encapsulation, the nanoparticles were further optimized with respect to pH of BSA solution, BSA loading and addition rate. At pH 3.5, up to 50% BSA encapsulation was achieved due to stronger interaction between protonated BSA and polyanionic ALG. Increasing the pH of BSA solutions led to drastic reduction in the encapsulation efficiency due to repulsion between negatively charged BSA and polyanionic ALG. The increment in BSA loading from 20 to 50% w/w increased the encapsulation efficiency of the nanoparticles (52% encapsulation at 50% w/w BSA loading). The BSA/DEAE polymer solution addition rate to the ALG polymer solution (between 0.6-1.2 ml/min) had no significant effect on encapsulation efficiency or particle size. However, the immediate addition of BSA solution and DEAE solution to ALG polymer solution led to decrease in the encapsulation of BSA as well as particle size. To further improve the BSA encapsulation, the ALG polymer solution was dialyzed against ultrapure Milli Q® water. This significantly improved the BSA encapsulation efficiency (~97%) due to the omission of the effect of sodium ions. The sodium ions bind firmly to the ALG polymer due to their small size and high charge density.

The formation of nanoparticle complexes was confirmed by studying the interactions by Fourier transform infrared (FTIR) spectroscopy. The FTIR analysis indicated that ionic interactions were predominant in the ALG-BSA-DEAE complex. Other interactions like hydrogen bonding also contributed to the complex formation. Stability of the BSA was assessed by gel electrophoresis and circular dichroism (CD) spectroscopic analysis. The gel electrophoresis (SDS-PAGE) confirmed the structural integrity while CD spectroscopic analysis confirmed the conformational stability of BSA. The strong ionic interactions between BSA, ALG and DEAE resulted in a controlled release of BSA from nanoparticles (~16% released in 8 hours). The release profile of BSA in phosphate buffer pH 6.0 and simulated nasal electrolyte solution (SNES) pH 6.0 was similar since the ionic strength of these two release media was also similar (~0.2 M). *In vitro* mucoadhesion studies performed by measuring detachment force with a texture analyzer and changes in net surface charge (zeta potential) of mucin particles by Zetasizer instrument confirmed the substantial mucoadhesive potential of the BSA-loaded nanoparticles.

Furthermore, *in vitro* cytotoxicity studies on human macrophages (THP-1 cell line) confirmed the non-toxic nature of the nanoparticles. To improve the storage stability of nanoparticles, the BSA-loaded nanoparticles were freeze-dried and the effect of different cryoprotectants and their concentration was studied. Sucrose, when used at 10% w/v concentration of nanoparticle suspension, effectively protected nanoparticles from freeze drying stress. Furthermore, it formed a porous cake which, after addition of Milli Q® water, redispersed into nanoparticles without significant effect on particle size and polydispersity index. The freeze dried nanoparticle formulation with sucrose as cryoprotectant maintained the particle size, PDI and zeta potential when stored at 2-8°C or 25°C/60% RH for 6 months. The formulations stored at 40°C/75% RH exhibited a significant increase in particle size and PDI over the period of 6 months. At this storage condition, the freeze-dried nanoparticle cake collapsed due to the high temperature and high humidity which led to nanoparticles aggregation. There was no significant effect on the structural integrity and conformational stability of BSA, irrespective of the storage conditions.

b) Preparation, characterization and *in vitro* and *in vivo* evaluation of Tetanus toxoid loaded novel mucoadhesive nanoparticles:

To assess the *in vivo* performance of the novel mucoadhesive nanoparticles, tetanus toxoid (TT) was encapsulated in the nanoparticles using previously optimized ionic gelation method. Aggregates formed in the formulation owing to the poor stability of the TT at lower pH. The method was modified and TT was first added to the dialyzed ALG polymer solution followed by lowering the pH. At pH 4.5, stable, monodisperse nanoparticles with high TT encapsulation (78 %), particle size < 200 nm and optimal zeta potential of -25.68±3.22 mV were obtained. The single band in the gel electrophoretic (SDS-PAGE) analysis confirmed the structural integrity of the TT encapsulated in the nanoparticles. Analogous to the *in vitro* release of BSA nanoparticles, the release of TT from the nanoparticles was slow and controlled without any burst effect (~15% released in 8 hours).

The *in vitro* proliferation assay performed on human nasal epithelial cells (RPMI 2650) showed no significant effect on the metabolic activity of the cells at 20 and 50 µg/ml concentration of TT-loaded and blank nanoparticles. At higher concentration of TT nanoparticles (100 µg/ml), the metabolic activity of nasal epithelial cells was reduced, which might be due to the higher number of nanoparticles and thus a higher number of surface-bound DEAE polymer available to interact with cells. The quaternary ammonium groups of DEAE might have affected the

metabolic activity of the cells. The uptake of nanoparticles and thus vaccine antigen into macrophages defines the quality and quantity of the immune response modulated against a specific antigen. The uptake of fluorescein isothiocyanate (FITC) dye-labeled nanoparticles into macrophages was time dependent with more than 50% nanoparticles entered in macrophages within 60 min of incubation.

Ideally, a vaccine should stimulate both humoral and cellular arms of the immune system to assure maximum protection. To evaluate the efficacy of TT loaded mucoadhesive polymeric nanoparticles, an *in vivo* immunization study was performed on Balb/c mice. The mice were treated with intranasal administration of blank nanoparticles (BNP_*i.n.*), TT nanoparticles (TTNP_*i.n.*), free TT solution (FTT_*i.n.*) and intramuscular administration of the marketed TT formulation (BE tt™). The TT specific serum IgG levels were measured in serum samples from different treatment groups using ELISA. The TT specific serum IgG levels were significantly higher for TTNP_*i.n.* and BE tt_*i.m.* treatment groups as compared to FTT_*i.n.* treatment group. This was ascribed to a higher uptake of TT nanoparticles as well as the controlled release of TT. Nasal administration of blank nanoparticles, TT loaded nanoparticles and free TT formulations did not lead to elevated sIgA levels in the nasal secretions. This indicates that the formulations did not evoke a mucosal immune response. However, it might also be due to the fact that the nasal washing procedure was complex and time-consuming and the presence of proteolytic enzymes often resulted in the destruction of these antibodies. The cytokine analysis from the spleen homogenate did not show any significant difference in IFN-γ and IL-2 cytokines secretion between all treatment groups. The reason behind this might be the immune homeostasis, which downregulates the secretion of cytokines and chemokines after complete elimination of processed antigen or infectious agents. To assess the cytokine (IFN-γ and IL-2) production by the splenocytes after immunization study, splenocytes were stimulated *ex vivo* with Concanavalin A (ConA), a strong T cell stimulant. The cytokine IFN-γ and IL-2 levels in the supernatant of the splenocyte culture were measured after 72 hours of stimulation. The IFN-γ and the IL-2 level was significantly upregulated in BNP_*i.n.*, TTNP_*i.n.* and BE tt_*i.m.* treatment groups as compared to the control and FTT_*i.n.* groups. The higher production of IFN-γ and IL-2 after stimulation with ConA in these treatment groups indicated the shift towards Th1 immune response. On the other hand, higher TT specific serum IgG levels for TT nanoparticles and marketed TT formulation confirmed the activation of Th2 immune response. This mixed Th1-Th2 response for the TT loaded novel mucoadhesive nanoparticles formulation will ensure the success of the immunization through nasal route.

c) Mechanistic understanding of immune response modulated by Ovalbumin loaded novel mucoadhesive nanoparticles:

The conventional development of vaccines pays very little or no attention to the mechanism with which they activate the immune system. Thus, a rational development of vaccine antigen or vaccine formulation, based on the systematic study of their impact on the immune effectors, has emerged recently.

In present work, the influence of the OVA-loaded nanoparticles (OVA NP) on various components of the immune system was studied qualitatively and quantitatively. C57BL/6J mice were immunized by intranasal administration (*i.n.*) of OVA NP, blank nanoparticles (BNP) and OVA adsorbed on aluminum hydroxide (OVA_Ads) and intramuscular administration (*i.m.*) of OVA_Ads as a positive control. OVA-specific IgG was analyzed in the serum samples of treated mice. A higher serum IgG level in mice treated with OVA NP intranasally confirmed better humoral response as compared to other treatment groups. The higher uptake of nanoparticles and controlled release of OVA primarily contributed to the higher serum IgG levels.

The mechanism by which the OVA NP modulate the immune response was studied in detail by analyzing the immune cells activated after treatment in blood and spleen by flow cytometry (FACS). After completion of immunization study, the spleen cells (splenocytes) from treated mice were restimulated *ex vivo* with immune stimulants (PMA+Ionomycin) and OVA in order to check the type and amount of the secreted cytokines by immune cells (CD4 and CD8 T cells).

The flow cytometric analysis of immune cells in the blood of mice treated with OVA NP showed increased upregulation of CD69 and MHCII surface co-stimulatory molecules on dendritic cells (DC) and macrophages. These results confirmed higher stimulation of innate immune system and higher antigen uptake and processing by DCs.

The expression of co-stimulatory molecules (CD69, MHCII, CD80, and CD86) on different splenic cell populations like dendritic cells ($CD11c^+$), T cells ($CD4^+$ T cells) and B cells ($B220^+$) was also studied after completion of immunization study. Similar to the observations with blood sample flow cytometric analysis, $CD11c^+$ cells (dendritic cells) showed significantly higher upregulation in $CD69^+$ ($p<0.01$) and $MHCII^+$ ($p<0.05$) while $CD4^+$ T cells showed higher upregulation of only $MHCII^+$ ($p<0.05$) co-stimulatory molecules in OVA NP treatment group. The results indicated a better uptake and presentation of antigen (OVA) by DCs to the $CD4^+$ T cells. This further stimulated the adaptive immune responses resulting in higher OVA-specific IgG antibody levels in OVA NP treated mice. Further, OVA NP *i.n.*

treatment also showed significantly higher upregulation in $CD86^+$ co-stimulatory molecules on B-lymphocytes as compared to OVA_Ads *i.n.* group, indicating a higher IgG antibody production (humoral immune response).

The *ex vivo* stimulation of splenocytes with PMA and Ionomycin stimulant combination produced a higher amount of IFN-γ and IL-10 cytokine secreting CD8 T cells in the OVA NP treatment group. This further confirmed the activation of both cellular and humoral immune responses.

To further analyze the OVA-specific cytokines secreted *in vitro*, splenocytes collected at the end of the immunization study were stimulated in presence or absence of OVA. Significant increase in IFN-γ ($p<0.001$), IL-6 ($p<0.05$) and IL-17a ($p<0.01$) levels were observed in mice treated with OVA NP *i.n.* as compared to mice treated with OVA_Ads *i.n.* as well as a control group. While no significant difference was observed in the anti-inflammatory IL-10 cytokine levels, indicating no sign of inflammation.

In conclusion, a mixed Th1, Th2 and Th17 type of immune response elicited by OVA-loaded polymeric nanoparticles activated all components of the immune system which in turn ensured better protection and thus success of the delivery system.

To conclude the entire work, controlled release, biocompatible nanoparticles with high encapsulation of proteins/vaccine antigen were successfully prepared without affecting the integrity and conformational stability of incorporated proteins. The efficacy of Tetanus toxoid loaded nanoparticles administered by the nasal route was comparable to the marketed intramuscular formulation (BE tt™). Cumulatively, an immune stimulation mechanism of the developed novel nanoparticles was established and the efficacy was compared with the OVA adsorbed on aluminum hydroxide, an adjuvant most widely used in commercial vaccine formulations. These key achievements can be translated into a promising, cost-effective vaccine delivery system for the nasal route.

5. Zusammenfassung

Die Einführung von Impfungen/Immunisierungen hat die durch Infektionskrankheiten verursachte Belastung signifikant reduziert. Impfen hat das Pockenvirus gänzlich ausgerottet, während der Poliomyelitis-Erreger beinahe ausgerottet ist. In den letzten Jahren hat die Impftechnologie gewaltige Fortschritte gemacht. Trotzdem sind bis heute für viele lebensbedrohliche Infektionen wie das Humane Immundefizienz-Virus (HIV) und andere neuartige, virale Infektionen keine Impfungen vorhanden. Außerdem sind die auf dem Markt verfügbaren Impfungen bei schwer immunkomprimierten Personen aufgrund der mangelhaften oder fehlenden Immunkomponenten in deren Körper unwirksam. Bei solchen Patienten werden die Impfantigene zusammen mit Adjuvantien, die als initiale Trigger für die Immunantwort dienen, verabreicht. Die meisten der erhältlichen Impfungen enthalten Aluminumsalze als Adjuvantien. Obwohl die Sicherheit von Aluminiumsalzen als Adjuvantien belegt ist, können sie in manchen Fällen schwere allergische Reaktionen auslösen.

Die meisten Impfungen werden parenteral appliziert. Dies verursacht bei manchen Personen Schmerzen und lokale Irritationen und führt somit zu Unannehmlichkeiten für die Patienten. Seit ein paar Jahren liegt der Schwerpunkt der wissenschaftlichen Forschung auf der Formulierung von Impfungen für die orale oder nasale Anwendung. In den letzten Jahren wurden Nanopartikel als potentielle Dareichungsform für Impfstoffe getestet, jedoch mit wenig Erfolg. Da Nanopartikel meist nicht in der Lage sind eine Immunreaktion auszulösen, ist die Zugabe von Adjuvantien zu Nanopartikelformulierungen notwendig. Dies erhöhte die Kosten der Formulierung zusätzlich und es kann die Stabilität der Nanopartikelsuspensionen beeinträchtigen.

Das Ziel dieser Arbeit war es, Nanopartikel zu herzustellen, welche die nasale Aufnahme des Antigens verbessern und die initiale Kaskade der Immunantwort triggern. Neuartige Polymernanopartikel mit zusätzlichem Adjuvantien-Effekt wurden durch das Kombinieren eines mukoadhäsiven Polymers und eines immunstimulierenden Polymers entwickelt. Die Arbeit gliedert sich in drei Teile mit den Schwerpunkten auf **a)** Entwicklung und Charakterisierung von neuartigen mukoadhäsiven Polymernanopartikeln, **b)** *in vitro* und *in vivo* Prüfung von mit Tetanustoxoid beladenen mukoadhäsiven Polymernanopartikeln und **c)** mechanistische Einsicht in die durch mukoadhäsive Polymernanopartikel ausgelöste Immunantwort.

a) Herstellung und Charakterisierung von mit dem Modelprotein „Rinderserumalbumin“ beladenen, neuartigen mukoadhäsiven Polymernanopartikeln:

Mit dem Modelprotein Rinderserumalbumin (BSA, engl. bovine serum albumin) beladene, mukoadhäsive Polymernanopartikel wurden durch ionische Vernetzung hergestellt. Verschiedene polyanionische, mukoadhäsive Polymere wie Natriumalginat (ALG), Natrium-Carboxymethylcellulose (CMC), Natriumhyaluronat (HA) und Natriumpektinat (PCT) wurden getestet, um stabile Nanopartikel mit kleiner Partikelgröße und hoher BSA-Einschlusseffizienz zu erreichen. Diethylaminoethyldextran (DEAE), ein immunstimulierendes Polymer wurde in die Nanopartikel eingearbeitet um eine Immunreaktion zu erzielen. ALG als mukoadäsives Polymer führte zu Nanopartikeln mit der höchsten BSA-Einschlusseffizienz, der kleinsten Partikelgröße (~100 nm), dem niedrigstem Polydispersitätsindex (PDI) und optimalem Zeta-Potenzial (-34.7 mV). Um eine höhere BSA-Einschlusseffizienz zu erreichen, wurden die Nanopartikel bezüglich dem pH der BSA-Lösung, der BSA-Beladung und der Zugabegeschwindigkeit weiter optimiert. Bei pH 3,5 konnte, aufgrund der stärkeren Interaktion zwischen dem protonierten BSA und dem polyanionischen ALG eine BSA-Einschlusseffizienz bis zu 50% erzielt werden. Eine Erhöhung des pHs der BSA-Lösung führte wegen der elektrostatischen Abstoßung zwischen dem negativ geladenen BSA und dem polyanionischen ALG zu einer starken Abnahme der Einschlusseffizienz. Die Erhöhung der BSA-Beladung von 20 auf 50% erhöhte die Einschlusseffizienz der Nanopartikel (52% Einschlusseffizienz bei 50% w/w BSA-Beladung). Die Zugabegeschwindigkeit der BSA/DEAE-Lösung zur ALG-Polymerlösung (zwischen 0,6-1,2 ml/min) hatte keinen signifikanten Einfluss auf die Einschlusseffizienz oder die Partikelgröße. Jedoch führte die sofortige Zugabe der BSA-Lösung und DEAE-Lösung zur ALG-Polymerlösung zu einer Reduktion der Einschlusseffizienz und der Partikelgröße. Um die BSA-Einschlusseffizienz weiter zu verbessern, wurde die ALG-Polymerlösung gegen hochreines Milli Q®- Wasser dialysiert. Dies verbesserte die BSA-Einschlusseffizienz signifikant (~97%), da der Effekt der Natrium-Ionen wegfiel. Die Natrium-Ionen binden stark an das ALG-Polymer aufgrund ihrer kleinen Größe und hohen Ladungsdichte.

Die Ausbildung von Nanopartikel-Komplexen wurde durch die Untersuchung der Interaktionen mittels Fourier-Transform-Infrarot (FTIR)-Spektroskopie bestätigt. Die FTIR-Untersuchung deutete darauf hin, dass die ionischen Interaktionen im ALG-BSA-DEAE-Komplex prädominant waren. Andere Interaktionen wie Wasserstoffbrücken trugen ebenfalls zur Komplexbildung bei. Die Stabilität von BSA wurde mittels Gelelektrophorese und Zirkulardichroismus (CD)-Spektroskopie untersucht. Die Gelelektrophorese (SDS-PAGE)

bestätigte die strukturelle Intaktheit während die Stabilität der Konformation von BSA durch die CD-Spektroskopie nachgewiesen wurde. Die starken Interaktionen zwischen BSA, ALG und DEAE führten aus den Nanopartikeln zu einer kontrollierten Freisetzung von BSA (~16% freigesetzt nach 8 Stunden). Das Freisetzungsprofil von BSA in Phosphatpuffer pH 6,0 und simulierter nasaler Elektrolytlösung (SNES) pH 6,0 war fast gleich, da die Ionenstärke der beiden Freisetzungsmedien ebenfalls ähnlich war (~0,2 M). Bei *in vitro* Mukoadhäsionstests wurde die Ablösekraft mit Hilfe eines Texture Analyzers gemessen, sowie die Veränderung der Netto-Oberflächenladung (Zeta-Potenzial) von Muzin-Partikeln mit einem Zetasizer-Apparat bestimmt. Die Tests bestätigten das beachtliche mukoadhäsive Potenzial der mit BSA beladenen Nanopartikel.

Des Weiteren zeigten *in vitro* Zytotoxizitätsstudien mit humanen Makrophagen (Zelllinie THP-1), dass die Nanopartikel nicht toxisch waren. Um die Lagerstabilität der Nanopartikel zu verbessern, wurden die mit BSA beladenen Nanopartikel gefriergetrocknet. Dabei wurde der Effekt verschiedener Kryoprotektiva und ihrer Konzentration untersucht. Saccharose schützte die Nanopartikel effizient vor der Belastung beim Gefriertrocknen, wenn die Konzentration bei 10% w/v der Nanopartikelsuspension lag. Außerdem bildete sich mit Saccharose ein lockerer Lyophilisat, das nach Zugabe von Milli Q® Wasser ohne signifikanten Effekt auf die Partikelgröße oder den Polydispersitätsindex in Nanopartikel redispergiert werden konnte. Partikelgröße, PDI und Zeta-Potenzial der gefriergetrockneten Nanopartikelformulierung mit Saccharose als Kryoprotektivum veränderte sich nicht während 6 monatiger Lagerung bei 2-8°C oder 25°C/60% RH. Wurde die Formulierung über einen Zeitraum von 6 Monaten bei 40°C/75% RH gelagert, nahmen die Partikelgröße und der PDI signifikant zu. Bei diesen Lagerbedingungen kollabierte das gefriergetrocknete Gut aufgrund der hohen Temperatur und Luftfeuchtigkeit, was zur Aggregation der Nanopartikel führte. Die strukturelle Intaktheit und die Konformation von BSA veränderten sich unabhängig von den Lagerbedingungen während der Lagerung nicht signifikant.

b) Herstellung, Charakterisierung und *in vitro* sowie *in vivo* Untersuchung von mit Tetanustoxoid beladenen neuartigen mukoadhäsiven Nanopartikeln:

Um das *in vivo*-Leistungsvermögen der neuartigen mukoadhäsiven Nanopartikel zu untersuchen wurde Tetanustoxoid (TT) mit der zuvor optimierten Methode der ionische Vernetzung in die Nanopartikel eingearbeitet. Aufgrund der schlechten Stabilität von TT bei niedrigem pH bildeten sich Aggregate in der Formulierung. Die Methode wurde verändert und

TT wurde zuerst zur dialysierten ALG-Polymerlösung zugegeben, gefolgt von der Absenkung des pHs. Bei pH 4,5 wurden stabile, monodisperse Nanopartikel mit hoher TT-Einschlusseffizienz (78%), einer Partikelgröße von < 200 nm und einem optimalen Zeta-Potenzial von -25.68±3.22 mV erhalten. Die einzelne Bande in der Gelelektrophoreseuntersuchung (SDS-PAGE) zeigte, dass das in den Nanopartikeln eingeschlossene TT strukturell intakt war. Analog zur *in vitro*-Freisetzung von BSA war auch die Freisetzung von TT aus den Nanopartikeln langsam und kontrolliert und ohne Burst-Effekt (~15% freigesetzt nach 8 Stunden).

In einem *in vitro*-Zellvermehrungstest mit humanen Nasenepithelzellen (RPMI 2650) hatten TT- und Placebo-Nanopartikel keinen signifikanten Effekt auf die metabolische Aktivität der Zellen bei Konzentrationen von 20 und 50 µg/ml. Bei höherer Konzentration von TT-Nanopartikeln (100 µg/ml) war die metabolische Aktivität der Nasenepithelzellen verringert. Dies könnte mit der größeren Anzahl von Nanopartikeln und der resultierenden größeren Menge von oberflächengebundenem DEAE-Polymer zusammenhängen, welches mit den Zellen interagieren kann. Die quartäre Ammoniumgruppen des DEAE könnten die metabolische Aktivität der Zellen beeinträchtigen. Die Aufnahme der Nanopartikel und somit des Impfantigens in Makrophagen ist ausschlaggebend für die Qualität und Quantität der Immunreaktion, welche gegen ein spezifisches Antigen erzeugt wird. Die Aufnahme von mit Fluorescinisothiocyanat (FITC) markierten Nanopartikeln in Makrophagen war zeitabhängig. Mehr als 50% der Nanopartikel waren nach 60 Minuten Inkubationszeit in die Makrophagen eingedrungen.

Idealerweise sollten Impfungen sowohl die humorale als auch die zelluläre Immunantwort stimulieren, um einen maximalen Impfschutz zu gewährleisten. Um die Wirksamkeit von mit TT beladenen mukoadhäsiven Polymernanopartikeln zu untersuchen, wurde eine *in vivo*-Immunisierungsstudie mit Balb/c-Mäusen durchgeführt. Die Mäuse wurden mit intranasal verabreichten Placebo-Nanopartikeln (BNP_*i.n.*), TT-Nanopartikeln (TTNP_*i.n.*), TT-Lösung (FTT_*i.n.*) und einer auf dem Markt zugelassen, intramuskulär verabreichten TT-Formulierung (BE tt™) behandelt. Die TT-spezifische IgG-Konzentration wurde in Serumproben der verschiedenen Behandlungsgruppen mittels ELISA bestimmt. Die Gesamtkonzentrationen der TT-spezifischen IgG im Serum waren für TTNP_*i.n.*- und BE tt_*i.m.*-Behandlungsgruppen im Vergleich zur FTT_*i.n.*-Gruppe signifikant höher. Dies wurde einer höheren Aufnahme der TT-Nanopartikel und der kontrollierten Freisetzung von TT zugeschrieben. Die nasale Verabreichung von Placebo-Nanopartikeln, TT-Nanopartikeln und TT-Lösung führte nicht zu erhöhten sIgA-Konzentrationen im Nasensekret. Dies deutet darauf hin, dass keine

Immunreaktion in der Schleimhaut ausgelöst wurde. Jedoch könnte es auch damit zusammenhängen, dass das Nasenwaschprozedere komplex und zeitaufwendig war und diese Antikörper oftmals durch die vorhandenen proteolytischen Enzyme abgebaut wurden. Die Zytokinanalyse der Milzhomogenisate zeigte keinen signifikanten Unterschied der in IFN-γ- und IL-2-Zytokinsekretion zwischen den verschiedenen Behandlungsgruppen. Der Grund dafür könnte die Immun-Homöostase sein, welche die Ausschüttung von Zytokinen und Chemokinen herunterregelt, wenn das abgebaute Antigen oder der Infektionserreger vollständig eliminiert ist. Um die Zytokin (IFN-γ und IL-2)-Produktion der Splenozyten nach der Immunisierungsstudie zu untersuchen, wurden die Splenozyten *ex vivo* mit Concanavalin A (ConA), einem starken T-Zell-Stimulanz, stimuliert. Die Konzentrationen der Zytokine IFN-γ und IL-2 im Überstand der Splenozytenkultur wurde 72 Stunden nach der Stimulation gemessen. Die IFN-γ- und IL-2-Konzentrationen waren in BNP_*i.n.*-, TTNP_*i.n.*- und BE tt_*i.m.*-Behandlungsgruppen im Vergleich zu den Kontroll- und FTT_*i.n.*-Gruppen signifikant erhöht. Die vermehrte Produktion von IFN-γ und IL-2 nach der Stimulation mit ConA in diesen Behandlungsgruppen deutet auf eine Verschiebung Richtung Th1-Immunantwort hin. Andererseits weist die erhöhte Konzentration von TT-spezifischen IgG im Serum nach der Behandlung mit TT-Nanopartikeln oder der auf dem Markt zugelassenen TT-Formulierung eine Aktivierung der Th2-Immunanwort nach. Diese gemischte Th1-Th2-Antwort auf die mit TT beladene, neuartige mukoadhäsive Nanopartikelformulierung wird eine erfolgreiche Immunisierung über die nasale Applikation sicherstellen.

c) Mechanistische Verständnis der Immunantwort ausgelöst durch neuartige, mit Ovalbumin beladene, mukoadhäsive Nanopartikel:

Bei der konventionellen Entwicklung von Impfstoffen wurde nur sehr wenig Aufmerksamkeit auf den Mechanismus, mit dem die Immunantwort aktiviert wird, gelegt. Jedoch gewinnt die rationale Entwicklung von Impfstoff-Antigenen bzw. Impfstoff-Formulierungen, basierend auf einer systematischen Untersuchung der Auswirkungen auf die Immuneffektoren, heute an Bedeutung.

In dieser Arbeit wurde der Einfluss von Ovalbumin-beladenen Nanopartikeln (OVA NP) auf die diversen Komponenten des Immunsystems qualitativ und quantitativ untersucht.

C57BL/6L-Mäuse wurden immunisiert durch intranasale (*i.n.*) Applizierung von OVA NP, unbeladenen Nanopartikeln (BNP) und an Aluminiumhydroxid adsorbiertes Ovalbumin (OVA_Ads), sowie durch intramuskuläre Applizierung (*i.m.*) von OVA_Ads als positiv

Kontrollgruppe. OVA-spezifische IgG-Antikörper wurden in Serumproben der behandelten Mäuse analysiert. Ein höherer IgG-Serumspiegel bei den mit OVA NP nasal behandelten Mäusen bestätigte eine bessere humorale Reaktion im Vergleich zu den anderen Behandlungsgruppen. Hauptgründe für die höheren IgG-Serumkonzentrationen waren die erhöhte Aufnahme der Nanopartikel und die kontrollierte Freisetzung von OVA.

Der Mechanismus, mit dem die OVA NP die Immunantwort modulieren, wurde im Detail analysiert, indem nach der Behandlung die aktivierten Immunzellen des Blutes und der Milz mithilfe der Durchflusszytometrie (FACS) untersucht wurden. Nach Abschluss der Immunisierungs-Studie wurden die Milzzellen (Splenocyten) der behandelten Mäuse *ex vivo* mit Immunstimulantien (PMA+Ionomycin) und OVA nochmals stimuliert um die Menge und Art der ausgeschütteten Zytokine der Immunzellen (CD4 und CD8 T-Zellen) zu kontrollieren. Die Durchflusszytometrie-Analyse der Immunzellen im Blut der mit OVA NP behandelten Mäuse zeigte eine gesteigerte Hochregulierung der co-stimulierenden Oberflächenmoleküle CD69 und MHCII auf dendritischen Zellen (DC) und Makrophagen. Diese Ergebnisse bestätigen die verstärkte Stimulation des angeborenen Immunsystems und eine gesteigerte Antigenaufnahme und -Verarbeitung der dendritischen Zellen.

Die Expression von co-stimulierenden Molekülen (CD69, MHCII, CD80 und CD86) auf verschiedenen Zellpopulationen der Milz wie den dendritischen Zellen ($CD11c^+$), T-Zellen ($CD4^+$ T-Zellen) und B-Zellen ($B220^+$) wurde zusätzlich nach Beendigung der Immunisierungsstudie untersucht. Ähnlich zu den Beobachtungen bei der durchflusszytometrischen Analyse der Blutproben zeigten $CD11c^+$-Zellen (dendritische Zellen) der OVA NP Behandlungsgruppe eine signifikant verstärkte Hochregulierung von $CD69^+$ ($p<0,01$) und $MHCII^+$ ($p<0,05$) während $CD4^+$ T-Zellen nur eine verstärkte Hochregulierung der $MHCII^+$ ($p<0,05$) co-stimulierenden Molekülen aufwiesen. Diese Ergebnisse weisen auf eine bessere Aufnahme und Präsentation des Antigens (OVA) durch dendritischen Zellen für $CD4^+$ T-Zellen hin. Dies stimulierte zusätzlich die adaptive Immunantwort, was zu einer höheren Konzentration von OVA-spezifischen IgG-Antikörpern in mit OVA NP behandelten Mäusen führte. Intranasale Behandlung mit OVA NP führte außerdem zu einer signifikant verstärkten Hochregulierung der $CD86^+$ co-timulierenden Moleküle auf B-Lymphozyten im Vergleich zur OVA_Ads intranasalen Gruppe, was auf eine höhere IgG-Antikörperproduktion (humorale Immunantwort) hinweist.

Die *ex vivo* Stimulierung der Splenocyten mithilfe der Kombination von PMA und Ionomycin führte in der mit OVA NP behandelten Gruppe zu einer erhöhten Anzahl von CD8 T-Zellen,

welche IFN-γ und IL-10 sekretieren. Dies bestätigte nochmals die Aktivierung sowohl der zellulären als auch der humoralen Immunantwort.
Zur weiteren *in vitro*-Analyse der OVA-spezifischen Zytokin-Sekretion wurden Splenocyten am Ende der Immunisierungsuntersuchung entweder mit oder ohne Zugabe von OVA stimuliert. Eine signifikante Steigerung der Konzentrationen von IFN-γ ($p<0,001$), IL-6 ($p<0,05$) und IL-17a ($p<0,01$) konnte bei den mit OVA NP *i.n.* behandelten Mäusen im Vergleich zu den Mäusen, die mit OVA_Ads *i.n.* behandelt wurden sowie im Vergleich zur Kontrollgruppe beobachtet werden. Kein signifikanter Unterschied wurde bei der Konzentration des antientzündlichen IL-10-Zytokins festgestellt, was zeigt, dass keine Entzündung stattfand.
Zusammenfassend kann gesagt werden, dass eine kombinierte Th1-, Th2- und Th17-Immunantwort, hervorgerufen durch OVA-beladene polymerische Nanopartikel, alle Komponenten des Immunsystems aktivierte, was einen besseren Schutz und damit den Erfolg der Formulierung gewährleistet.

Als Fazit der ganzen Arbeit ist Folgendes festzuhalten: kontrolliert freisetzende, biokompatible Nanopartikel mit hoher Einschlusseffizienz von Proteinen/Impfstoffantigenen wurden erfolgreich hergestellt, ohne dass die Integrität und die Stabilität der Konformation der eingeschlossenen Proteine beeinträchtigt wurde. Die Wirksamkeit von mit Tetanustoxoid beladenen, intranasal applizierten Nanopartikeln war mit derjenigen der auf dem Markt zugelassenen, intramuskulären Formulierung (BE tt™) vergleichbar. Der Mechanismus der Immunstimulation durch die entwickelten, neuartigen Nanopartikel wurde aufgezeigt und die Wirksamkeit verglichen mit OVA, welches an Aluminiumhydroxid adsorbiert war, einem häufig genutzten Adjuvans in Impfprodukten.
Diese Erfolge können Anwendung finden als verheißungsvolles, kosteneffektives Impfstoff-Darreichungssystem zur nasalen Applikation.

6. References

Abdelwahed, W., Degobert, G., Fessi, H., 2006a. Investigation of nanocapsules stabilization by amorphous excipients during freeze-drying and storage. European Journal of Pharmaceutics and Biopharmaceutics 63, 87-94.

Abdelwahed, W., Degobert, G., Stainmesse, S., Fessi, H., 2006b. Freeze-drying of nanoparticles: Formulation, process and storage considerations. Advanced Drug Delivery Reviews 58, 1688-1713.

Adm, F.D., CDER, CBER, 2013. Guidance for Industry: Immunogenicity Assessment for Therapeutic Protein Products. Biotechnology Law Report 32, 172-185.

Aguado, M.T., 1993. Future Approaches to Vaccine Development - Single-Dose Vaccines Using Controlled-Release Delivery Systems. Vaccine 11, 596-597.

Aguado, T., Engers, H., Pang, T., Pink, R., 1999. Novel adjuvants currently in clinical testing November 2-4, 1998, Fondation Merieux, Annecy, France: a meeting sponsored by the World Health Organization. Vaccine 17, 2321-2328.

Ahire, V.J., Sawant, K.K., Doshi, J.B., Ravetkar, S.D., 2007. Chitosan Microparticles as Oral Delivery System for Tetanus Toxoid. Drug Development and Industrial Pharmacy 33, 1112-1124.

Akagi, T., Baba, M., Akashi, M., 2012. Biodegradable Nanoparticles as Vaccine Adjuvants and Delivery Systems: Regulation of Immune Responses by Nanoparticle-Based Vaccine. Polymers in Nanomedicine 247, 31-64.

Akagi, T., Kaneko, T., Kida, T., Akashi, M., 2005. Preparation and characterization of biodegradable nanoparticles based on poly(gamma-glutamic acid) with L-phenylalanine as a protein carrier. Journal of Controlled Release 108, 226-236.

Ali, M.S., Al-Lohedan, H.A., Rafiquee, M.Z.A., Atta, A.M., Ezzat, A.O., 2015. Spectroscopic studies on the interaction between novel polyvinylthiol-functionalized silver nanoparticles with lysozyme. Spectrochimica Acta Part A: Molecular and Biomolecular Spectroscopy 135, 147-152.

Allémann, E., Gurny, R., Doelker, E., 1992. Preparation of aqueous polymeric nanodispersions by a reversible salting-out process: influence of process parameters on particle size. International Journal of Pharmaceutics 87, 247-253.

Almeida, P.F., Almeida, A.J., 2004. Cross-linked alginate-gelatine beads: a new matrix for controlled release of pindolol. Journal of controlled release 97, 431-439.

Alonso, M.J., Losa, C., Calvo, P., Vilajato, J.L., 1991. Approaches to Improve the Association of Amikacin Sulfate to Poly(Alkylcyanoacrylate) Nanoparticles. International Journal of Pharmaceutics 68, 69-76.

Ambrose, C.S., Wu, X.H., Jones, T., Mallory, R.M., 2012. The role of nasal IgA in children vaccinated with live attenuated influenza vaccine. Vaccine 30, 6794-6801.

Amidi, M., Romeijn, S.G., Borchard, G., Junginger, H.E., Hennink, W.E., Jiskoot, W., 2006. Preparation and characterization of protein-loaded N-trimethyl chitosan nanoparticles as nasal delivery system. Journal of controlled release 111, 107-116.

Anal, A.K., Stevens, W.F., Remuñán-López, C., 2006. Ionotropic cross-linked chitosan microspheres for controlled release of ampicillin. International Journal of Pharmaceutics 312, 166-173.

Andrade, F., Goycoolea, F., Chiappetta, D.A., das Neves, J., Sosnik, A., Sarmento, B., 2011. Chitosan-grafted copolymers and chitosan-ligand conjugates as matrices for pulmonary drug delivery. International Journal of Carbohydrate Chemistry 2011.

Anggard, A., 1974. Capillary and shunt blood flow in the nasal mucosa of the cat. Acta Otorrinolaringologica 78, 418-422.

Annunziato, F., Cosmi, L., Santarlasci, V., Maggi, L., Liotta, F., Mazzinghi, B., Parente, E., Fili, L., Ferri, S., Frosali, F., Giudici, F., Romagnani, P., Parronchi, P., Tonelli, F., Maggi, E., Romagnani, S., 2007. Phenotypic and functional features of human Th17 cells. Journal of Experimental Medicine 204, 1849-1861.

Avadi, M.R., Sadeghi, A.M.M., Mohammadpour, N., Abedin, S., Atyabi, F., Dinarvand, R., Rafiee-Tehrani, M., 2010. Preparation and characterization of insulin nanoparticles using chitosan and Arabic gum with ionic gelation method. Nanomedicine 6, 58-63.

Axelsson, I., 1978. Characterization of Proteins and Other Macromolecules by Agarose-Gel Chromatography. Journal of Chromatography A 152, 21-32.

Bacon, A., Makin, J., Sizer, P.J., Jabbal-Gill, I., Hinchcliffe, M., Illum, L., Chatfield, S., Roberts, M., 2000. Carbohydrate biopolymers enhance antibody responses to mucosally delivered vaccine antigens. Infection and Immunity 68, 5764-5770.

Badovinac, V.P., Harty, J.T., 2000. Intracellular staining for TNF and IFN-gamma detects different frequencies of antigen-specific CD8(+) T cells. Journal of Immunological Methods 238, 107-117.

Bal, S.M., Slutter, B., Verheul, R., Bouwstra, J.A., Jiskoot, W., 2012. Adjuvanted, antigen loaded N-trimethyl chitosan nanoparticles for nasal and intradermal vaccination: Adjuvant- and site-dependent immunogenicity in mice. European Journal of Pharmaceutical Sciences 45, 475-481.

Barichello, J.M., Morishita, M., Takayama, K., Nagai, T., 1999. Encapsulation of hydrophilic and lipophilic drugs in PLGA nanoparticles by the nanoprecipitation method. Drug Development and Industrial Pharmacy 25, 471-476.

Batchelor, H., 2014. Nasal, Ocular and Otic Drug Delivery, in: Bar-Shalom, D., Rose, K. (Eds.), Pediatric Formulations: A Roadmap. Springer New York, New York, NY, pp. 273-301.

Baudner, B.C., Giuliani, M.M., Verhoef, J.C., Rappuoli, R., Junginger, H.E., Giudice, G.D., 2003. The concomitant use of the LTK63 mucosal adjuvant and of chitosan-based

delivery system enhances the immunogenicity and efficacy of intranasally administered vaccines. Vaccine 21, 3837-3844.

Belshe, R.B., Newman, F.K., Anderson, E.L., Wright, P.F., Karron, R.A., Tollefson, S., Henderson, F.W., Meissner, H.C., Madhi, S., Roberton, D., Marshall, H., Loh, R., Sly, P., Murphy, B., Tatem, J.M., Randolph, V., Hackell, J., Gruber, W., Tsai, T.F., 2004. Evaluation of combined live, attenuated respiratory syncytial virus and parainfluenza 3 virus vaccines in infants and young children. Journal of Infectious Diseases 190, 2096-2103.

Bende, M., Flisberg, K., Larsson, I., Ohlin, P., Olsson, P., 1983. A method for determination of blood flow with 133Xe in human nasal mucosa. Acta Otorrinolaringologica 96, 277-285.

Benichou, A., Aserin, A., Garti, N., 2002. Protein-polysaccharide interactions for stabilization of food emulsions. Journal of Dispersion Science and Technology 23, 93-123.

Bernkop-Schnurch, A., Kast, C.E., Richter, M.F., 2001. Improvement in the mucoadhesive properties of alginate by the covalent attachment of cysteine. Journal of controlled release 71, 277-285.

Bertram, U., Bodmeier, R., 2006. In situ gelling, bioadhesive nasal inserts for extended drug delivery: In vitro characterization of a new nasal dosage form. European Journal of Pharmaceutical Sciences 27, 62-71.

Bhardwaj, V., Hariharan, S., Bala, I., Lamprecht, A., Kumar, N., Panchagnula, R., Ravi Kumar, M., 2005. Pharmaceutical aspects of polymeric nanoparticles for oral drug delivery. Journal of Biomedical Nanotechnology 1, 235-258.

Bienenstock, J., McDermott, M.R., 2005. Bronchus- and nasal-associated lymphoid tissues. Immunological Reviews 206, 22-31.

Bilensoy, E., Rouf, M.A., Vural, I., Sen, M., Hincal, A.A., 2006. Mucoadhesive, thermosensitive, prolonged-release vaginal gel for clotrimazole: beta-cyclodextrin complex. AAPS PharmSciTech 7:E54.

Boateng, J.S., Matthews, K.H., Stevens, H.N.E., Eccleston, G.M., 2008. Wound Healing Dressings and Drug Delivery Systems: A Review. Journal of Pharmaceutical Sciences 97, 2892-2923.

Bodmeier, R., Oh, K.H., Pramar, Y., 1989. Preparation and Evaluation of Drug-Containing Chitosan Beads. Drug Development and Industrial Pharmacy 15, 1475-1494.

Boonyo, W., Junginger, H.E., Waranuch, N., Polnok, A., Pitaksuteepong, T., 2007. Chitosan and trimethyl chitosan chloride (TMC) as adjuvants for inducing immune responses to ovalbumin in mice following nasal administration. Journal of Controlled Release 121, 168-175.

Borges, O., Borchard, G., Verhoef, J.C., de Sousa, A., Junginger, H.E., 2005. Preparation of coated nanoparticles for a new mucosal vaccine delivery system. International Journal of Pharmaceutics 299, 155-166.

Borges, O., Cordeiro-da-Silva, A., Tavares, J., Santarem, N., de Sousa, A., Borchard, G., Junginger, H.E., 2008a. Immune response by nasal delivery of hepatitis B surface antigen and codelivery of a CpG ODN in alginate coated chitosan nanoparticles. European Journal of Pharmaceutics and Biopharmaceutics 69, 405-416.

Borges, O., Silva, M., de Sousa, A., Borchard, G., Junginger, H.E., Cordeiro-da-Silva, A., 2008b. Alginate coated chitosan nanoparticles are an effective subcutaneous adjuvant for hepatitis B surface antigen. International Immunopharmacology 8, 1773-1780.

Borges, O., Tavares, J., de Sousa, A., Borchard, G., Junginger, H.E., Cordeiro-Da-Silva, A., 2007. Evaluation of the immune response following a short oral vaccination schedule with hepatitis B antigen encapsulated into alginate-coated chitosan nanoparticles. European Journal of Pharmaceutical Sciences 32, 278-290.

Braun, A., Alsenz, J., 1997. Development and use of enzyme-linked immunosorbent assays (ELISA) for the detection of protein aggregates in interferon-alpha (IFN-alpha) formulations. Pharmaceutical Research 14, 1394-1400.

Brewer, S.H., Glomm, W.R., Johnson, M.C., Knag, M.K., Franzen, S., 2005. Probing BSA binding to citrate-coated gold nanoparticles and surfaces. Langmuir 21, 9303-9307.

Broere, F., Apasov, S.G., Sitkovsky, M.V., van Eden, W., 2011. A2 T cell subsets and T cell-mediated immunity, Principles of immunopharmacology. Springer, pp. 15-27.

Bromberg, L., 1998. Properties of aqueous solutions and gels of poly(ethylene oxide)-b-poly(propylene oxide)-b-poly(ethylene oxide)-g-poly(acrylic acid). The Journal of Physical Chemistry B 102, 10736-10744.

Bromberg, L., Hatton, T.A., Barreiro-Iglesias, R., Alvarez-Lorenzo, C., Concheiro, A., 2007. Controlled release camptothecin tablets based on pluronic and poly(acrylic acid) copolymer. Effect of fabrication technique on drug stability, tablet structure, and release mode. Drug Development and Industrial Pharmacy 33, 607-615.

Bromberg, L., Temchenko, M., Alakhov, V., Hatton, T.A., 2004. Bioadhesive properties and rheology of polyether-modified poly(acrylic acid) hydrogels. International Journal of Pharmaceutics 282, 45-60.

Bujacz, A., Zielinski, K., Sekula, B., 2014. Structural studies of bovine, equine, and leporine serum albumin complexes with naproxen. Proteins 82, 2199-2208.

Butoescu, N., Jordan, O., Doelker, E., 2009. Intra-articular drug delivery systems for the treatment of rheumatic diseases: A review of the factors influencing their performance. European Journal of Pharmaceutics and Biopharmaceutics 73, 205-218.

Calvo, P., RemunanLopez, C., VilaJato, J.L., Alonso, M.J., 1997. Novel hydrophilic chitosan-polyethylene oxide nanoparticles as protein carriers. The Journal of Applied Polymer Science 63, 125-132.

Cannon, G.J., Swanson, J.A., 1992. The Macrophage Capacity for Phagocytosis. Journal of Cell Science 101, 907-913.

Castaldello, A., Brocca-Cofano, E., Voltan, R., Triulzi, C., Altavilla, G., Laus, M., Sparnacci, K., Ballestri, M., Tondelli, L., Fortini, C., Gavioli, R., Ensoli, B., Caputo, A., 2006. DNA prime and protein boost immunization with innovative polymeric cationic core-shell nanoparticles elicits broad immune responses and strongly enhance cellular responses of HIV-1 tat DNA vaccination. Vaccine 24, 5655-5669.

Cesta, M.F., 2006. Normal structure, function, and histology of mucosa-associated lymphoid tissue. Toxicologic Pathology 34, 599-608.

Chacon, M., Molpeceres, J., Berges, L., Guzman, M., Aberturas, M.R., 1999. Stability and freeze-drying of cyclosporine loaded poly(D,L lactide-glycolide) carriers. European Journal of Pharmaceutical Sciences 8, 99-107.

Chadwick, S., Kriegel, C., Amiji, M., 2010. Nanotechnology solutions for mucosal immunization. Advanced Drug Delivery Reviews 62, 394-407.

Chang, D., Chang, R.K., 2007. Review of current issues in pharmaceutical excipients. Pharmaceutical Technology 31, 56-66.

Charalambos D, P., 2000. Intranasal vaccines: forthcoming challenges. Pharmaceutical Science and Technology Today 3, 273-281.

Chen, M.C., Mi, F.L., Liao, Z.X., Hsiao, C.W., Sonaje, K., Chung, M.F., Hsu, L.W., Sung, H.W., 2013. Recent advances in chitosan-based nanoparticles for oral delivery of macromolecules. Advanced Drug Delivery Reviews 65, 865-879.

Chen, W.X., Cheng, Y.F., Wang, B.H., 2012. Dual-Responsive Boronate Crosslinked Micelles for Targeted Drug Delivery. Angewandte Chemie International Edition 51, 5293-5295.

Chiappetta, D.A., Sosnik, A., 2007. Poly(ethylene oxide)-poly(propylene oxide) block copolymer micelles as drug delivery agents: Improved hydrosolubility, stability and bioavailability of drugs. European Journal of Pharmaceutics and Biopharmaceutics 66, 303-317.

Cleary, J., Bromberg, L., Magner, E., 2004. Adhesion of polyether-modified poly(acrylic acid) to mucin. Langmuir 20, 9755-9762.

Cleland, J.L., Powell, M.F., Shire, S.J., 1993. The Development of Stable Protein Formulations - a Close Look at Protein Aggregation, Deamidation, and Oxidation. Critical Reviews in Therapeutic Drug Carrier Systems 10, 307-377.

Cohn, D., Lando, G., Sosnik, A., Garty, S., Levi, A., 2006. PEO-PPO-PEO-based poly(ether ester urethane)s as degradable reverse thermo-responsive multiblock copolymers. Biomaterials 27, 1718-1727.

Cohn, D., Sosnik, A., 2003. Novel reverse thermoresponsive injectable poly(ether carbonate)s. Journal of Materials Science: Materials in Medicine 14, 175-180.

Cohn, D., Sosnik, A., Levy, A., 2003. Improved reverse thermo-responsive polymeric systems. Biomaterials 24, 3707-3714.

Cohn, D., Sosnik, A., Malal, R., Zarka, R., Garty, S., Levy, A., 2007. Chain extension as a strategy for the development of improved reverse thermo-responsive polymers. Polymers for Advanced Technologies 18, 731-736.

Cordeiro, A.S., Alonso, M.J., de la Fuente, M., 2015. Nanoengineering of vaccines using natural polysaccharides. Biotechnology Advances 33, 1279-1293.

Couper, K.N., Blount, D.G., Riley, E.M., 2008. IL-10: the master regulator of immunity to infection. The Journal of Immunology 180, 5771-5777.

Couvreur, P., Barratt, G., Fattal, E., Legrand, P., Vauthier, C., 2002. Nanocapsule technology: A review. Critical Reviews in Therapeutic Drug Carrier Systems 19, 99-134.

Couvreur, P., Dubernet, C., Puisieux, F., 1995. Controlled Drug-Delivery with Nanoparticles - Current Possibilities and Future-Trends. European Journal of Pharmaceutics and Biopharmaceutics 41, 2-13.

Cox, J.C., Coulter, A.R., 1997. Adjuvants - A classification and review of their modes of action. Vaccine 15, 248-256.

Craven, C.J., Dawson, D.J., 1973. The chain composition of tetanus toxin. Biochimica et Biophysica Acta 317, 277-285.

Csaba, N., Garcia-Fuentes, M., Alonso, M.J., 2009. Nanoparticles for nasal vaccination. Advanced Drug Delivery Reviews 61, 140-157.

Dahl, T.C., Allen, L.V., Luner, P.E., Kanbir, M.A., Reo, P.E., 2009. Handbook of pharmaceutical excipients, 6th ed. Pharmaceutical Press.

Dahlin, M., Jansson, B., Bjork, E., 2001. Levels of dopamine in blood and brain following nasal administration to rats. European Journal of Pharmaceutical Sciences 14, 75-80.

Dalum, I., Jensen, M.R., Gregorius, K., Thomasen, C.M., Elsner, H.I., Mouritsen, S., 1997. Induction of cross-reactive antibodies against a self protein by immunization with a modified self protein containing a foreign T helper epitope. Molecular Immunology 34, 1113-1120.

das Neves, J., Bahia, M.F., Amiji, M.M., Sarmento, B., 2011. Mucoadhesive nanomedicines: characterization and modulation of mucoadhesion at the nanoscale. Expert Opinion on Drug Delivery 8, 1085-1104.

das Neves, J., Michiels, J., Arien, K.K., Vanham, G., Amiji, M., Bahia, M.F., Sarmento, B., 2012. Polymeric nanoparticles affect the intracellular delivery, antiretroviral activity and cytotoxicity of the microbicide drug candidate dapivirine. Pharmaceutical Research 29, 1468-1484.

Davda, J., Labhasetwar, V., 2002. Characterization of nanoparticle uptake by endothelial cells. International Journal of Pharmaceutics 233, 51-59.

De Jaeghere, F., Allemann, E., Leroux, J.C., Stevels, W., Feijen, J., Doelker, E., Gurny, R., 1999. Formulation and lyoprotection of poly(lactic acid-co-ethylene oxide) nanoparticles: Influence on physical stability and in vitro cell uptake. Pharmaceutical Research 16, 859-866.

de la Fuente, M., Ravina, M., Paolicelli, P., Sanchez, A., Seijo, B., Alonso, M.J., 2010. Chitosan-based nanostructures: A delivery platform for ocular therapeutics. Advanced Drug Delivery Reviews 62, 100-117.

de Vos, P., Faas, M.M., Strand, B., Calafiore, R., 2006. Alginate-based microcapsules for immunoisolation of pancreatic islets. Biomaterials 27, 5603-5617.

Demento, S.L., Cui, W.G., Criscione, J.M., Stern, E., Tulipan, J., Kaech, S.M., Fahmy, T.M., 2012. Role of sustained antigen release from nanoparticle vaccines in shaping the T cell memory phenotype. Biomaterials 33, 4957-4964.

Devadasu, V.R., Bhardwaj, V., Kumar, M.N.V.R., 2013. Can Controversial Nanotechnology Promise Drug Delivery? Chemical Reviews 113, 1686-1735.

Douglas, K.L., Tabrizian, M., 2005. Effect of experimental parameters on the formation of alginate-chitosan nanoparticles and evaluation of their potential application as DNA carrier. Journal of biomaterials science. Polymer edition 16, 43-56.

Draget, K.I., Smidsrød, O., Skjåk-Bræk, G., 2005. Alginates from Algae, Biopolymers Online. Wiley-VCH Verlag GmbH & Co. KGaA.

Duchateau, G.S.M.J.E., Graamans, K., Zuidema, J., Merkus, F.W.H.M., 1985. Correlation between Nasal Ciliary Beat Frequency and Mucus Transport Rate in Volunteers. The Laryngoscope 95, 854-859.

Dufes, C., Olivier, J.C., Gaillard, F., Gaillard, A., Couet, W., Muller, J.M., 2003. Brain delivery of vasoactive intestinal peptide (VIP) following nasal administration to rats. International Journal of Pharmaceutics 255, 87-97.

Duque, G.A., Descoteaux, A., 2014. Macrophage cytokines: involvement in immunity and infectious diseases. Frontiers in Immunology 5, 1-12.

Eidi, H., Joubert, O., Attik, G., Duval, R.E., Bottin, M.C., Hamouia, A., Maincent, P., Rihn, B.H., 2010. Cytotoxicity assessment of heparin nanoparticles in NR8383 macrophages. International Journal of Pharmaceutics 396, 156-165.

Ekman, B., Sjoholm, I., 1978. Improved Stability of Proteins Immobilized in Microparticles Prepared by a Modified Emulsion Polymerization Technique. Journal of Pharmaceutical Sciences 67, 693-696.

El-Shabouri, M.H., 2002. Positively charged nanoparticles for improving the oral bioavailability of cyclosporin-A. International Journal of Pharmaceutics 249, 101-108.

Eldridge, J.H., Hammond, C.J., Meulbroek, J.A., Staas, J.K., Gilley, R.M., Tice, T.R., 1990. Controlled Vaccine Release in the Gut-Associated Lymphoid-Tissues .1. Orally-Administered Biodegradable Microspheres Target the Peyers Patches. Journal of Controlled Release 11, 205-214.

Ellis, G.A., Palte, M.J., Raines, R.T., 2012. Boronate-mediated biologic delivery. Journal of the American Chemical Society 134, 3631-3634.

Fallouh, N.A.K., Roblot-Treupel, L., Fessi, H., Devissaguet, J.P., Puisieux, F., 1986. Development of a new process for the manufacture of polyisobutylcyanoacrylate nanocapsules. International Journal of Pharmaceutics 28, 125-132.

Fan, W., Yan, W., Xu, Z., Ni, H., 2012. Formation mechanism of monodisperse, low molecular weight chitosan nanoparticles by ionic gelation technique. Colloids and Surfaces B: Biointerfaces 90, 21-27.

Feng, G.Z., Jiang, Q.T., Xia, M., Lu, Y.L., Qiu, W., Zhao, D., Lu, L.W., Peng, G.Y., Wang, Y.W., 2013. Enhanced Immune Response and Protective Effects of Nano-chitosan-based DNA Vaccine Encoding T Cell Epitopes of Esat-6 and FL against Mycobacterium Tuberculosis Infection. PloS One 8.

Fischer, D., Li, Y.X., Ahlemeyer, B., Krieglstein, J., Kissel, T., 2003. In vitro cytotoxicity testing of polycations: influence of polymer structure on cell viability and hemolysis. Biomaterials 24, 1121-1131.

Fokkens, W.J., Vroom, T.M., Rijntjes, E., Mulder, P.G., 1989. CD-1 (T6), HLA-DR-expressing cells, presumably Langerhans cells, in nasal mucosa. Allergy 44, 167-172.

Folttmann, H., Quadir, A., 2008. Polyvinylpyrrolidone (PVP)—one of the most widely used excipients in pharmaceuticals: an overview. Drug Delivery Technology 8, 22-27.

Fu, K., Griebenow, K., Hsieh, L., Klibanov, A.M., Langer, R., 1999. FTIR characterization of the secondary structure of proteins encapsulated within PLGA microspheres'. Journal of Controlled Release 58, 357-366.

Gamvrellis, A., Leong, D., Hanley, J.C., Xiang, S.D., Mottram, P., Plebanski, M., 2004. Vaccines that facilitate antigen entry into dendritic cells. Immunology and Cell Biology 82, 506-516.

Gan, Q., Wang, T., 2007. Chitosan nanoparticle as protein delivery carrier - Systematic examination of fabrication conditions for efficient loading and release. Colloids and Surfaces B: Biointerfaces 59, 24-34.

Ganachaud, F., Katz, J.L., 2005. Nanoparticles and Nanocapsules Created Using the Ouzo Effect: Spontaneous Emulsification as an Alternative to Ultrasonic and High-Shear Devices. ChemPhysChem 6, 209-216.

Garinot, M., Fievez, V., Pourcelle, V., Stoffelbach, F., des Rieux, A., Plapied, L., Theate, I., Freichels, H., Jerome, C., Marchand-Brynaert, J., Schneider, Y.J., Preat, V., 2007.

PEGylated PLGA-based nanoparticles targeting M cells for oral vaccination. Journal of Controlled Release 120, 195-204.

Gåserød, O., Jolliffe, I.G., Hampson, F.C., Dettmar, P.W., Skjåk-Bræk, G., 1998. The enhancement of the bioadhesive properties of calcium alginate gel beads by coating with chitosan. International Journal of Pharmaceutics 175, 237-246.

Ge, S.R., Kojio, K., Takahara, A., Kajiyama, T., 1998. Bovine serum albumin adsorption onto immobilized organotrichlorosilane surface: Influence of the phase separation on protein adsorption patterns. Journal of Biomaterials Science, Polymer Edition 9, 131-150.

Gettins, P.G.W., 2002. Serpin structure, mechanism, and function. Chemical Reviews 102, 4751-4803.

Gizurarson, S., 1990. Animal-Models for Intranasal Drug Delivery Studies - a Review Article. Acta Pharmaceutica Nordica 2, 105-122.

Gizurarson, S., 2012. Anatomical and Histological Factors Affecting Intranasal Drug and Vaccine Delivery. Current Drug Delivery 9, 566-582.

Gogev, S., de Fays, K., Versali, M.F., Gautier, S., Thiry, E., 2004. Glycol chitosan improves the efficacy of intranasally administrated replication defective human adenovirus type 5 expressing glycoprotein D of bovine herpesvirus 1. Vaccine 22, 1946-1953.

Goh, C.H., Heng, P.W.S., Chan, L.W., 2012. Alginates as a useful natural polymer for microencapsulation and therapeutic applications. Carbohydrate Polymers 88, 1-12.

Gonzalez, M.J., Plummer, E.M., Rae, C.S., Manchester, M., 2009. Interaction of Cowpea Mosaic Virus (CPMV) Nanoparticles with Antigen Presenting Cells In Vitro and In Vivo. PloS One 4.

Goshisht, M.K., Moudgil, L., Khullar, P., Singh, G., Kaura, A., Kumar, H., Kaur, G., Bakshi, M.S., 2015. Surface Adsorption and Molecular Modeling of Biofunctional Gold Nanoparticles for Systemic Circulation and Biological Sustainability. ACS Sustainable Chemistry & Engineering 3, 3175-3187.

Grabovac, V., Guggi, D., Bernkop-Schnurch, A., 2005. Comparison of the mucoadhesive properties of various polymers. Advanced Drug Delivery Reviews 57, 1713-1723.

Greenfield, N., 1982. Citation Classic - Computed Circular-Dichroism Spectra for the Evaluation of Protein Conformation. Current Contents/Life Science, 28-28.

Gross-Heitfeld, C., Linders, J., Appel, R., Selbach, F., Mayer, C., 2014. Polyalkylcyanoacrylate Nanocapsules: Variation of Membrane Permeability by Chemical Cross-Linking. Journal of Physical Chemistry B 118, 4932-4939.

Guggi, D., Langoth, N., Hoffer, M.H., Wirth, M., Bernkop-Schnurch, A., 2004. Comparative evaluation of cytotoxicity of a glucosamine-TBA conjugate and a chitosan-TBA conjugate. International Journal of Pharmaceutics 278, 353-360.

Hamdy, S., Elamanchili, P., Alshamsan, A., Molavi, O., Satou, T., Samuel, J., 2007. Enhanced antigen-specific primary CD4(+) and CD8(+) responses by codelivery of ovalbumin and toll-like receptor ligand monophosphoryl lipid A in poly(D,L-lactic-co-glycolic acid) nanoparticles. Journal of Biomedical Materials Research Part A 81a, 652-662.

Harde, H., Agrawal, A.K., Jain, S., 2014. Development of stabilized glucomannosylated chitosan nanoparticles using tandem crosslinking method for oral vaccine delivery. Nanomedicine 9, 2511-2529.

Harde, H., Agrawal, A.K., Jain, S.Y., 2015. Tetanus Toxoids Loaded Glucomannosylated Chitosan Based Nanohoming Vaccine Adjuvant with Improved Oral Stability and Immunostimulatory Response. Pharmaceutical Research 32, 122-143.

Hasegawa, K., Noguchi, Y., Koizumi, F., Uenaka, A., Tanaka, M., Shimono, M., Nakamura, H., Shiku, H., Gnjatic, S., Murphy, R., Hiramatsu, Y., Old, L.J., Nakayama, E., 2006. In vitro Stimulation of CD8 and CD4 T Cells by Dendritic Cells Loaded with a Complex of Cholesterol-Bearing Hydrophobized Pullulan and NY-ESO-1 Protein: Identification of a New HLA-DR15–Binding CD4 T-Cell Epitope. Clinical Cancer Research 12, 1921-1927.

Hassan, R.M., 1991. Alginate Polyelectrolyte Ionotropic Gels .3. Kinetics of Exchange of Chelated Divalent Transition-Metal Ions Especially Cobalt(Ii) and Copper(Ii) by Hydrogen-Ions in Capillary Ionotropic Metal Alginate Polymembrane Gels. Journal of Materials Science 26, 5806-5810.

Haug, A., Larsen, B., Smidsrød, O., 1974. Uronic acid sequence in alginate from different sources. Carbohydrate Research 32, 217-225.

He, C., Hu, Y., Yin, L., Tang, C., Yin, C., 2010. Effects of particle size and surface charge on cellular uptake and biodistribution of polymeric nanoparticles. Biomaterials 31, 3657-3666.

Hinchcliffe, M., Illum, L., 1999. Intranasal insulin delivery and therapy. Advanced Drug Delivery Reviews 35, 199-234.

Hirayama, K., Akashi, S., Furuya, M., Fukuhara, K., 1990. Rapid Confirmation and Revision of the Primary Structure of Bovine Serum-Albumin by Esims and Frit-Fab Lc Ms. Biochemical and Biophysical Research Communications 173, 639-646.

Honda-Okubo, Y., Saade, F., Petrovsky, N., 2012. Advax (TM), a polysaccharide adjuvant derived from delta inulin, provides improved influenza vaccine protection through broad-based enhancement of adaptive immune responses. Vaccine 30, 5373-5381.

Hua, X.Y., Zeman, K.L., Zhou, B.Q., Hua, Q.Q., Senior, B.A., Tilley, S.L., Bennett, W.D., 2010. Noninvasive real-time measurement of nasal mucociliary clearance in mice by pinhole gamma scintigraphy. Journal of Applied Physiology 108, 189-196.

Hunter, C.A., Jones, S.A., 2015. IL-6 as a keystone cytokine in health and disease. Nature Immunology 16, 448-457.

Huntington, J.A., Stein, P.E., 2001. Structure and properties of ovalbumin. Journal of Chromatography B: Biomedical Sciences and Applications 756, 189-198.

Illum, L., 1996. Nasal delivery. The use of animal models to predict performance in man. Journal of Drug Targeting 3, 427-442.

Illum, L., 2000. Transport of drugs from the nasal cavity to the central nervous system. European Journal of Pharmaceutical Sciences 11, 1-18.

Illum, L., 2015. Intranasal Delivery to the Central Nervous System, Blood-Brain Barrier in Drug Discovery. John Wiley & Sons, Inc, pp. 535-565.

Illum, L., Fisher, A.N., 1997. Intranasal delivery of peptides and proteins, in: Adjei, A.L., Gupta, P.K. (Eds.), Inhalation delivery of therapeutic peptides and proteins. Marcel Dekker Inc., New York, pp. 135-184.

Illum, L., Jabbal-Gill, I., Hinchcliffe, M., Fisher, A.N., Davis, S.S., 2001. Chitosan as a novel nasal delivery system for vaccines. Advanced Drug Delivery Reviews 51, 81-96.

Iovescu, A., Băran, A., Stîngă, G., Cantemir-Leontieş, A.R., Maxim, M.E., Anghel, D.F., 2015. A combined binding mechanism of nonionic ethoxylated surfactants to bovine serum albumin revealed by fluorescence and circular dichroism. Journal of Photochemistry and Photobiology B: Biology 153, 198-205.

Irache, J.M., Huici, M., Konecny, M., Espuelas, S., Campanero, M.A., Arbos, P., 2005. Bioadhesive properties of Gantrez nanoparticles. Molecules 10, 126-145.

Issa, M.M., Koping-Hoggard, M., Artursson, P., 2005. Chitosan and the mucosal delivery of biotechnology drugs. Drug Discovery Today: Technologies 2, 1-6.

Ivanov, A.E., Eccles, J., Panahi, H.A., Kumar, A., Kuzimenkova, M.V., Nilsson, L., Bergenstahl, B., Long, N., Phillips, G.J., Mikhalovsky, S.V., Galaev, I.Y., Mattiasson, B., 2009. Boronate-containing polymer brushes: Characterization, interaction with saccharides and mammalian cancer cells. Journal of Biomedical Materials Research Part A 88a, 213-225.

Ivanov, A.E., Galaev, I.Y., Mattiasson, B., 2006. Interaction of sugars, polysaccharides and cells with boronate-containing copolymers: from solution to polymer brushes. Journal of Molecular Recognition 19, 322-331.

Jabbal-Gill, I., 2010. Nasal vaccine innovation. Journal of Drug Targeting 18, 771-786.

Jabbal-Gill, I., Fisher, A.N., Rappuoli, R., Davis, S.S., Illum, L., 1998. Stimulation of mucosal and systemic antibody responses against Bordetella pertussis filamentous haemagglutinin and recombinant pertussis toxin after nasal administration with chitosan in mice. Vaccine 16, 2039-2046.

Jain, S., Harde, H., Indulkar, A., Agrawal, A.K., 2014. Improved stability and immunological potential of tetanus toxoid containing surface engineered bilosomes following oral administration. Nanomedicine 10, 431-440.

Jain, S., Khomane, K., K. Jain, A., Dani, P., 2011a. Nanocarriers for Transmucosal Vaccine Delivery. Current Nanoscience 7, 160-177.

Jain, S., Uchegbu, I.F., Betageri, G., Pastorin, G., 2011b. Nanotechnology in advanced drug delivery. Journal of Drug Delivery 2011, 343082.

Janes, K.A., Fresneau, M.P., Marazuela, A., Fabra, A., Alonso, M.J., 2001. Chitosan nanoparticles as delivery systems for doxorubicin. Journal of Controlled Release 73, 255-267.

Jimenez-Castellanos, M.R., Zia, H., Rhodes, C.T., 1993. Mucoadhesive Drug Delivery Systems. Drug Development and Industrial Pharmacy 19, 143-194.

Jones, N., 2001. The nose and paranasal sinuses physiology and anatomy. Advanced Drug Delivery Reviews 51, 5-19.

Jones, N., Rog, D., 1998. Olfaction: a review. Journal of Laryngology and Otology 112, 11-24.

Jones, S.A., 2005. Directing transition from innate to acquired immunity defining a role for IL-6. Journal of Immunology 175, 3463-3468.

Jung, T., Kamm, W., Breitenbach, A., Hungerer, K.D., Hundt, E., Kissel, T., 2001. Tetanus toxoid loaded nanoparticles from sulfobutylated poly(vinyl alcohol)-graft-poly(lactide-co-glycolide): evaluation of antibody response after oral and nasal application in mice. Pharmaceutical Research 18, 352-360.

Kaliner, M., Shelhamer, J.H., Borson, B., Nadel, J., Patow, C., Marom, Z., 1986. Human Respiratory Mucus. American Review of Respiratory Disease 134, 612-621.

Kalkanidis, M., Pietersz, G.A., Xiang, S.D., Mottram, P.L., Crimeen-Irwin, B., Ardipradja, K., Plebanski, M., 2006. Methods for nano-particle based vaccine formulation and evaluation of their immunogenicity. Methods 40, 20-29.

Kallas, E.G., Gibbons, D.C., Soucier, H., Fitzgerald, T., Treanor, J.J., Evans, T.G., 1999. Detection of Intracellular Antigen-Specific Cytokines in Human T Cell Populations. Journal of Infectious Diseases 179, 1124-1131.

Kamel, S., Ali, N., Jahangir, K., Shah, S.M., El-Gendy, A.A., 2008. Pharmaceutical significance of cellulose: A review. eXPRESS Polymer Letters 2, 758-778.

Kapsenberg, M.L., 2003. Dendritic-cell control of pathogen-driven T-cell polarization. Nature Reviews Immunology 3, 984-993.

Kataoka, K., Fujihashi, K., 2009. Dendritic cell-targeting DNA-based mucosal adjuvants for the development of mucosal vaccines. Expert Review of Vaccines 8, 1183-1193.

Kean, T., Thanou, M., 2010. Biodegradation, biodistribution and toxicity of chitosan. Advanced Drug Delivery Reviews 62, 3-11.

Khutoryanskiy, V.V., 2011. Advances in Mucoadhesion and Mucoadhesive Polymers. Macromolecular Bioscience 11, 748-764.

Kim, S.Y., Doh, H.J., Jang, M.H., Ha, Y.J., Chung, S.I., Park, H.J., 1999. Oral immunization with Helicobacter pylori-loaded poly(D,L-lactide-co-glycolide) nanoparticles. Helicobacter 4, 33-39.

Kimchi-Sarfaty, C., Schiller, T., Hamasaki-Katagiri, N., Khan, M.A., Yanover, C., Sauna, Z.E., 2013. Building better drugs: developing and regulating engineered therapeutic proteins. Trends in Pharmacological Sciences 34, 534-548.

Komiyama, Y., Nakae, S., Matsuki, T., Nambu, A., Ishigame, H., Kakuta, S., Sudo, K., Iwakura, Y., 2006. IL-17 plays an important role in the development of experimental autoimmune encephalomyelitis. Journal of Immunology 177, 566-573.

Kreuter, J., 1982. On the Mechanism of Termination in Heterogeneous Polymerization. Journal of Polymer Science Part C: Polymer Letters 20, 543-545.

Kreuter, J., 1991. Nanoparticle-Based Drug Delivery Systems. Journal of Controlled Release 16, 169-176.

Kumar, S., Anselmo, A.C., Banerjee, A., Zakrewsky, M., Mitragotri, S., 2015. Shape and size-dependent immune response to antigen-carrying nanoparticles. Journal of Controlled Release 220, Part A, 141-148.

Kuper, C.F., Koornstra, P.J., Hameleers, D.M.H., Biewenga, J., Spit, B.J., Duijvestijn, A.M., Vriesman, P.J.C.V., Sminia, T., 1992. The Role of Nasopharyngeal Lymphoid-Tissue. Immunology Today 13, 219-224.

Kwak, L.W., Longo, D.L., 1996. Modern vaccine adjuvants, in: Chabner, B.A., Longo, D.L. (Eds.), In Cancer Chemotherapy and Biotherapy. Lippincott–Raven, pp. 749-763.

Labala, S., Mandapalli, P.K., Kurumaddali, A., Venuganti, V.V.K., 2015. Layer-by-Layer Polymer Coated Gold Nanoparticles for Topical Delivery of Imatinib Mesylate To Treat Melanoma. Molecular Pharmaceutics 12, 878-888.

Lamprecht, A., Ubrich, N., Perez, M.H., Lehr, C.M., Hoffman, M., Maincent, P., 1999. Biodegradable monodispersed nanoparticles prepared by pressure homogenization-emulsification. International Journal of Pharmaceutics 184, 97-105.

Lee, J., Cho, E.C., Cho, K., 2004. Incorporation and release behavior of hydrophobic drug in functionalized poly (D, L-lactide)-block–poly (ethylene oxide) micelles. Journal of Controlled Release 94, 323-335.

Leitner, V.M., Walker, G.F., Bernkop-Schnurch, A., 2003. Thiolated polymers: evidence for the formation of disulphide bonds with mucus glycoproteins. European Journal of Pharmaceutics and Biopharmaceutics 56, 207-214.

Lemarchand, C., Gref, R., Passirani, C., Garcion, E., Petri, B., Muller, R., Costantini, D., Couvreur, P., 2006. Influence of polysaccharide coating on the interactions of nanoparticles with biological systems. Biomaterials 27, 108-118.

Lewis, P.A., Loomis, D., 1924. Allergic Irritability : The Formation of Anti-Sheep Hemolytic Amboceptor in the Normal and Tuberculous Guinea Pig. Journal of Experimental Medicine 40, 503-515.

Li, P., Luo, Z.C., Liu, P., Gao, N.N., Zhang, Y.J., Pan, H., Liu, L.L., Wang, C., Cai, L.T., Ma, Y.F., 2013. Bioreducible alginate-poly(ethylenimine) nanogels as an antigen-delivery system robustly enhance vaccine-elicited humoral and cellular immune responses. Journal of Controlled Release 168, 271-279.

Li, T., Shi, X.W., Du, Y.M., Tang, Y.F., 2007. Quaternized chitosan/alginate nanoparticles for protein delivery. Journal of Biomedical Materials Research Part A 83, 383-390.

Li, Y.P., Xiao, W.W., Xiao, K., Berti, L., Luo, J.T., Tseng, H.P., Fung, G., Lam, K.S., 2012. Well-Defined, Reversible Boronate Crosslinked Nanocarriers for Targeted Drug Delivery in Response to Acidic pH Values and cis-Diols. Angewandte Chemie International Edition 51, 2864-2869.

Longer, M.A., Robinson, J.R., 1986. Fundamental-Aspects of Bioadhesion. Pharmacy International 7, 114-117.

Lowe, P.J., Temple, C.S., 1994. Calcitonin and Insulin in Isobutylcyanoacrylate Nanocapsules - Protection against Proteases and Effect on Intestinal-Absorption in Rats. Journal of Pharmacy and Pharmacology 46, 547-552.

Lu, J.M., Wang, X.W., Marin-Muller, C., Wang, H., Lin, P.H., Yao, Q.Z., Chen, C.Y., 2009. Current advances in research and clinical applications of PLGA-based nanotechnology. Expert Review of Molecular Diagnostics 9, 325-341.

Lu, W., Zhang, Y., Tan, Y.Z., Hu, K.L., Jiang, X.G., Fu, S.K., 2005. Cationic albumin-conjugated pegylated nanoparticles as novel drug carrier for brain delivery. Journal of Controlled Release 107, 428-448.

Luckheeram, R.V., Zhou, R., Verma, A.D., Xia, B., 2012. CD4(+)T Cells: Differentiation and Functions. Clinical and Developmental Immunology, 1-12.

Ma, Z., Lim, T.M., Lim, L.Y., 2005. Pharmacological activity of peroral chitosan-insulin nanoparticles in diabetic rats. International Journal of Pharmaceutics 293, 271-280.

Madsen, F., Eberth, K., Smart, J.D., 1998. A rheological examination of the mucoadhesive/mucus interaction: the effect of mucoadhesive type and concentration. Journal of Controlled Release 50, 167-178.

Majithiya, R.J., Ghosh, P.K., Umrethia, M.L., Murthy, R.S.R., 2006. Thermoreversible-mucoadhesive gel for nasal delivery of sumatriptan. AAPS PharmSciTech 7.

Makhlof, A., Werle, M., Tozuka, Y., Takeuchi, H., 2010. Nanoparticles of glycol chitosan and its thiolated derivative significantly improved the pulmonary delivery of calcitonin. International Journal of Pharmaceutics 397, 92-95.

Mansouri, S., Lavigne, P., Corsi, K., Benderdour, M., Beaumont, E., Fernandes, J.C., 2004. Chitosan-DNA nanoparticles as non-viral vectors in gene therapy: strategies to improve transfection efficacy. European Journal of Pharmaceutics and Biopharmaceutics 57, 1-8.

Mao, H.Q., Roy, K., Troung-Le, V.L., Janes, K.A., Lin, K.Y., Wang, Y., August, J.T., Leong, K.W., 2001. Chitosan-DNA nanoparticles as gene carriers: synthesis, characterization and transfection efficiency. Journal of Controlled Release 70, 399-421.

Marcato, P.D., Duran, N., 2008. New aspects of nanopharmaceutical delivery systems. Journal of Nanoscience and Nanotechnology 8, 2216-2229.

Marciani, D.J., 2003. Vaccine adjuvants: role and mechanisms of action in vaccine immunogenicity. Drug Discovery Today 8, 934-943.

Mbela, T.K.M., Poupaert, J.H., Dumont, P., 1992. Poly (diethylmethylidene malonate) nanoparticles as primaquine delivery system to liver. International Journal of Pharmaceutics 79, 29-38.

Menchicchi, B., Fuenzalida, J.P., Hensel, A., Swamy, M.J., David, L., Rochas, C., Goycoolea, F.M., 2015. Biophysical Analysis of the Molecular Interactions between Polysaccharides and Mucin. Biomacromolecules 16, 924-935.

Merkus, F.W.H.M., Verhoef, J.C., 1994. Nasal drug delivery: trends and perspectives. Encyclopedia of Pharmaceutical Technology 10, 191-220.

Mestecky, J., Moldoveanu, Z., Michalek, S.M., Morrow, C.D., Compans, R.W., Schafer, D.P., Russell, M.W., 1997. Current options for vaccine delivery systems by mucosal routes. Journal of Controlled Release 48, 243-257.

Minigo, G., Scholzen, A., Tang, C.K., Hanley, J.C., Kalkanidis, M., Pietersz, G.A., Apostolopoulos, V., Plebanski, M., 2007. Poly-L-lysine-coated nanoparticles: A potent delivery system to enhance DNA vaccine efficacy. Vaccine 25, 1316-1327.

Mitchell, D.A., Batich, K.A., Gunn, M.D., Huang, M.N., Sanchez-Perez, L., Nair, S.K., Congdon, K.L., Reap, E.A., Archer, G.E., Desjardins, A., Friedman, A.H., Friedman, H.S., Herndon, J.E., Coan, A., McLendon, R.E., Reardon, D.A., Vredenburgh, J.J., Bigner, D.D., Sampson, J.H., 2015. Tetanus toxoid and CCL3 improve dendritic cell vaccines in mice and glioblastoma patients. Nature 519, 366-369.

Mittal, A., Schulze, K., Ebensen, T., Weißmann, S., Hansen, S., Lehr, C.M., Guzmán, C.A., 2015. Efficient nanoparticle-mediated needle-free transcutaneous vaccination via hair follicles requires adjuvantation. Nanomedicine: Nanotechnology, Biology and Medicine 11, 147-154.

Moingeon, P., de Taisne, C., Almond, J., 2002. Delivery technologies for human vaccines. British Medical Bulletin 62, 29-44.

Moingeon, P., Haensler, J., Lindberg, A., 2001. Towards the rational design of Th1 adjuvants. Vaccine 19, 4363-4372.

Molina-Bolivar, J.A., Galisteo-Gonzalez, F., Hidalgo-Alvarez, R., 1999. The role played by hydration forces in the stability of protein-coated particles: non-classical DLVO behaviour. Colloids and Surfaces B: Biointerfaces 14, 3-17.

Molpeceres, J., Guzman, M., Aberturas, M.R., Chacon, M., Berges, L., 1996. Application of central composite designs to the preparation of polycaprolactone nanoparticles by solvent displacement. Journal of Pharmaceutical Sciences 85, 206-213.

Montecucco, C., Schiavo, G., 1995. Structure and function of tetanus and botulinum neurotoxins. Quarterly Reviews of Biophysics 28, 423-472.

Mora-Huertas, C.E., Fessi, H., Elaissari, A., 2011. Influence of process and formulation parameters on the formation of submicron particles by solvent displacement and emulsification–diffusion methods: Critical comparison. Advances in Colloid and Interface Science 163, 90-122.

Morgan, D.M., Larvin, V.L., Pearson, J.D., 1989. Biochemical characterisation of polycation-induced cytotoxicity to human vascular endothelial cells. Journal of Cell Science 94, 553-559.

Mosmann, T.R., Coffman, R.L., 1989. TH1 and TH2 cells: different patterns of lymphokine secretion lead to different functional properties. Annual Review of Immunology 7, 145-173.

Murray, H.W., Rubin, B.Y., Carriero, S.M., Harris, A.M., Jaffee, E.A., 1985. Human Mononuclear Phagocyte Antiprotozoal Mechanisms - Oxygen-Dependent Vs Oxygen-Independent Activity against Intracellular Toxoplasma-Gondii. Journal of Immunology 134, 1982-1988.

Muzzarelli, R.A.A., Muzzarelli, C., 2005. Chitosan chemistry: Relevance to the biomedical sciences. Advances in Polymer Science 186, 151-209.

Mygind, N., Dahl, R., 1998. Anatomy, physiology and function of the nasal cavities in health and disease. Advanced Drug Delivery Reviews 29, 3-12.

Nakae, S., Komiyama, Y., Nambu, A., Sudo, K., Iwase, M., Homma, I., Sekikawa, K., Asano, M., Iwakura, Y., 2002. Antigen-specific T cell Sensitization is impaired in IL-17-deficient mice, causing suppression of allergic cellular and humoral responses. Immunity 17, 375-387.

Nakamura, F., Ohta, R., Machida, Y., Nagai, T., 1996. In vitro and in vivo nasal mucoadhesion of some water-soluble polymers. International Journal of Pharmaceutics 134, 173-181.

Nemati, F., Dubernet, C., Fessi, H., deVerdiere, A.C., Poupon, M.F., Puisieux, F., Couvreur, P., 1996. Reversion of multidrug resistance using nanoparticles in vitro: Influence of the nature of the polymer. International Journal of Pharmaceutics 138, 237-246.

Nembrini, C., Stano, A., Dane, K.Y., Ballester, M., van der Vlies, A.J., Marsland, B.J., Swartz, M.A., Hubbell, J.A., 2011. Nanoparticle conjugation of antigen enhances cytotoxic T-

cell responses in pulmonary vaccination. Proceedings of the National Academy of Sciences USA 108, E989-E997.

NIAID, 2012. Types of vaccines, Vaccines. National Institute of Allergy and Infectious Diseases.

Niemann, H., 1991. Molecular Biology of Clostridial Neurotoxins, in: Alouf, J.E., Freer, J.H. (Eds.), Sourcebook of Bacterial Protein Toxins. Academic Press, pp. 303-348.

Nisbet, A.D., Saundry, R.H., Moir, A.J.G., Fothergill, L.A., Fothergill, J.E., 1981. The Complete Amino-Acid-Sequence of Hen Ovalbumin. European Journal of Biochemistry 115, 335-345.

Nordly, P., Madsen, H.B., Nielsen, H.M., Foged, C., 2009. Status and future prospects of lipid-based particulate delivery systems as vaccine adjuvants and their combination with immunostimulators. Expert Opinion on Drug Delivery 6, 657-672.

O'Garra, A., Robinson, D., 2004. Development and function of T helper 1 cells. Advances in Immunology 83, 133-162.

O'Hagan, D.T., Fox, C.B., 2015. New generation adjuvants - From empiricism to rational design. Vaccine 33, B14-B20.

Obrosovaserova, N.P., Slepushkin, A.N., Kendal, A.P., Harmon, M.W., Burtseva, E.I., Bebesheva, N.I., Beljaev, A.L., Lonskaja, N.I., Medvedeva, T.E., Egorov, A.Y., Peklisova, L.V., Alexandrova, G.I., 1990. Evaluation in Children of Cold-Adapted Influenza-B Live Attenuated Intranasal Vaccine Prepared by Reassortment between Wild-Type B/Ann-Arbor/1/86 and Cold-Adapted B/Leningrad/14/55 Viruses. Vaccine 8, 57-60.

Oftung, F., Naess, L.M., Wetzler, L.M., Korsvold, G.E., Aase, A., Hoiby, E.A., Dalseg, R., Holst, J., Michaelsen, T.E., Haneberg, B., 1999. Antigen-specific T-cell responses in humans after intranasal immunization with a meningococcal serogroup B outer membrane vesicle vaccine. Infection and Immunity 67, 921-927.

Oyarzun-Ampuero, F.A., Brea, J., Loza, M.I., Torres, D., Alonso, M.J., 2009. Chitosan-hyaluronic acid nanoparticles loaded with heparin for the treatment of asthma. International Journal of Pharmaceutics 381, 122-129.

Oyarzun-Ampuero, F.A., Rivera-Rodriguez, G.R., Alonso, M.J., Torres, D., 2013. Hyaluronan nanocapsules as a new vehicle for intracellular drug delivery. European Journal of Pharmaceutical Sciences 49, 483-490.

Partidos, C.D., 2000. Intranasal vaccines: forthcoming challenges. Pharmaceutical Science and Technology Today 3, 273-281.

Parveen, S., Misra, R., Sahoo, S.K., 2012. Nanoparticles: a boon to drug delivery, therapeutics, diagnostics and imaging. Nanomedicine 8, 147-166.

Peng, Z.G., Hidajat, K., Uddin, M.S., 2004. Adsorption of bovine serum albumin on nanosized magnetic particles. Journal of Colloid and Interface Science 271, 277-283.

Penman, A., Sanderson, G.R., 1972. A method for the determination of uronic acid sequence in alginates. Carbohydrate Research 25, 273-282.

Perez, C., Sanchez, A., Putnam, D., Ting, D., Langer, R., Alonso, M.J., 2001. Poly(lactic acid)-poly(ethylene glycol) nanoparticles as new carriers for the delivery of plasmid DNA. Journal of Controlled Release 75, 211-224.

Petruson, B., Hansson, H.A., Karlsson, G., 1984. Structural and Functional-Aspects of Cells in the Nasal Mucociliary System. Archives of Otolaryngology 110, 576-581.

Pinto Reis, C., Neufeld, R.J., Ribeiro, A.J., Veiga, F., 2006. Nanoencapsulation I. Methods for preparation of drug-loaded polymeric nanoparticles. Nanomedicine 2, 8-21.

Pires, A., Fortuna, A., Alves, G., Falcao, A., 2009. Intranasal drug delivery: how, why and what for? Journal of Pharmacy and Pharmaceutical Sciences 12, 288-311.

Plotkin, S.A., 2005. Vaccines: past, present and future. Nature medicine 11, S5-11.

Ponchel, G., Touchard, F., Wouessidjewe, D., Duchene, D., Peppas, N.A., 1987. Bioadhesive Analysis of Controlled-Release Systems .3. Bioadhesive and Release Behavior of Metronidazole-Containing Poly(Acrylic Acid)-Hydroxypropyl Methylcellulose Systems. International Journal of Pharmaceutics 38, 65-70.

Pontiroli, A.E., Calderara, A., Pozza, G., 1989. Intranasal Drug Delivery - Potential Advantages and Limitations from a Clinical Pharmacokinetic Perspective. Clinical Pharmacokinetics 17, 299-307.

Press, J.B., Reynolds, R.C., May, R.D., Marciani, D.J., 2000. Structure/Function Relationships of Immunostimulating Saponins, in: Atta ur, R. (Ed.), Studies in Natural Products Chemistry. Elsevier, pp. 131-174.

Price, N.C., 2000. Conformational issues in the characterization of proteins. Biotechnology and Applied Biochemistry 31, 29-40.

Priebe, G.P., Walsh, R.L., Cederroth, T.A., Kamei, A., Coutinho-Sledge, Y.S., Goldberg, J.B., Pier, G.B., 2008. IL-17 is a critical component of vaccine-induced protection against lung infection by lipopolysaccharide-heterologous strains of Pseudomonas aeruginosa. Journal of Immunology 181, 4965-4975.

Quintanar-Guerrero, D., Allémann, E., Fessi, H., Doelker, E., 1998. Preparation techniques and mechanisms of formation of biodegradable nanoparticles from preformed polymers. Drug Development and Industrial Pharmacy 24, 1113-1128.

Quraishi, M.S., Jones, N.S., Mason, J., 1998. The rheology of nasal mucus: a review. Clinical Otolaryngology 23, 403-413.

Rahimi, M., Wadajkar, A., Subramanian, K., Yousef, M., Cui, W.N., Hsieh, J.T., Nguyen, K.T., 2010. In vitro evaluation of novel polymer-coated magnetic nanoparticles for controlled drug delivery. Nanomedicine 6, 672-680.

Rahimian, S., Kleinovink, J.W., Fransen, M.F., Mezzanotte, L., Gold, H., Wisse, P., Overkleeft, H., Amidi, M., Jiskoot, W., Löwik, C.W., Ossendorp, F., Hennink, W.E., 2015. Near-infrared labeled, ovalbumin loaded polymeric nanoparticles based on a hydrophilic polyester as model vaccine: In vivo tracking and evaluation of antigen-specific CD8+ T cell immune response. Biomaterials 37, 469-477.

Rahmat, D., Sakloetsakun, D., Shahnaz, G., Perera, G., Kaindl, R., Bernkop-Schnurch, A., 2011. Design and synthesis of a novel cationic thiolated polymer. International Journal of Pharmaceutics 411, 10-17.

Rajaonarivony, M., Vauthier, C., Couarraze, G., Puisieux, F., Couvreur, P., 1993. Development of a New Drug Carrier Made from Alginate. Journal of Pharmaceutical Sciences 82, 912-917.

Ramdas, M., Dileep, K.J., Anitha, Y., Paul, W., Sharma, C.P., 1999. Alginate encapsulated bioadhesive chitosan microspheres for intestinal drug delivery. Journal of Biomaterials Applications 13, 290-296.

Rao, J.P., Geckeler, K.E., 2011. Polymer nanoparticles: preparation techniques and size-control parameters. Progress in Polymer Science 36, 887-913.

Ribeiro, A.J., Silva, C., Ferreira, D., Veiga, F., 2005. Chitosan-reinforced alginate microspheres obtained through the emulsification/internal gelation technique. European Journal of Pharmaceutical Sciences 25, 31-40.

Richardson, S.C.W., Kolbe, H.J.V., Duncan, R., 1999. Potential of low molecular mass chitosan as a DNA delivery system: biocompatibility, body distribution and ability to complex and protect DNA. International Journal of Pharmaceutics 178, 231-243.

Rinaudo, M., 2006. Chitin and chitosan: Properties and applications. Progress in Polymer Science 31, 603-632.

Rowley, J.A., Madlambayan, G., Mooney, D.J., 1999. Alginate hydrogels as synthetic extracellular matrix materials. Biomaterials 20, 45-53.

Saade, F., Honda-Okubo, Y., Trec, S., Petrovsky, N., 2013. A novel hepatitis B vaccine containing Advax (TM), a polysaccharide adjuvant derived from delta inulin, induces robust humoral and cellular immunity with minimal reactogenicity in preclinical testing. Vaccine 31, 1999-2007.

Sahana, D.K., Mittal, G., Bhardwaj, V., Kumar, M.N.V.R., 2008. PLGA nanoparticles for oral delivery of hydrophobic drugs: influence of organic solvent on nanoparticle formation and release behavior in vitro and in vivo using estradiol as a model drug. Journal of Pharmaceutical Sciences 97, 1530-1542.

Sakuma, S., Matsumoto, T., Yamashita, S., Wang, Y., Lu, Z.R., 2007. Conjugation of poorly absorptive drugs with mucoadhesive polymers for the improvement of oral absorption of drugs. Journal of Controlled Release 123, 195-202.

Sakuma, S., Sudo, R., Suzuki, N., Kikuchi, H., Akashi, M., Hayashi, M., 1999. Mucoadhesion of polystyrene nanoparticles having surface hydrophilic polymeric chains in the gastrointestinal tract. International Journal of Pharmaceutics 177, 161-172.

Salamat-Miller, N., Chittchang, M., Johnston, T.P., 2005. The use of mucoadhesive polymers in buccal drug delivery. Advanced Drug Delivery Reviews 57, 1666-1691.

Sandford, P.A., Steinnes, A., 1991. Biomedical Applications of High-Purity Chitosan, Water-Soluble Polymers. American Chemical Society, pp. 430-445.

Santander-Ortega, M.J., Peula-Garcia, J.M., Goycoolea, F.M., Ortega-Vinuesa, J.L., 2011. Chitosan nanocapsules: Effect of chitosan molecular weight and acetylation degree on electrokinetic behaviour and colloidal stability. Colloids and Surfaces B: Biointerfaces 82, 571-580.

Sarmento, B., Ferreira, D., Veiga, F., Ribeiro, A., 2006. Characterization of insulin-loaded alginate nanoparticles produced by ionotropic pre-gelation through DSC and FTIR studies. Carbohydrate Polymers 66, 1-7.

Sarti, F., Iqbal, J., Muller, C., Shahnaz, G., Rahmat, D., Bernkop-Schnurch, A., 2012. Poly(acrylic acid)-cysteine for oral vitamin B12 delivery. Analytical Biochemistry 420, 13-19.

Sarti, F., Staaf, A., Sakloetsakun, D., Bernkop-Schnurch, A., 2010. Thiolated hydroxyethylcellulose: Synthesis and in vitro evaluation. European Journal of Pharmaceutics and Biopharmaceutics 76, 421-427.

Schijns, V.E., 2000. Immunological concepts of vaccine adjuvant activity. Current Opinion in Immunology 12, 456-463.

Schmitt, C., Sanchez, C., Desobry-Banon, S., Hardy, J., 1998. Structure and technofunctional properties of protein-polysaccharide complexes: a review. Critical Reviews in Food Science and Nutrition 38, 689-753.

Schwarz, C., Mehnert, W., 1997. Freeze-drying of drug-free and drug-loaded solid lipid nanoparticles (SLN). International Journal of Pharmaceutics 157, 171-179.

Serp, D., Cantana, E., Heinzen, C., Von Stockar, U., Marison, I.W., 2000. Characterization of an encapsulation device for the production of monodisperse alginate beads for cell immobilization. Biotechnology and Bioengineering 70, 41-53.

Serra, L., Domenech, J., Peppas, N.A., 2006. Design of poly(ethylene glycol)-tethered copolymers as novel mucoadhesive drug delivery systems. European Journal of Pharmaceutics and Biopharmaceutics 63, 11-18.

Shaikh, J., Ankola, D.D., Beniwal, V., Singh, D., Kumar, M.N.V.R., 2009. Nanoparticle encapsulation improves oral bioavailability of curcumin by at least 9-fold when compared to curcumin administered with piperine as absorption enhancer. European Journal of Pharmaceutical Sciences 37, 223-230.

Shang, L., Wang, Y., Jiang, J., Dong, S., 2007. pH-dependent protein conformational changes in albumin:gold nanoparticle bioconjugates: a spectroscopic study. Langmuir 23, 2714-2721.

Shen, J., Wang, Y., Ping, Q., Xiao, Y., Huang, X., 2009. Mucoadhesive effect of thiolated PEG stearate and its modified NLC for ocular drug delivery. Journal of Controlled Release 137, 217-223.

Shephard, M.J., Todd, D., Adair, B.M., Po, A.L.W., Mackie, D.P., Scott, E.M., 2003. Immunogenicity of bovine parainfluenza type 3 virus proteins encapsulated in nanoparticle vaccines, following intranasal administration to mice. Research in Veterinary Science 74, 187-190.

Shilpa, A., Agrawal, S.S., Ray, A.R., 2003. Controlled delivery of drugs from alginate matrix. Journal of Macromolecular Science-Polymer Reviews C43, 187-221.

Shire, S.J., Shahrokh, Z., Liu, J., 2004. Challenges in the development of high protein concentration formulations. Journal of Pharmaceutical Sciences 93, 1390-1402.

Shu, X.Z., Zhu, K.J., 2002. The influence of multivalent phosphate structure on the properties of ionically cross-linked chitosan films for controlled drug release. European Journal of Pharmaceutics and Biopharmaceutics 54, 235-243.

Shukla, R., Bansal, V., Chaudhary, M., Basu, A., Bhonde, R.R., Sastry, M., 2005. Biocompatibility of gold nanoparticles and their endocytotic fate inside the cellular compartment: A microscopic overview. Langmuir 21, 10644-10654.

Siddhapura, K., Harde, H., Jain, S., 2016. Immunostimulatory effect of tetanus toxoid loaded chitosan nanoparticles following microneedles assisted immunization. Nanomedicine 12, 213-222.

Siegrist, C.A., 2008. Vaccine immunology, in: Plotkin SA, O.W., Offit PA (Ed.), Vaccines, 5 ed. Elsevier, New York, pp. 17-36.

Silva, A.L., Rosalia, R.A., Sazak, A., Carstens, M.G., Ossendorp, F., Oostendorp, J., Jiskoot, W., 2013. Optimization of encapsulation of a synthetic long peptide in PLGA nanoparticles: Low-burst release is crucial for efficient CD8(+) T cell activation. European Journal of Pharmaceutics and Biopharmaceutics 83, 338-345.

Sleigh, M.A., Blake, J.R., Liron, N., 1988. The Propulsion of Mucus by Cilia. American Review of Respiratory Disease 137, 726-741.

Slutter, B., Bal, S., Keijzer, C., Mallants, R., Hagenaars, N., Que, I., Kaijzel, E., van Eden, W., Augustijns, P., Lowik, C., Bouwstra, J., Broere, F., Jiskoot, W., 2010. Nasal vaccination with N-trimethyl chitosan and PLGA based nanoparticles: Nanoparticle characteristics determine quality and strength of the antibody response in mice against the encapsulated antigen. Vaccine 28, 6282-6291.

Slutter, B., Jiskoot, W., 2010. Dual role of CpG as immune modulator and physical crosslinker in ovalbumin loaded N-trimethyl chitosan (TMC) nanoparticles for nasal vaccination. Journal of Controlled Release 148, 117-121.

Smith, J.R.H., Bailey, M.R., Etherington, G., Shutt, A.L., Youngman, M.J., 2011. An experimental study of clearance of inhaled particles from the human nose. Experimental Lung Research 37, 109-129.

Sogias, I.A., Williams, A.C., Khutoryanskiy, V.V., 2008. Why is chitosan mucoadhesive? Biomacromolecules 9, 1837-1842.

Soppimath, K.S., Aminabhavi, T.M., Kulkarni, A.R., Rudzinski, W.E., 2001. Biodegradable polymeric nanoparticles as drug delivery devices. Journal of Controlled Release 70, 1-20.

Sosnik, A., Cohn, D., 2005. Reverse thermo-responsive poly(ethylene oxide) and poly(propylene oxide) multiblock copolymers. Biomaterials 26, 349-357.

Sosnik, A., das Neves, J., Sarmento, B., 2014. Mucoadhesive polymers in the design of nano-drug delivery systems for administration by non-parenteral routes: A review. Progress in Polymer Science 39, 2030-2075.

Sproul, T.W., Cheng, P.C., Dykstra, M.L., Pierce, S.K., 2000. A role for MHC class II antigen processing in B cell development. International Reviews of Immunology 19, 139-155.

Srivastava, I.K., Singh, M., 2005. DNA Vaccines. International Journal of Pharmaceutical Medicine 19, 15-28.

Staprans, I., Watanabe, S., 1970. Optical Properties of Troponin, Tropomyosin, and Relaxing Protein of Rabbit Skeletal Muscle. The Journal of Biological Chemistry 245, 5962-5966.

Stein, P.E., Leslie, A.G., Finch, J.T., Carrell, R.W., 1991. Crystal structure of uncleaved ovalbumin at 1.95 A resolution. Journal of Molecular Biology 221, 941-959.

Striebel, H.W., Kramer, J., Luhmann, I., Rohierse-Hohler, I., Rieger, A., 1993. Pharmakokinetische Studie zur intranasalen Gabe von Fentanyl. Der Schmerz 7, 122-125.

Tachaprutinun, A., Pan-In, P., Wanichwecharungruang, S., 2013. Mucosa-plate for direct evaluation of mucoadhesion of drug carriers. International Journal of Pharmaceutics 441, 801-808.

Takahashi, T., Takayama, K., Machida, Y., Nagai, T., 1990. Characteristics of Polyion Complexes of Chitosan with Sodium Alginate and Sodium Polyacrylate. International Journal of Pharmaceutics 61, 35-41.

Takeuchi, H., Thongborisute, J., Matsui, Y., Sugihara, H., Yamamoto, H., Kawashima, Y., 2005. Novel mucoadhesion tests for polymers and polymer-coated particles to design optimal mucoadhesive drug delivery systems. Advanced Drug Delivery Reviews 57, 1583-1594.

Tang, Q., Cao, B., Lei, X., Sun, B.B., Zhang, Y.Q., Cheng, G., 2014. Dextran-Peptide Hybrid for Efficient Gene Delivery. Langmuir 30, 5202-5208.

Taylor Nordgård, C., Draget, K.I., 2011. Oligosaccharides As Modulators of Rheology in Complex Mucous Systems. Biomacromolecules 12, 3084-3090.

Teixeira, L.K., Fonseca, B.P., Vieira-de-Abreu, A., Barboza, B.A., Robbs, B.K., Bozza, P.T., Viola, J.P., 2005. IFN-gamma production by CD8+ T cells depends on NFAT1 transcription factor and regulates Th differentiation. Journal of Immunology 175, 5931-5939.

Thanou, M., Verhoef, J.C., Junginger, H.E., 2001a. Chitosan and its derivatives as intestinal absorption enhancers. Advanced Drug Delivery Reviews 50, S91-S101.

Thanou, M., Verhoef, J.C., Junginger, H.E., 2001b. Oral drug absorption enhancement by chitosan and its derivatives. Advanced Drug Delivery Reviews 52, 117-126.

Thomann-Harwood, L.J., Kaeuper, P., Rossi, N., Milona, P., Herrmann, B., McCullough, K.C., 2013. Nanogel vaccines targeting dendritic cells: Contributions of the surface decoration and vaccine cargo on cell targeting and activation. Journal of Controlled Release 166, 95-105.

Thomas, C., Rawat, A., Hope-Weeks, L., Ahsan, F., 2011. Aerosolized PLA and PLGA Nanoparticles Enhance Humoral, Mucosal and Cytokine Responses to Hepatitis B Vaccine. Molecular Pharmaceutics 8, 405-415.

Tønnesen, H.H., Karlsen, J., 2002. Alginate in Drug Delivery Systems. Drug Development and Industrial Pharmacy 28, 621-630.

Torres-Lugo, M., Peppas, N.A., 2002. Preparation and characterization of P(MAA-g-EG) nanospheres for protein delivery applications. Journal of Nanoparticle Research 4, 73-81.

Tos, M., 1983. Distribution of Mucus Producing Elements in the Respiratory-Tract - Differences between Upper and Lower Airway. European Journal of Respiratory Diseases 64, 269-279.

Treanor, J., Nolan, C., O'Brien, D., Burt, D., Lowell, G., Linden, J., Fries, L., 2006. Intranasal administration of a proteosome-influenza vaccine is well-tolerated and induces serum and nasal secretion influenza antibodies in healthy human subjects. Vaccine 24, 254-262.

Treanor, J.J., Mattison, H.R., Dumyati, G., Yinnon, A., Erb, S., Obrien, D., Dolin, R., Betts, R.F., 1992. Protective Efficacy of Combined Live Intranasal and Inactivated Influenza-a Virus-Vaccines in the Elderly. Annals of Internal Medicine 117, 625-633.

Uenaka, A., Wada, H., Isobe, M., Saika, T., Tsuji, K., Sato, E., Sato, S., Noguchi, Y., Kawabata, R., Yasuda, T., Doki, Y., Kumon, H., Iwatsuki, K., Shiku, H., Monden, M., Jungbluth, A.A., Ritter, G., Murphy, R., Hoffman, E., Old, L.J., Nakayama, E., 2007. T cell immunomonitoring and tumor responses in patients immunized with a complex of

cholesterol-bearing hydrophobized pullulan (CHP) and NY-ESO-1 protein. Cancer Immunology 7, 9.

Ueno, H., Mori, T., Fujinaga, T., 2001. Topical formulations and wound healing applications of chitosan. Advanced Drug Delivery Reviews 52, 105-115.

Ugwoke, M.I., Agu, R.U., Verbeke, N., Kinget, R., 2005a. Nasal mucoadhesive drug delivery: Background, applications, trends and future perspectives. Advanced Drug Delivery Reviews 57, 1640-1665.

Ugwoke, M.I., Agu, R.U., Verbeke, N., Kinget, R., 2005b. Nasal mucoadhesive drug delivery: background, applications, trends and future perspectives. Advanced Drug Delivery Reviews 57, 1640-1665.

Van Kampen, K.R., Shi, Z.K., Gao, P., Zhang, J.F., Foster, K.W., Chen, D.T., Marks, D., Elmets, C.A., Tang, D.C.C., 2005. Safety and immunogenicity of adenovirus-vectored nasal and epicutaneous influenza vaccines in humans. Vaccine 23, 1029-1036.

Varchi, G., Benfenati, V., Pistone, A., Ballestri, M., Sotgiu, G., Guerrini, A., Dambruoso, P., Liscio, A., Ventura, B., 2013. Core-shell poly-methylmethacrylate nanoparticles as effective carriers of electrostatically loaded anionic porphyrin. Photochemical & Photobiological Sciences 12, 760-769.

Vargas, A., Pegaz, B., Debefve, E., Konan-Kouakou, Y., Lange, N., Ballini, J.P., van den Bergh, H., Gurny, R., Delie, F., 2004. Improved photodynamic activity of porphyrin loaded into nanoparticles: an in vivo evaluation using chick embryos. International Journal of Pharmaceutics 286, 131-145.

Vasi, A.M., Popa, M.I., Tanase, E.C., Butnaru, M., Verestiuc, L., 2014. Poly(Acrylic Acid)-Poly(Ethylene Glycol) Nanoparticles Designed for Ophthalmic Drug Delivery. Journal of Pharmaceutical Sciences 103, 676-686.

Vauthier, C., Dubernet, C., Fattal, E., Pinto-Alphandary, H., Couvreur, P., 2003. Poly(alkylcyanoacrylates) as biodegradable materials for biomedical applications. Advanced Drug Delivery Reviews 55, 519-548.

Verwey, E.J.W., Overbeek, J.T.G., 1999. Theory of the stability of lyophobic colloids. Courier Corporation.

Vignali, D.A.A., Collison, L.W., Workman, C.J., 2008. How regulatory T cells work. Nature Reviews Immunology 8, 523-532.

Vila, A., Sanchez, A., Evora, C., Soriano, I., Jato, J.L.V., Alonso, M.J., 2004a. PEG-PLA nanoparticles as carriers for nasal vaccine delivery. Journal of Aerosol Medicine 17, 174-185.

Vila, A., Sanchez, A., Evora, C., Soriano, I., Vila Jato, J.L., Alonso, M.J., 2004b. PEG-PLA nanoparticles as carriers for nasal vaccine delivery. Journal of Aerosol Medicine 17, 174-185.

Vila, A., Sanchez, A., Tobio, M., Calvo, P., Alonso, M.J., 2002. Design of biodegradable particles for protein delivery. Journal of Controlled Release 78, 15-24.

Washington, N., McGlashan, J.A., Jackson, S.J., Bush, D., Pitt, K.G., Rawlins, D.A., Gill, D.A., 2000. The effect of nasal patency on the clearance of radiolabeled saline in healthy volunteers. Pharmaceutical Research 17, 733-736.

Weaver, C.T., Harrington, L.E., Mangan, P.R., Gavrieli, M., Murphy, K.M., 2006. Th17: An effector CD4 T cell lineage with regulatory T cell ties. Immunity 24, 677-688.

Weller, U., Dauzenroth, M.E., Heringdorf, D.M.Z., Habermann, E., 1989. Chains and Fragments of Tetanus Toxin - Separation, Reassociation and Pharmacological Properties. European Journal of Biochemistry 182, 649-656.

Wendorf, J., Singh, M., Chesko, J., Kazzaz, J., Soewanan, E., Ugozzoli, M., O'Hagan, D., 2006. A practical approach to the use of nanoparticles for vaccine delivery. Journal of Pharmaceutical Sciences 95, 2738-2750.

Westerink, M.A., Smithson, S.L., Srivastava, N., Blonder, J., Coeshott, C., Rosenthal, G.J., 2001. ProJuvant (Pluronic F127/chitosan) enhances the immune response to intranasally administered tetanus toxoid. Vaccine 20, 711-723.

Widdicombe, J., 1997. Microvascular anatomy of the nose. Allergy 52, 7-11.

Wischke, C., Schneider, C., Neffe, A.T., Lendlein, A., 2013. Polyalkylcyanoacrylates as in situ formed diffusion barriers in multimaterial drug carriers. Journal of Controlled Release 169, 321-328.

Wong, C.F., Yuen, K.H., Peh, K.K., 1999. An in-vitro method for buccal adhesion studies: importance of instrument variables. International Journal of Pharmaceutics 180, 47-57.

Xie, J., Wang, C.H., 2007. Encapsulation of proteins in biodegradable polymeric microparticles using electrospray in the Taylor cone-jet mode. Biotechnology and Bioengineering 97, 1278-1290.

Xu, Y., Du, Y., Huang, R., Gao, L., 2003. Preparation and modification of N-(2-hydroxyl) propyl-3-trimethyl ammonium chitosan chloride nanoparticle as a protein carrier. Biomaterials 24, 5015-5022.

Yang, P., Gao, F., 2002. The principle of bioinorganic chemistry. Science, Beijing 349.

Yoo, H.S., Oh, J.E., Lee, K.H., Park, T.G., 1999. Biodegradable nanoparticles containing doxorubicin-PLGA conjugate for sustained release. Pharmaceutical Research 16, 1114-1118.

Zarate, J., Virdis, L., Orive, G., Igartua, M., Hernandez, R.M., Pedraz, J.L., 2011. Design and characterization of calcium alginate microparticles coated with polycations as protein delivery system. Journal of Microencapsulation 28, 614-620.

Zhang, H., Oh, M., Allen, C., Kumacheva, E., 2004. Monodisperse chitosan nanoparticles for mucosal drug delivery. Biomacromolecules 5, 2461-2468.

Zhao, F.J., Zhang, X.H., Liu, S.Q., Zeng, T.B., Yu, J., Gu, W.M., Zhang, Y.J., Chen, X., Wu, Y.M., 2013. Assessment of the immune responses to Treponema pallidum Gpd DNA vaccine adjuvanted with IL-2 and chitosan nanoparticles before and after Treponema pallidum challenge in rabbits. Science China Life Sciences 56, 174-180.

Zhou, L., Ivanov, I.I., Spolski, R., Min, R., Shenderov, K., Egawa, T., Levy, D.E., Leonard, W.J., Littman, D.R., 2007. IL-6 programs TH-17 cell differentiation by promoting sequential engagement of the IL-21 and IL-23 pathways. Nature Immunology 8, 967-974.

Zinkernagel, R.M., 2000. Localization dose and time of antigens determine immune reactivity. Seminars in Immunology 12, 163-171.

7. Publications and presentations

Publications

1. Research article entitled "Solid lipid nanoparticles loaded topical gel containing combination drugs: An approach to offset psoriasis" published in Expert Opinion on Drug Delivery. (Impact factor: 4.84, DOI: 10.1517/17425247.2014.938634).
2. Indian Patent application entitled "A NOVEL SUBMICRONIC TOPICAL PHARMACEUTICAL FORMULATION FOR THE EFFECTIVE TREATMENT OF PSORIASIS" has been filed in 2012 (Application number: 1394/DEL/2011).
3. Manuscript entitled “Novel mucoadhesive polymeric nanocarriers for nasal delivery of vaccines” is under preparation.
4. Manuscript entitled “Nasal delivery of Tetanus toxoid loaded mucoadhesive polymeric nanoparticles with additional adjuvant effect” is under preparation.
5. Manuscript entitled “Mechanistic understanding of Immune response modulated by Ovalbumin loaded mucoadhesive nanoparticles” is under preparation.

Poster/Oral presentations

1. Poster entitled "Nasal Delivery of Tetanus Toxoid Loaded Polymeric Nanoparticles with Additional Adjuvant Effect” was presented at American Association of Pharmaceutical Scientists (AAPS) 2015 conference held in Orlando, Florida, USA.
2. Poster entitled "Mucoadhesive Polymeric Nanocarriers for Nasal Delivery of Vaccines" was presented at American Association of Pharmaceutical Scientists (AAPS) 2014 conference held in San Diego, California, USA.
3. Oral presentation "SLNs Loaded Topical Gel Containing Combination Drugs: An Approach to Offset Psoriasis" was delivered in Fourth Winter School on "Nanotechnology in Advanced Drug Delivery" held at NIPER, Mohali, India.
4. Attended 2nd International Symposium on “Drug Metabolism and Pharmacokinetics” held at NIPER, S.A.S. Nagar, Mohali, India. (February 2010).

8. Curriculum vitae

For reasons of data protection,
the curriculum vitae is not included in the online version